University of Southampton

Faculty of Engineering, Sciences and Mathematics
School of Ocean and Earth Science

Diagnostics of diapycnal diffusion in z-level ocean models

by

Julia Getzlaff

Thesis for the degree of Doctor of Philosophy

March 2008

University of Southampton

Abstract

Faculty of Engineering, Sciences and Mathematics
School of Ocean and Earth Science

Doctor of Philosophy

Diagnostics of diapycnal diffusion in z-level ocean models

by Julia Getzlaff

In general ocean circulation models (OGCMs) diapycnal diffusion arises not only from the discretisation of the explicit diffusion, but also by numerically induced diffusion, caused, e.g., by common discretisations of advective transport.

In the present study, three different diagnostics to analyse the mean diapycnal diffusivities of individual tracers (vertically and horizontally) are introduced: (i) The divergence method based on the work of Ledwell et al. (1998) infers the mean diapycnal diffusivity from the advection-diffusion equation. (ii) The tracer flux method based on the work of Griffies et al. (2000), that determines the diapycnal flux crossing an isopycnal layer, is modified for the analysis of mean diapycnal diffusivities of a passive tracer. (iii) The variance method based on the work of Morales Maqueda and Holloway (2006) is a more general approach as the diapycnal diffusion is analysed by the variance decay of the total tracer concentration.

These methods can be used for the analysis of the diffusivity of passive tracer independent of the model set-up, e.g. the advection scheme used, but support only information about mean diapycnal diffusivity of that tracer field rather than for each individual layer. The applicability of these methods is tested in a set of 1- and 2-dimensional case studies. The effect of vertical advection and of diverging and converging isopycnals is shown separately. In all three methods used, the transformation of the tracer onto isopycnals leads to errors in the diagnosed diffusivities. It turns out that the tracer flux method is the most robust method and therefore the method of choice. In order to keep the errors as small as possible, longer time mean values should be analysed.

To Klaus, Leonie and Paulina

Contents

List of Figures

List of Tables

Author's declaration

I, **Julia Getzlaff**, declare that the thesis entitled **"Diagnostics of diapycnal diffusion in z-level ocean models"** and the work presented in the thesis are both my own, and have been generated by me as the result of my own original research. I confirm that:

- this work was done mainly while in candidature for a research degree at this University;
- where any part of this thesis has previously been submitted for a degree or any other qualification at this University or any other institution, this has been clearly stated;
- where I have consulted the published work of others, this is always clearly attributed;
- where I have quoted from the work of others, the source is always given. With the exception of such quotations, this thesis is entirely my own work;
- I have acknowledged all main sources of help;
- where the thesis is based on work done by myself jointly with others, I have made clear exactly what was done by others and what I have contributed myself;
- none of this work has been published before submission

Signed: .....

Date: .....

Acknowledgements

First, I would like to thank my supervisor Andreas Oschlies for providing his support and encouragement in this project, the time for discussion and the nice and easy start in Southampton. He gave me the opportunity to start this thesis at the IFM-GEOMAR in Kiel (Germany) and change to the National Oceanography Centre in Southampton for the second half.

George Nurser agreed to be my co-supervisor, when I moved to Southampton and became my main supervisor after Andreas moved back to Germany. I would like to thank him for his effort, encouragement and exactness which helped me to solve nearly all my problems.

I would also like to thank David Smeed, who joined into my panel as the co-supervisor for the second half of my thesis, for his helpful comments and Duncan Purdie as my panel chair.

Thanks to Carsten Eden and Heiner Dietze for the very helpful discussions during the last months of my PhD and for proof-reading. I thank also Jens Schafstall, Mirjam Glessmer and Friederike Prowe for proof-reading.

Thanks to John Armitage, Caroline Scott, Lisa Weber, Ralf Schiebel, Uta Krebs, Torsten Kanzow for the nice time in Southampton.

I would like to thank my parents, for their constant support and help. And also the distance to Southampton didn't matter, when there was some need for babysitting. I would also like to thank Roswitha Getzlaff for her help.

Finally, I would like to thank Klaus for his love, his constant support and his belief, that I can solve any problem. My special thanks go to Leonie and Paulina.

Chapter 1

Introduction

In this thesis, methods to analyse diapycnal mixing in z-level models will be developed and tested in idealised 1- and 2-dimensional case studies in order to estimate values for the numerically induced diffusivity. To motivate this work, the following questions are discussed:

1. What is diapycnal diffusion and why is it important?
2. How significant is the implicit diffusion induced by numerical schemes in ocean general circulation models?

In the following, the process of diapycnal mixing will be explained including its role in the ocean circulation. Additionally a status of science will be given, first from the observational side and second in the view of the modeller, including an explanation of numerically induced diffusivity.

What is diapycnal diffusion and why is it important?

In general, diffusion describes the mixing of molecules as a result of random thermal motion. A mathematical description of diffusion is derived from Fick's law (Fick, 1855): The net movement of a diffusing substance per unit area of a cross section (the direct flux) is proportional to the spatial derivative of the concentration and towards lower concentration. The constant of proportionality is the diffusion coefficient (diffusivity).

The diapycnal diffusion is this small scale mixing process across surfaces of equal density. In a motionless case with a horizontal stratification, the diapycnal diffusion is only determined by the Brownian motion. In the ocean, this process is intensified by small-scale turbulence and also known as turbulent diffusion. The resulting effect of the diapycnal mixing is the change of the water mass properties, hence the position of the centre of mass of the water column is changed. That means that part of the kinetic energy contained in the turbulence is transformed into potential energy.

In order to understand the role of diapycnal diffusion in the ocean, it is necessary to get an overview of the large scale circulation. The meridional overturning circulation (MOC) is the zonally integrated volume transport, which results in a vertical circulation loop. In the Atlantic ocean, the MOC is characterised by the northwards flow of warm surface waters and the return flow of cold and dense waters at greater depth. In the high northern latitudes formation of dense water masses take place (e.g. Marshall and Schott, 1999). The meridional circulation loop is closed by upwelling of deep waters through the pycnocline in low latitudes and in the Southern Ocean.

The thermal forcing, heating and cooling at the surface is not able to drive the MOC, which is described earliest in its basic form in the theorem postulated by Sandström (1908) and discussed in many recent studies (e.g. Paparella and Young, 2002; Wunsch and Ferrari, 2004).

The thermal forcing is determined by the buoyancy exchange at the surface. One resulting process is the deep water formation in the high latitudes. The dense waters are formed by deep convection. The convective mixing of an unstable stratified water column reduces its potential energy. This potential energy needs to be resupplied. As both, the heating and the cooling happens at the surface, so at the same geopotential level, the thermal energy the ocean receives cannot be converted in an efficient way into kinetic energy. The thermohaline driving mechanism on its own results in a very weak horizontal circulation only in the upper layers, and homogenous cold waters in the deep ocean (Sandström, 1908; Wunsch and Ferrari, 2004). This is completely different from the observed

meridional circulation and the observed stable oceanic stratification.

In the traditional studies, Sandström (1908, 1916) and later Jeffreys (1925) suggested, that additionally to the thermohaline forcing small-scale mixing processes are necessary. These transport heat down from the surface into the deeper water masses across isopycnal surfaces (Wunsch and Ferrari, 2004) in order to drive the MOC and close the energy balance.

Since the observed oceanic structure is different from the scenarios described by Sandström (1908), the theorem itself says therefore, that the observed structure and the associated flow is not the result of direct buoyancy forcing. In addition to Sandström's theorem, Paparella and Young (2002) showed that a flow that is generated by buoyancy forces acting at the surface alone cannot generate interior turbulence. This mechanism is described in detail by Munk and Wunsch (1998). What can generate the interior turbulence in that case? By a combination of winds and tides, internal waves are generated in the ocean, which dissipate into small-scale motion and therefore cause turbulent mixing. Without interior turbulence (diapycnal mixing), the fluid sinking to the seafloor cannot be lightened by the mixing necessary for it to reach the surface across the deep stable stratification. Consequently this raises the question of how big the diapycnal diffusion in the ocean really is.

Currently there are two distinct processes considered as driving mechanisms of the MOC: (i) the diapycnal mixing of heat and salt by small-scale turbulence, and (ii) the wind driven upwelling in the Southern Ocean (Wunsch and Ferrari, 2004; Kuhlbrodt et al., 2007). To what extent the diapycnal diffusion is the dominant driving mechanism of the MOC is currently under debate, but it is certainly an important factor.

Initially the diapycnal mixing coefficient was assumed to be uniform throughout the oceans interior, mainly because of the lack of data and in order to simplify matters. This implied a uniformly distributed slow upwelling over larger regions of the ocean (Stommel and Arons, 1960).

From observations of oceanic carbon-14, Munk (1966) was able to separately estimate global means of the vertical velocity w and the

eddy-coefficient κ , interpreted as diapycnal diffusivity ($1 \times 10^{-4}\, m^2/s$) for large scales. Since then, a diapycnal diffusivity of $1 \times 10^{-4}\, m^2/s$ was widely seen as the mixing coefficient needed in order to return the deep water masses back to the surface. In fact, Munk (1966) showed that the MOC strength and the global mean value of the diapycnal diffusivity are proportional to each other.

Osborn and Cox (1972) and Osborn (1980) estimated values for the diapycnal diffusivity in the upper $1000\, m$ below the mixed layer, using direct measurements on subcentimeter scales. However, the direct open-ocean estimates generally failed to produce values of κ exceeding about $0.1 \times 10^{-4}\, m^2/s$. This is only about one tenth of the value believed necessary to support the observed basin-wide circulation.

Given the uncertainties of the representativeness of the direct and local estimates of diffusivities and of the theoretical assumptions, there was a need for more direct measurements. With the North Atlantic Tracer Release Experiment (NATRE) Ledwell et al. (1993, 1998) introduced a method to estimate local diapycnal diffusivities from tracer measurements. An inert tracer dye (sulfur hexafluoride) was deployed in a controlled fashion on an isopycnal surface at about $300\, m$ depth in the eastern North Atlantic. The estimated diapycnal diffusivities of the order of $0.1 \times 10^{-4}\, m^2/s$ confirmed the estimates of Osborn and Cox (1972) and are also shown by Moum and Osborn (1986) and Oakey et al. (1994) for mixing rates away from topographic features and boundaries. Even lower values can be found close to the equator as shown by Gregg et al. (2003).

On the other hand, along continental slopes (Moum et al., 2002) or close to highly variable bottom topography (Polzin et al., 1997; Ledwell et al., 2000; Garabato et al., 2004) strong mixing with a diffusivity coefficient of up to $100 \times 10^{-4}\, m^2/s$ can be found. Additionally, experiments in boundary regions, primarily in easier settings such as lakes show, that there is enhanced diapycnal mixing in regions with strong isopycnal slopes (Ledwell and Hickey, 1995; Wuest and Lorke, 2003). Munk and Wunsch (1998) take into account such highly variable mixing and reestimated the basin average diapycnal diffusivity. They

hypothesised that the power which is required to mix water with a uniform diapycnal diffusion coefficient of $1 \times 10^{-4}\, m^2/s$ is the same as if concentrated mixing with a much higher coefficient as e.g. $100 \times 10^{-4}\, m^2/s$ occurs in only 1% of the oceans.

It appears straightforward to use numerical ocean general circulation models (OGCMs) in order to study regions where intense mixing is suggested and to gain insight into how the meridional overturning is influenced by the diapycnal mixing. Bryan (1987); Zhang et al. (1999) and Mignot et al. (2006) showed that the heat transport and the MOC are very sensitive to the diapycnal diffusivity used. Additionally, the studies by Marotzke (1997) and Scott and Marotzke (2002) showed the influence of mixing locations on the meridional overturning and the importance of mixing only at the boundaries. These studies conclude that mixing at the boundary is the more efficient driving process for the overturning circulation in comparison with the mixing in the interior.

In addition to the suggested influence of the diapycnal mixing on the large scale circulation such as the MOC, it is also an important process for the ecology, chemistry, optical properties and the spreading of water masses. Pelegri and Csanady (1991) and Pelegri et al. (1996) showed that diapycnal mixing has a maximum at the location of the nutrient stream associated with observed nutrient anomalies along the Gulf stream along the western boundary of the subtropical North Atlantic. They suggest that diapycnal mixing associated to the passage of steep meanders brings nutrients from the nutrient stream to the shallow photic layers. Jenkins and Doney (2003) suggested with the mechanism of the subtropical nutrient spiral, that diapycnal mixing is an important process for the nutrient supply in the surface waters near Bermuda.

In the analysis of biogeochemical models, Oschlies and Garcon (1999) showed in a model intercomparison that although the explicit diffusion is kept constant changes in the advection schemes lead to an increase of the primary production by a factor of two. This indicates that the diapycnal diffusion in these models depends strongly on the discretisation of the advection on the model grid, e.g. on numerically induced diffusion.

What is the numerically induced diffusion?

In general the motion of a fluid can be described by the Navier-Stokes equations, a set of coupled differential equations which establish relations among the rate of change of the variables of interest. Solving the Navier-Stokes equations numerically would require a very fine grid to resolve all turbulence scales and it would also require a fine resolution in time, as turbulent flow (diapycnal mixing) is always unsteady. This is not given in OGCMs, therefore the Reynolds-averaged Navier-Stokes equations are used. That means to ignore small-scale vortices (or eddies) in the motion and to calculate a large-scale motion with an eddy viscosity that characterises the transport and dissipation of energy in the smaller-scale flow and an eddy diffusivity.

The diapycnal mixing in models is not only determined by the parameterisation of the explicit diffusive mixing, but also by the numerically induced diffusion. Numerically induced diffusion in z-level models arises from discretisation errors, particulary of the advection terms or from problems to adequately resolve boundary layers on the model grid, as a result of the insufficient horizontal and vertical resolution. Lee et al. (2002) showed that the numerically induced diffusion associated with the advection scheme in high-resolution z-coordinate models may drive unrealistically high rates of diapycnal mixing.

The advection in numerical models can be realised by a wide range of advection schemes. Present advection schemes lead in general to spurious effects, given by two most important effects: First, the advection scheme can induce additional diffusion, e.g. in the upstream scheme. For tracers, these advection schemes do not conserve the variance. Second, the advection scheme can cause dispersion, which is the case when centred differences in space and time are used. Consider for instance the analytical case in which the tracer moves with a constant velocity. Numerical dispersion of the advection scheme will lead to different advection velocities depending on frequency. This means that in the model advection velocities are different to the analytical case, i.e. incorrectly represented. This effect

can be suppressed by an increase of the explicit diffusion in the model. Usually the advection schemes used in OGCMs generate both, numerically induced diffusion and dispersion. Note, that not only the spatial discretisation of the advection but also the discretisation in time may result in a numerically induced diffusion.

Before giving an overview of the different methods that are used in z-level models in order to diagnose the numerically induced diffusivity, it is necessary to introduce the terminology used in this study. In the following the explicit diffusivity is the diffusion which is used for the parameterisation of the diffusive mixing in the model input. Opposite to this, the diagnosed diffusivity denotes the sum of the explicit diffusivity and the numerically induced diffusivity. For the analysis of the diagnosed diffusivity only the fields of the model output are used. The difference between the diagnosed and the explicit diffusivity is the numerically induced diffusivity.

Following the work of Winters et al. (1995) and Winters and D'Asaro (1996), Griffies et al. (2000) analysed the diagnosed diffusivity by comparing the change in the density with time with the diapycnal flux of the density. This diagnostic only permits the analysis of the basin averaged diffusivity. However, they are able to quantify mean values for the induced diffusivity, the disadvantage of this method is the restriction to the analysis of basin wide parameters.

A different approach was carried out by Morales Maqueda and Holloway (2006). They analysed the decay of the tracer variance and related it to a diffusive term. Although they are able to analyse values for the induced diffusivity for each grid box, their analysis is restricted to models where the linear second-order moment (SOM) advection scheme is used. More generally, the diagnostic suggested by Burchard and Rennau (2007) also based on the variance decay of individual tracers, similar to the approach by Morales Maqueda and Holloway (2006). However, here, the tracer variance decay is used as a direct measure for the mixing.

In the present study, three different methods will be tested in order to

analyse diagnosed diffusivities of individual tracers. These tests will be done in idealised 1- and 2-dimensional case studies, in which it is possible to separate between different mechanisms, i.e. the effect of advection and/or of diverging and converging isopycnals with time. All methods analyse a mean value for the diagnosed diffusivity, which is depth independent (for the 2-dimensional case also independent of the horizontal axis), but time dependent.

The evolution of the tracer with time is a result of the dynamics in the model including the boundary (surface and lateral) tracer fluxes. Therefore diagnostic methods need to take account of tracer fluxes across the boundaries (and possible interior sources). However the passive tracer employed here does not have any such sources. For all three methods the temporally changing tracer field is used for the analysis of the diagnosed diffusivity. This has the advantage that the methods, so long as they work, can be used for the analysis of OGCMs in the same way as shown in this thesis for the analysis of the 1- and 2-dimensional case studies. The results show the patch-averaged diapycnal diffusion of the tracer. This leads to the possibility to directly compare the results of the OGCMs with those from observational studies. Releasing the tracer in different regions, such as the interior at the position where the NATRE studies took place or in more turbulent regions e.g. at the western boundary, provides information about local rates of diapycnal mixing in that region as well as the numerically induced diffusion.

Since the diagnosed diffusivity is the sum of the explicit diffusivity and the numerically induced diffusivity, it is necessary to weight the explicit diffusivity. The difference between the weighted and the diagnosed diffusivity is the numerically induced diffusivity.

Methods Before it is possible to analyse the diapycnal diffusivity in OGCMs by performing tracer experiments in close analogy to experiments that have been performed in the real ocean (Ledwell et al., 1998), it is necessary to test the robustness of the different diagnostics in a set of one- and two-dimensional case studies. The present work is restricted to results

of these case studies.

In the first method, it will be tested, in how far it is useful to use the same method as described by Ledwell et al. (1998) for the analysis of the diapycnal diffusivity in models. This method is denoted as the divergence method. In the second one, the same approach is used as done in Griffies et al. (2000), but modified in such a way that no longer is the basin wide mean analysed; instead the tracer mean diapycnal diffusivity is calculated for each time step. It will be denoted as the tracer flux method.

Since the method used by Burchard and Rennau (2007) is not differentiating between the diapycnal and the isopycnal component of the induced mixing, the last method described is a variation of the method introduced by Morales Maqueda and Holloway (2006). Instead of analysing the variance decay for each model box, the variance decay for the whole tracer volume is analysed. This will be denoted as the variance method.

Although all three methods are not able to resolve the model induced diffusion for each grid box, it is possible to analyse local rates depending on the tracer field. The advantage on the other hand is, that all methods are independent of the advection scheme used in the model and the model grid, equidistant or non-equidistant z-levels or layers.

In this thesis, the analysis is focused on methods to diagnose diapycnal diffusivities. This gives the possibility to directly compare the model results with the observational studies of e.g. Ledwell et al. (1998). Although the diagnosed diffusivity depends strongly on the actual tracer distribution, the analysis of e.g. tracer fluxes will not lead to different results in the divergence method and the tracer flux method. For these methods the diapycnal flux due to diffusion is directly correlated to the diagnosed diffusivity. Despite the difficulties in evaluating it, and its crudity as a measure of mixing, diffusivity is a familiar concept, whose values are immediately meaningful, and which can be compared with observation.

Outline The thesis is divided into two different parts, one concerned with the 1-dimensional case studies and the second part with the 2-dimensional case studies. In Part I, a detailed description of the three different methods is given (Chapter 2), restricted to the analysis of the one-dimensional experiments. In Chapter 3, the model set-up is introduced and the results for a set of experiments, where only the tracer is considered, are shown using an equidistant and a non-equidistant z-level grid.

Since for the analysis of experiments including vertical advection and/or diffusion in temperature and salinity, it is necessary to transform the tracer on isopycnals, Chapter 4 introduces the mapping scheme for the transformation of the tracer on isopycnal layers as well as the consequences in the diagnostics. Additionally the sensitivity of the three methods to the transformation of the tracers onto isopycnals will be shown. It turns out, that the method based on the analysis similar to Ledwell et al. (1998) (divergence method) is very sensitive to the transformation.

The two remaining methods, the tracer flux and the variance methods, analyse the diffusion from the temporal evolution of the tracer with time. In order to analyse the diapycnal diffusion for cases, with non-stationary isopycnals, the relative movement of the isopycnals with time can be divided into two different classes: (i) a parallel movement and (ii) divergence and convergence of the isopycnal layers. For the analysis of the tracer flux method, it is not important if these relative movements of the isopycnals are a result of vertical or horizontal flows, only the relative movement of the tracer to the isopycnal layers are important. Also horizontal flows are only able to generate a parallel displacement or divergence and convergence of the isopycnals. Therefore only case studies including vertical advection or diffusion are presented in this study.

In Chapter 5, the effect of the vertical advection on the results of the diagnosed diffusivity will be analysed. In this case, the vertical advection is restricted to an exact parallel movement of the isopycnals in order to suppress the consequences of diverging or converging isopycnals. The effect of converging and diverging isopycnals is separately analysed in Chapter 6, where diffusion acts on tracer, temperature and salinity. The results of the

first part are summarised in Chapter 7.

In Part II, the same experiments as shown in Part I for the 1-dimensional model are repeated for the 2-dimensional model. In Chapter 8, the results for the variance method, which is based on the work of Morales Maqueda and Holloway (2006), are shown including changes in the method according to the additional dimension. Chapter 9 is structured in the same way, only that here the results for the tracer flux method, which is based on the ideas of Griffies et al. (2000), are shown. Chapter 10 summarises the main results of the second part and gives an outlook for the application of these methods for the analysis of numerically induced diffusion in OGCMs.

It turns out that the tracer flux method, where temporal change of the total amount of tracer above an isopycnal equals the diapycnal flux through the isopycnal, can be used. In order to keep the errors as small as possible, it is useful to analyse longer time mean values as the combination of the advection and the transformation of the tracer onto isopycnals induces oscillations. The results of the variance method show that for the variance method it is not possible to separate the diapycnal from the isopycnal diffusion.

Part I

1-dimensional Experiments

Chapter 2

Methods to analyse diapycnal diffusion in z-level models

In the following, three different methods of diagnosing diffusion will be introduced. The divergence method is based on the description by Ledwell et al. (1998) and the tracer flux method on the description by Griffies et al. (2000) and their application in numerical models. Both of these methods derive from the assumptions of the advection-diffusion equation and their parameterisation in the model set-up. Finally, the variance method (Morales Maqueda and Holloway, 2006) will be used, where the diagnosed diffusivity is inferred from the variance decay of the tracer. All three methods give a mean value for the diagnosed diffusivity of the tracer volume.

For all three methods, the diagnosed diffusivity is estimated from the temporally changing tracer field in the model output. The diagnosed diffusivity is the sum of the explicit and the numerically induced diffusivity. In order to estimate values for the numerically induced diffusivity, it is necessary to weight the explicit diffusivity in such a way that it can be directly compared to the depth independent value of the diagnosed diffusivity. For all three implicit methods, a weighting of the explicit diffusion coefficient will be introduced as well.

The introduction of the three different methods, as shown in this chapter,

will be reduced to the analysis of simple 1-dimensional experiments, while diffusion of density is not considered here. In these special cases the vertical diffusion is equal to the diapycnal diffusion and the analysis can be done on z-coordinates. The adjustment of the diagnostics for the analysis of 2-dimensional experiments will be shown in the second part of this thesis.

2.1 The divergence method

The diagnostics of analysing the diapycnal diffusivity described by Ledwell et al. (1998) are based on the temporal evolution of the diapycnal spreading of the isopycnally integrated tracer field. This analysis uses the advection-diffusion equation and gives information only about vertical mean values for the diapycnal diffusivity and vertical velocity. Different to the approach of Ledwell et al. (1998), in the simplified 1-dimensional models considered here the tracer concentration only depends on the vertical dimension, thus no extra isopycnal interpolation is needed.

Following Ledwell et al. (1998), the diagnosed diffusivity is obtained by the advection-diffusion equation. The advection-diffusion equation in a 1-dimensional form is given by

$$\frac{\partial C}{\partial t} + \frac{\partial (w \cdot C)}{\partial z} = \frac{\partial}{\partial z}\left(\kappa \cdot \frac{\partial C}{\partial z}\right), \tag{2.1}$$

where $C = C(z,t)$ is the tracer concentration, $w = w(z,t)$ is the vertical velocity, $\kappa = \kappa(z,t)$ is the vertical diffusivity, z is the depth and t is the time. In close analogy to the method used in the observational studies (Ledwell et al., 1993, 1998), the diffusivity and the vertical velocity are taken as depth independent, leaving

$$\frac{\partial C}{\partial t} = \overline{\kappa} \cdot \frac{\partial^2 C}{\partial z^2} - \overline{w} \cdot \frac{\partial C}{\partial z}, \tag{2.2}$$

where $\overline{\kappa} = \overline{\kappa}(t)$ denotes the mean diffusivity and $\overline{w} = \overline{w}(t)$ the mean vertical velocity. In general, solving Equation 2.2 with the method of the

least squares fit gives values for the mean diffusivity and the mean vertical velocity.

In order to test the robustness of this method, in Chapter 3 experiments are analysed without vertical advection. In this case, the advection-diffusion equation (see Equation 2.2) can be reduced to

$$\frac{\partial C}{\partial t} = \overline{\kappa} \cdot \frac{\partial^2 C}{\partial z^2}. \tag{2.3}$$

In the following, this method will be referred to as the divergence method. The method of the least squares fit requires that the vertical integral of the square of the difference between the temporal development of the tracer and the diffusive term should be minimal, leading to

$$\int \left(\frac{\partial C}{\partial t} - \overline{\kappa} \frac{\partial^2 C}{\partial z^2} \right)^2 dz \doteq min,$$

where the integral is taken over the total depth. As the integral has to be a minimum, this also means that the derivative with respect to $\overline{\kappa}$ is required to be equal to zero.

$$\begin{aligned} &\frac{\partial}{\partial \overline{\kappa}} \int \left(\frac{\partial C}{\partial t} - \overline{\kappa} \frac{\partial^2 C}{\partial z^2} \right)^2 dz = 0 \\ \rightarrow &\int \left(\frac{\partial C}{\partial t} - \overline{\kappa} \frac{\partial^2 C}{\partial z^2} \right) \cdot \frac{\partial^2 C}{\partial z^2} \, dz = 0. \end{aligned} \tag{2.4}$$

This leads to the general form of the mean diffusivity $\overline{\kappa}$ for the case, in which only the tracer is diffusive ($w = 0$), as follows

$$\overline{\kappa} = \frac{\int \left(\frac{\partial C}{\partial t} \cdot \frac{\partial^2 C}{\partial z^2} \right) dz}{\int \left(\frac{\partial^2 C}{\partial z^2} \right)^2 dz} \tag{2.5}$$

The mean diffusivity $\overline{\kappa}$ depends only on the temporal derivative of the tracer and its curvature. In order to analyse the mean diffusivity in numerical models Equation 2.5 needs to be discretised on the model grid.

Different to the analysis of observational studies, in models the temporal derivative of the tracer can be estimated in two different ways.

First, the temporal derivative can be determined from the temporal evolution of the tracer field. The resulting diffusivity includes the explicit and the numerically induced diffusivities and will be denoted as diagnosed diffusivity $\kappa_{diag\_L} = \kappa_{diag\_L}(t)$ in the following. Second, in models the temporal derivative of the tracer can be reduced to explicit diffusive flux divergence which is generated in the model set-up by the explicit diffusion term. The resulting weighting of the explicit diffusivity is denoted as weighted diffusivity $\kappa_{w\_L} = \kappa_{w\_L}(t)$ in the following.

Diagnosed diffusivity For the analysis of the diagnosed diffusivity, the temporal derivative of the tracer is estimated from the temporal evolution of the tracer field. The discretisation of the temporal derivative of the tracer concentration is given by

$$\frac{\Delta C}{\Delta t} = \frac{C_k^{t+\Delta t} - C_k^t}{\Delta t}, \tag{2.6}$$

where k is the index of the depth levels, t the time index and Δt is the time-step. The dicretisation of the spatial derivative needs to be done in exactly the same way, as in the model set-up. Therefore it is also important to be aware of the integration scheme used. For the models used in this thesis, the implicit Eulerian backwards scheme is used. This means for the discretisation of the mean diffusivity (Equation 2.5) that the spatial derivative has to be taken at time-step $t + \Delta t$. Additionally, the discretisation of the spatial derivatives is realised by a centred differences scheme, leading to

$$\frac{\Delta^2 C}{\Delta z^2} = \frac{1}{\Delta z_k} \cdot \left(\frac{C_{k-1}^{t+\Delta t} - C_k^{t+\Delta t}}{\Delta \tilde{z}_{k-1}} - \frac{C_k^{t+\Delta t} - C_{k+1}^{t+\Delta t}}{\Delta \tilde{z}_k} \right), \tag{2.7}$$

where k is the index of the depth levels, Δz is the thickness of the z-levels and $\Delta \tilde{z}$ is the thickness of the levels of the temperature grid (for more detail see Section 3.1).

Discretising Equation 2.5 with the temporal derivative given in Equation 2.6 and the spatial derivative given in Equation 2.7 the diagnosed diffusivity κ_{diag_L} is defined as

$$\kappa_{diag\_L} = \frac{\sum_{k=1}^{n} \left(\frac{\Delta C}{\Delta t} \cdot \frac{\Delta^2 C}{\Delta z^2} \cdot \Delta z_k \right)}{\sum_{k=1}^{n} \left(\left(\frac{\Delta^2 C}{\Delta z^2} \right)^2 \cdot \Delta z_k \right)}, \tag{2.8}$$

where n is the number of model levels. The diagnosed diffusivity κ_{diag_L} is the sum of the explicit and the numerically induced diffusivities.

Weighted diffusivity On the other hand, the contribution towards the temporal change of the tracer field generated by the explicit diffusive flux divergence in the model set-up only is given by

$$\frac{\partial C}{\partial t} = \frac{\partial}{\partial z} \left(\kappa \cdot \frac{\partial C}{\partial z} \right). \tag{2.9}$$

In the following $\kappa_{expl} = \kappa_{expl}(z,t)$ denotes the explicit diffusion coefficient. The discretised form of the explicit diffusive flux divergence $\frac{\partial}{\partial z} \left(\kappa \cdot \frac{\partial C}{\partial z} \right) = \frac{\partial F_{expl}}{\partial z}$ is denoted as ΔF_{expl} in the following, leading to the discretisation of the temporal derivative as follows

$$\frac{\Delta C}{\Delta t} = \Delta F_{expl}. \tag{2.10}$$

In the model set-up used in this study, the parameterisation of the explicit diffusive flux divergence is defined by

$$\Delta F_{expl} = \frac{1}{\Delta z_k} \cdot \left({\kappa_{expl}}_{k-1}^{t+\Delta t} \cdot \frac{C_{k-1}^{t+\Delta t} - C_k^{t+\Delta t}}{\Delta \tilde{z}_{k-1}} - {\kappa_{expl}}_{k}^{t+\Delta t} \cdot \frac{C_k^{t+\Delta t} - C_{k+1}^{t+\Delta t}}{\Delta \tilde{z}_k} \right), \tag{2.11}$$

where Δz is the thickness of the z-levels and $\Delta \tilde{z}$ is the thickness of the levels of the temperature grid. The discretisation of the spatial derivative is the same as given in Equation 2.7.

Discretising Equation 2.5 with the temporal change of the tracer concentration given by the diffusive flux divergence in Equation 2.11 and the spatial derivative given in Equation 2.7, the weighted diffusivity κ_{w_L} is defined as

$$\kappa_{w\_L} = \frac{\sum_{k=1}^{n} \left(\Delta F_{expl} \cdot \frac{\Delta^2 C}{\Delta z^2} \cdot \Delta z_k \right)}{\sum_{k=1}^{n} \left(\left(\frac{\Delta^2 C}{\Delta z^2} \right)^2 \cdot \Delta z_k \right)}, \tag{2.12}$$

where n is the number of z-levels in the model. The weighted diffusivity κ_{w_L} is only a function of the explicit diffusivity κ_{expl} and the spatial derivatives of the tracer concentration, but does not depend on the temporal derivatives, which is different to the diagnosed diffusivity κ_{diag_L}. Note, both the weighted diffusivity κ_{w_L} and the diagnosed diffusivity κ_{diag_L} are time dependent, but depth independent values.

The definitions of the weighted and the diagnosed diffusivities are independent of the model grid. The method can also be used for all different model types, but the discretisation needs to be adjusted to the one used in the model set-up.

2.2 The tracer flux method

In the method of Griffies et al. (2000), the main interest is the amount of flux crossing a particular isopycnal surface, which can be found by analysing the temporal change of the tracer above the isopycnal. By using the cumulative integral of the advection-diffusion equation, the same flux is analysed. Similar to the approach in Griffies et al. (2000), the tracer flux method as defined here basically analyses the diapycnal flux crossing a particular isopycnal layer.

The cumulative integral of the advection-diffusion equation is given by

$$\frac{\partial}{\partial t} \int_{z'=z}^{0} C dz' = -\kappa \frac{\partial C}{\partial z}\Big|_z + w \cdot C\Big|_z, \tag{2.13}$$

where $C = C(z,t)$ is the tracer concentration, z denotes the depth, $\kappa = \kappa(z,t)$ the vertical diffusivity and $w = w(z,t)$ the vertical velocity. In principle Equation 2.13 can be solved with the method of the least squares fit finding depth and time depending values for the diffusivity κ and the vertical velocity w similar to the analysis described by Griffies et al. (2000). However, the focus of this study is the analysis of vertical mean values for κ and w, as those can be directly compared to the results of the divergence method and later to the diffusivities found in observational studies.

In the following $\overline{\kappa} = \overline{\kappa}(t)$ is the mean vertical diffusivity and $\overline{w} = \overline{w}(t)$ the mean vertical velocity. In this case the cumulative integrated advection-diffusion equation is given by

$$\frac{\partial}{\partial t}\int_{z'=z}^{0} C dz' = -\overline{\kappa}\frac{\partial C}{\partial z}\Big|_z + \overline{w}\cdot C\Big|_z. \tag{2.14}$$

Solving Equation 2.14 with the method of the least squares fit, mean values for the vertical diffusivity and the vertical velocity can be found. For a better illustration, it will be focused on the solution of the case with no explicit vertical velocity ($w = 0$). In this case Equation 2.14 can be reduced to

$$\frac{\partial}{\partial t}\int_{z'=z}^{0} C dz' = -\overline{\kappa}\frac{\partial C}{\partial z}\Big|_z. \tag{2.15}$$

This means that the change of the total amount of tracer above one level is equal to the diffusive flux through that level. Therefore the method is denoted as tracer flux method. Equation 2.15 can now be solved with the method of the least squares fit, which leads to

$$\int_{z=-h}^{0}\left(\frac{\partial}{\partial t}\int_{z'=z}^{0} C dz' + \overline{\kappa}\frac{\partial C}{\partial z}\Big|_z\right)^2 dz \doteq min,$$

where h denotes the total depth of the water column. As the integral over dz is required to be a minimum, the drivative $\partial/\partial\overline{\kappa}$ has to equal zero, giving

$$\frac{\partial}{\partial \overline{\kappa}} \int_{z=-h}^{0} \left(\frac{\partial}{\partial t} \int_{z'=z}^{0} C dz' + \overline{\kappa} \frac{\partial C}{\partial z}\Big|_z \right)^2 dz = 0,$$

$$\rightarrow \int_{z=-h}^{0} \left(\left(\frac{\partial}{\partial t} \int_{z'=z}^{0} C dz' + \overline{\kappa} \frac{\partial C}{\partial z}\Big|_z \right) \cdot \frac{\partial C}{\partial z}\Big|_z \right) dz = 0. \tag{2.16}$$

Solving Equation 2.16 for the mean diffusivity $\overline{\kappa}$ gives

$$\overline{\kappa} = \frac{\int_{z=-h}^{0} \left(\frac{\partial}{\partial t} \int_{z'=z}^{0} C dz' \cdot \frac{\partial C}{\partial z}\Big|_z \right) dz}{\int_{z=-h}^{0} \left(\frac{\partial C}{\partial z}\Big|_z \right)^2 dz} \tag{2.17}$$

The result of the least squares fit (see Equation 2.17) shows how the mean value is weighted. Different to the result of the divergence method, the mean diffusivity analysed by the tracer flux method is weighted by the tracer gradient. For the analysis of numerical models, Equation 2.17 needs to be discretised on the model grid. This discretisation can be done in two different ways, leading to the definitions of the diagnosed and the weighted diffusivities.

Diagnosed diffusivity The diagnosed diffusivity is the total diffusivity of the tracer patch, including the explicit and the numerically induced diffusivity. For the analysis of the diagnosed diffusivity, denoted as $\kappa_{diag\_G} = \kappa_{diag\_G}(t)$ in the following, the temporal change of the total amount of tracer above an isopycnal is determined by the temporal evolution of the tracer field. For the analysis the change of the total amount of tracer above an isopycnal with time needs to be discretised in the model grid:

$$\sum_{m=1}^{k} \frac{\Delta \left(C \cdot \Delta z \right)}{\Delta t} = \sum_{m=1}^{k} \frac{C_m^{t+\Delta t} \cdot \Delta z_m - C_m^t \cdot \Delta z_m}{\Delta t}, \tag{2.18}$$

where the cumulative sum is taken over the m levels. The vertical tracer gradient at the level $k+1$ for the model parameterisation used in this thesis (centred differences) is given by

$$\frac{\Delta C}{\Delta z}\Big|_{k+1} = \frac{C_k^{t+\Delta t} - C_{k+1}^{t+\Delta t}}{\Delta \tilde{z}_k}, \tag{2.19}$$

where $\Delta\tilde{z}$ is the thickness of the temperature grid. Discretising Equation 2.17 with the temporal change of the total amount of tracer above an isopycnal given in Equation 2.18 and the tracer gradient given in Equation 2.19, the diagnosed diffusivity κ_{diag_G} is defined as

$$\kappa_{diag\_G} = \frac{-\sum_{k=1}^{n}\left(\frac{\Delta C}{\Delta z}\Big|_{k+1} \cdot \sum_{m=1}^{k}\frac{\Delta(C\cdot\Delta z)}{\Delta t}\cdot\Delta\tilde{z}_k\right)}{\sum_{k=1}^{n}\left(\left(\frac{\Delta C}{\Delta z}\Big|_{k+1}\right)^2\cdot\Delta\tilde{z}_k\right)}, \tag{2.20}$$

where n is the number of model levels. As already mentioned for the diagnostics of the divergence method, the discretisation of the derivative in time and space needs to be done in the same way as in the model set-up.

Weighted diffusivity The weighted diffusivity includes only the explicit diffusion of the tracer. Different to the analysis of the diagnosed diffusivity, the change of the total amount of tracer above an isopycnal is discretised by the explicit diffusive flux:

$$\frac{\partial}{\partial t}\int_{z'=z}^{0} C dz' = -\kappa\frac{\partial C}{\partial z}\Big|_z. \tag{2.21}$$

The explicit diffusive flux $F_{expl} = \kappa\frac{\partial C}{\partial z}\big|_{k+1}$ as defined in the model set-up is given by

$$F_{expl} = \kappa_{expl}\cdot\frac{C_k^{t+\Delta t} - C_{k+1}^{t+\Delta t}}{\Delta\tilde{z}_k}, \tag{2.22}$$

where $\kappa_{expl} = \kappa_{expl}(z,t)$ denotes the explicit diffusion coefficient as defined in the model and $\Delta\tilde{z}$ is the thickness of the temperature grid. The discretisation of the tracer gradient is identical to the one shown in Equation 2.19. Discretising Equation 2.17 with the explicit diffusive flux

(Equation 2.22) and the tracer gradient (Equation 2.19), the weighted diffusivity κ_{w_G} is defined as

$$\kappa_{w\_G} = \frac{\sum_{k=1}^{n} \left(\frac{\Delta C}{\Delta z}\Big|_{k+1} \cdot F_{expl} \cdot \Delta \tilde{z}_k \right)}{\sum_{k=1}^{n} \left(\left(\frac{\Delta C}{\Delta z}\Big|_{k+1} \right)^2 \cdot \Delta \tilde{z}_k \right)}, \tag{2.23}$$

where n is the number of model levels. The definitions of the depth independent values for the weighted diffusivity κ_{w_G} and the diagnosed diffusivity κ_{diag_G} can be analysed independent on the model set-up used, but it is important to choose the discretisation of the different terms in exactly the same way as done in the model set-up. For implicit time-stepping schemes, the spatial derivative needs to be estimated at time-step $t + \Delta t$.

2.3 The variance method

A different way to analyse numerically induced diffusion is introduced by Morales Maqueda and Holloway (2006). In their work they calculate the numerically induced diffusivity by considering the variance decay of the tracer within a constant volume.

The tracer variance of one model box is calculated after applying the diffusion (and before the advection). Then the variance of the same volume is estimated. Finally, the change in the variance after applying the advection operator of that special volume is linked to a diffusive term. This is the diffusivity, which is only caused by the parameterisation of the advection in the model since the analytical form of the advection operator would not lead to a change in the tracer variance.

The aim of the variance method is, to find a more general method inferred from the variance decay of the tracer, which is not restricted by the model set-up. By estimating the variance decay of the whole tracer volume, this requirement is fulfilled.

The variance method links the temporal change in the variance of the whole tracer volume to a mean diffusivity. This is a depth independent parameter and gives a more general approach, which can be used independent of the used advection scheme in the model set-up.

Diagnosed diffusivity The total variance of the tracer concentration C is denoted as σ^2 and defined as follows:

$$\sigma^2 = \frac{1}{2}\sum_{k=1}^{n} C_k^2 \Delta z_k, \tag{2.24}$$

where n denotes the number of model levels and Δz the level thickness. According to Morales Maqueda and Holloway (2006), the link between the diffusion κ_{var} and the temporal change of the variance σ^2 can be written as

$$\frac{\Delta\sigma^2}{\Delta t} = -\kappa_{var} \cdot \sum_{k=1}^{n} \left[\left(\frac{\Delta C}{\Delta z} \right)^2 \cdot \Delta \tilde{z}_k \right], \tag{2.25}$$

where $\frac{\Delta\sigma^2}{\Delta t}$ is the variance decay and $\frac{\Delta C}{\Delta z}$ the tracer gradient.

The tracer gradient is given by

$$\frac{\Delta C}{\Delta z} = \frac{C_{k-1}^{t+\Delta t} - C_k^{t+\Delta t}}{\Delta \tilde{z}_{k-1}}, \tag{2.26}$$

where $C_k^{t+\Delta t}$ denotes the tracer concentration at the depth index k and the time-step $t + \Delta t$ and $\Delta\tilde{z}$ denotes the level thickness of the temperature grid. The temporal change in the tracer variance is given by

$$\frac{\Delta\sigma^2}{\Delta t} = \frac{1}{\Delta t} \cdot \left(\frac{1}{2}\sum_{k=1}^{n} (C_k^{t+\Delta t})^2 \Delta z_k - \frac{1}{2}\sum_{k=1}^{n} (C_k^t)^2 \Delta z_k \right), \tag{2.27}$$

where n is the number of model levels. Solving Equation 2.25 for the diagnosed diffusivity κ_{var} leads to

$$\kappa_{var} = \frac{-\frac{\Delta\sigma^2}{\Delta t}}{\sum_{k=1}^{n}\left(\left(\frac{\Delta C}{\Delta z}\right)^2 \cdot \Delta\tilde{z}_k\right)}, \tag{2.28}$$

where n is the number of model levels as well. This is the formulation of diagnosing diffusivity according to changes in the tracer variance as used below.

Weighted diffusivity In order to compare the diagnosed diffusivity κ_{var} with the explicit diffusion coefficient, κ_{expl} needs to be weighted in the same way as κ_{var} is weighted, which is by the square of the tracer gradient. The weighted diffusivity for the variance method is denoted as κ_w. The variance decay, which is given by the term of the explicit diffusivity is given by

$$\frac{\Delta\sigma^2}{\Delta t} = -\sum_{k=1}^{n}\left[\kappa_{expl} \cdot \left(\frac{\Delta C}{\Delta z}\right)^2 \cdot \Delta\tilde{z}_k\right]. \tag{2.29}$$

The discretisation of the tracer gradient is the same as given in Equation 2.26. Similarly, the variance decay according to the weighted diffusivity κ_w is given by

$$\frac{\Delta\sigma^2}{\Delta t} = -\kappa_w \cdot \sum_{k=1}^{n}\left[\left(\frac{\Delta C}{\Delta z}\right)^2 \cdot \Delta\tilde{z}_k\right]. \tag{2.30}$$

By substituting Equation 2.29 in 2.30, the weighted diffusivity κ_w is given by

$$\kappa_w = \frac{\sum_{k=1}^{n}\left(\kappa_{expl} \cdot \left(\frac{\Delta C}{\Delta z}\right)^2 \cdot \Delta\tilde{z}_k\right)}{\sum_{k=1}^{n}\left(\left(\frac{\Delta C}{\Delta z}\right)^2 \cdot \Delta\tilde{z}_k\right)}. \tag{2.31}$$

The discretisation of the tracer gradient is the same as given in Equation 2.26. In order to compare the variance method with the tracer flux method (see Section 2.4), the tracer flux through an isopycnal layer, given by $\kappa_{expl} \cdot \frac{\partial C}{\partial z} = F_{expl}$ is discretised in the same way as in Equation 2.22

method	diagnosed diffusivity	weighted diffusivity
divergence	$\kappa_{diag\_L} = \frac{-\sum_{k=1}^{n}\left(\frac{\Delta C}{\Delta t}\cdot\frac{\Delta^2 C}{\Delta z^2}\right)\Delta z_k}{\sum_{k=1}^{n}\left(\frac{\Delta^2 C}{\Delta z^2}\right)^2\Delta z_k}$	$\kappa_{w\_L} = \frac{\sum_{k=1}^{n}\left(\frac{\Delta F_{expl}}{\Delta z}\cdot\frac{\Delta^2 C}{\Delta z^2}\right)\Delta z_k}{\sum_{k=1}^{n}\left(\frac{\Delta^2 C}{\Delta z^2}\right)^2\Delta z_k}$
tracer flux	$\kappa_{diag\_G} = \frac{-\sum_{k=1}^{n-1}\left(\frac{\Delta C}{\Delta z}\Big\vert_{k+1}\cdot\sum_{m=1}^{k}\frac{\Delta(C\cdot\Delta z)}{\Delta t}\right)\Delta\tilde{z}_k}{\sum_{k=1}^{n-1}\left(\frac{\Delta C}{\Delta z}\Big\vert_{k+1}\right)^2\Delta\tilde{z}_k}$	$\kappa_{w\_G} = \frac{\sum_{k=1}^{n-1}\left(F_{expl}\cdot\frac{\Delta C}{\Delta z}\Big\vert_{k+1}\right)\Delta\tilde{z}_k}{\sum_{k=1}^{n-1}\left(\frac{\Delta C}{\Delta z}\Big\vert_{k+1}\right)^2\Delta\tilde{z}_k}$
variance	$\kappa_{var} = \frac{-\frac{\Delta\sigma^2}{\Delta t}}{\sum_{k=1}^{n}\left(\frac{\Delta C}{\Delta z}\right)^2\cdot\Delta\tilde{z}_k}$	$\kappa_{w} = \frac{\sum_{k=1}^{n}\left(F_{expl}\cdot\frac{\Delta C}{\Delta z}\right)\Delta\tilde{z}_k}{\sum_{k=1}^{n}\left(\frac{\Delta C}{\Delta z}\right)^2\Delta\tilde{z}_k}$

Table 2.1: Summary of the diagnosed and the weighted diffusivity for all three different methods, the discretised form is shown.

$$F_{expl} = \kappa_{expl}\cdot\frac{C_k^{t+\Delta t} - C_{k+1}^{t+\Delta t}}{\Delta\tilde{z}_k^{t+\Delta t}}.$$

That leaves the general form of the discretisation of the weighted diffusivity

$$\kappa_w = \frac{\sum_{k=1}^{n}\left(F_{expl}\cdot\frac{\Delta C}{\Delta z}\cdot\Delta\tilde{z}_k\right)}{\sum_{k=1}^{n}\left(\left(\frac{\Delta C}{\Delta z}\right)^2\cdot\Delta\tilde{z}_k\right)}, \tag{2.32}$$

where n is the number of model levels.

2.4 Summary and comparison

In Table 2.1, the discretised forms of the diagnosed and the weighted diffusivities for all three different methods are summarised. This makes a direct comparison of the different methods easier. In all three methods, the weighted diffusivity gives the mean value of the explicit model diffusion.

Comparing the weighted diffusivity analysed by the divergence method

with the weighted diffusivity diagnosed by the tracer flux method shows that the results are generally different. Whereas the diffusivity in the divergence method is weighted by the curvature of the tracer, the diffusivity of the tracer flux method is weighted by the tracer gradient. Only in experiments, where the explicit diffusivity coefficient is constant with depth, the results for the weighted diffusivities for both methods are identical. In general, it cannot be expected that the results for the divergence and the tracer flux methods are the same.

A comparison between the weighted diffusivity of the tracer flux and the variance method shows that both discretised forms are identical. Thus a direct comparison between these two methods is possible and the results for the weighted diffusivity should be consistent in all shown experiments. Note, the diagnosed diffusivity analysed by the variance method is identical to the one analysed by the tracer flux method, when diffusion and advection are discretised by the Crack-Nicholson scheme (centred differences in space and time), as the variance is conseved.

Chapter 3

1-dimensional case study: The simple tracer problem

In the previous chapter, three different methods for analysing diagnosed diffusivities have been introduced: the divergence method, the tracer flux method and the variance method. In order to test the robustness of these methods, in the following a set of 1-dimensional experiments will be analysed, where diffusion acts on tracer only.

First, the model set-up and the configuration of the different experiments will be introduced. Then, the results for these experiments using an equidistant and a non-equidistant vertical grid will be shown.

3.1 Model configuration

The model used is a 1-dimensional z-level model. The implemented tracer spreads only in a diffusive manner. In this case the weighted and the diagnosed diffusivity analysed by the divergence or the tracer flux method should give the same results.

The diffusion is implemented into the model as a Eulerian backward time stepping scheme. This scheme is usually chosen to discretise diffusion in OGCMs, as it is more stable compared to e.g. the Eulerian forward scheme.

Depending on the size of the explicit diffusion coefficient κ_{expl}, the model using the Eulerian forward scheme might become unstable. In that case, it is necessary to reduce the time-step; then the results converge towards the ones of the model with the Eulerian backward scheme. The temperature and salinity fields, hence the density, and the used explicit diffusion coefficients stay constant with time for the experiments shown in this chapter.

For the case, in which the tracer spreads only in a diffusive manner, the tracer evolves by:

$$\frac{\partial C(z,t)}{\partial t} = \frac{\partial}{\partial z}\left(\kappa_{expl}(z) \cdot \frac{\partial C(z,t)}{\partial z}\right), \tag{3.1}$$

where C is the concentration of the tracer, κ_{expl} is the explicit diffusivity coefficient, z is the depth and t is the time. Note, the explicit diffusivity coefficient κ_{expl} is taken as time independent, but depth dependent. For the Eulerian backward scheme, Equation 3.1 needs to be discretised in time on the model grid as follows:

$$C(z,t+\Delta t) = C(z,t) + \frac{\partial}{\partial z}\left(\kappa_{expl}(z) \cdot \frac{\partial C(z,t+\Delta t)}{\partial z}\right) \cdot \Delta t, \tag{3.2}$$

where Δt is the time-step, which is one day for the experiments shown. The effect of this choice on the results of the experiments will be discussed later. As the analysis for the diffusivity requires tracer conservation, noflux boundary conditions are considered in this model.

For the discretisation, the same definition of the grid as in MOM 2 described in Pacanowski (1995) is used, where the grid is u-centered, where the w-points are in the centre of two T-points. This means, the tracer concentration is not necessarily defined in the middle of each box. As already mentioned in Chapter 2, Δz is the thickness of the model box of the tracer and $\Delta\tilde{z}$ is the vertical distance between two tracer points (the thickness of the temperature box). The discretisation of the explicit diffusion is realised by the centred differences scheme. Note, according to the analysis of the diagnosed diffusivity, it is important to discretise the

Experiment	expl. diff. coefficient
A_const	constant
A_incr	lin. increase
A_decr	lin. decrease
A_oc	non-linear

Table 3.1: Experiments of the 1-dimensional case studies, for both initial tracer conditions.

methods always in exactly the same way as the model itself is dicretised.

To work out step by step the way of analysing diapycnal diffusivities and numerical influences on the method, first the results of all experiments using a uniform grid with a level thickness of $20\,m$ will be shown. After that, the same experiments using non-equidistant z-levels will be repeated. The non-equidistant grid has got 45 vertical levels, with spacing of $10\,m$ in the uppermost level and a smooth increase to $250\,m$ at $2500\,m$ depth. Below $2500\,m$ the vertical grid box thickness is constantly $250\,m$ up to a maximum depth of $5500\,m$. All experiments are integrated over a period of six months.

3.1.1 Experiments

In the following a set of experiments will be introduced, which only vary in the explicit diffusion coefficient used in order to analyse the sensitivity of the three methods. In these experiments the diffusion acts on the tracer only and the explicit diffusivity is constant with time. Temperature and salinity are also constant with time, hence the density is stationary. The experiments differing in the explicit diffusion coefficient are denoted as:

(i) **A_const**: κ_{expl} is constant with depth

(ii) **A_incr**: κ_{expl} increases linearly with depth

(iii) **A_decr**: κ_{expl} decreases linearly with depth

(iv) **A_oc**: κ_{expl} is non-linear with depth.

An overview of the experiments is also shown in Table 3.1. The constant explicit diffusion coefficient in experiment *A_const* has a value of $4cm^2/s$. Figure 3.1 shows the explicit diffusion coefficients for experiment *A_incr*

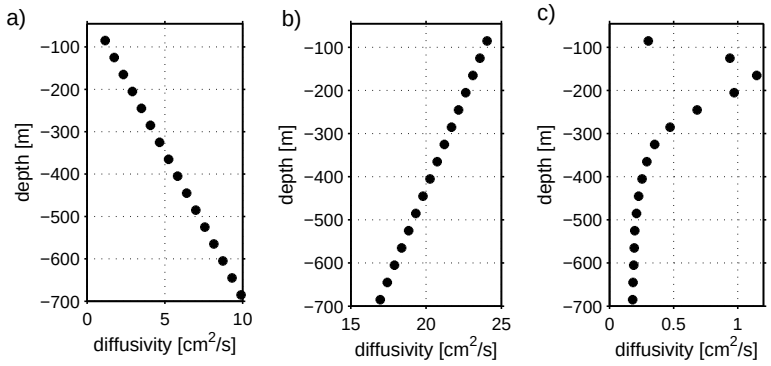

Figure 3.1: Time invariant diffusion coefficient for three different experiments: a) linearly increasing with depth (A_incr), b) linearly decreasing with depth (A_decr) and c) non-linear, as expected in the interior of the ocean (A_oc).

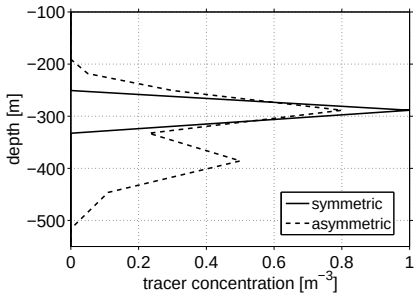

Figure 3.2: Symmetric (solid) and asymmetric (dashed) initial profiles of the tracer distribution.

(a), A_decr (b) and A_oc (c) for the equidistant model grid. The non-linear explicit diffusivity is chosen to be similiar to values typically found in the ocean interior in OGCMs with a coarse horizontal resolution of 4/3°. As, in general, OGCMs have a non-equidistant depth grid with a higher resolution at the surface, the linear interpolation of the explicit diffusivity coefficient onto an uniform grid with a level thickness of $20\,m$ is smoothing the maximum of the explicit diffusivity coefficient directly at the surface.

In the NATRE experiments, described e.g. by Ledwell et al. (1998), the tracer (sulfur hexafluoride) was released into the ocean in controlled fashion at a depth of $300\,m$. In order to mimic this initial condition, the tracer with a concentration of $1\,mol/m^3$ is initialised in one grid box at a depth of $300\,m$ (see Figure 3.2, solid line).

In the ocean, or also in OGCMs, the tracer distribution with depth does not necessarily stay symmetric with depth, as a result of diffusion and

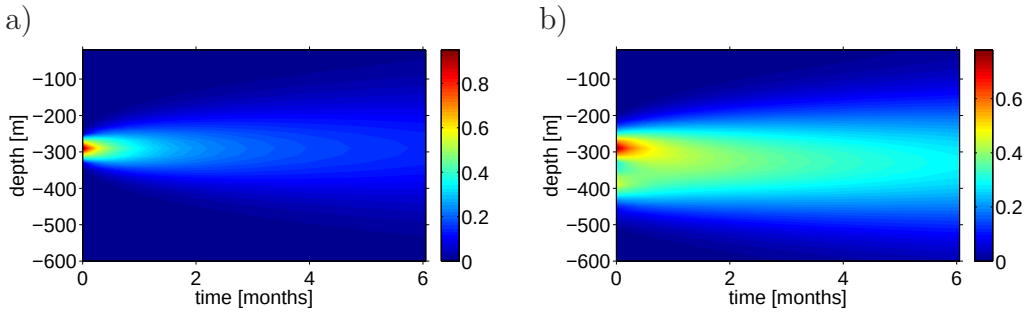

Figure 3.3: Spreading of the tracer concentration with time for experiment *A_const*, a) using the symmetric initial tracer condition and b) using the asymmetric initial tracer condition.

advection. To get more general information about the robustness of the methods, experiments using a second initial condition as shown in Figure 3.2 (dashed line) will be presented as well. The vertical structure of the second initial tracer condition is asymmetric with depth with a second weaker maximum in the tracer concentration at a depth of $350\,m$.

In order to get similar results for the experiments using the uniform and the non-uniform grid, the initial tracer condition is defined on the non-uniform grid and linearly interpolated onto the uniform grid.

3.2 Experiments with equidistant z-levels

In this section, the results of the experiments *A_const*, *A_incr*, *A_decr* and *A_oc* are shown using the equidistant depth grid in the model set-up with a level thickness of $20\,m$. The diagnostics will be divided by showing the results using the divergence and the tracer flux method first, as both methods infer from the advection-diffusion equation. Second, the results of the variance method will be presented.

To give an overview, Figure 3.3 shows the temporal evolution of the tracer field using a) the symmetric and b) the asymmetric initial tracer condition for experiment *A_const* ($\kappa_{expl} = 4cm^2/s$). The spreading of the tracer with time is similar for the other experiments with different explicit diffusion coefficients and therefore is not separately shown.

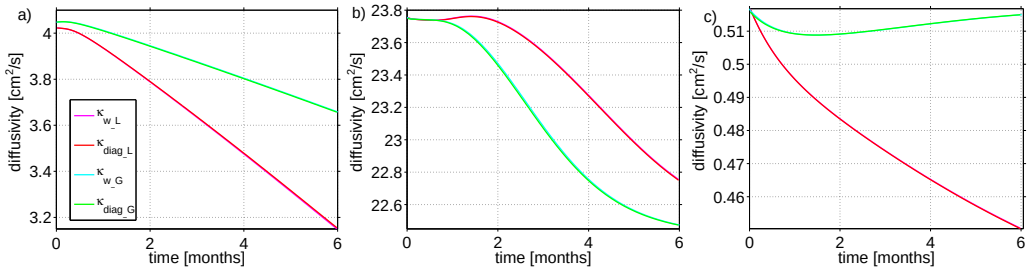

Figure 3.4: Diagnosed diffusivities κ_{diag_L} (red) and κ_{diag_G} (green) and weighted diffusivities κ_{w_L} (magenta) and κ_{w_G} (cyan) for the experiments: a) *A_incr*, b) *A_decr* and c) *A_oc* with symmetric initial tracer condition (weighted diffusion overlaid by diagnosed diffusion).

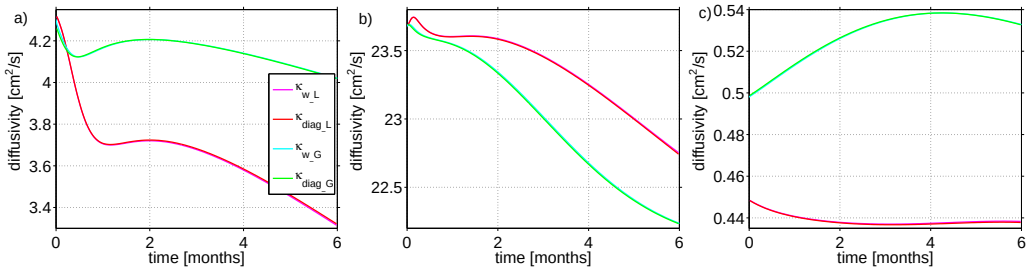

Figure 3.5: Diagnosed diffusivities κ_{diag_L} (red) and κ_{diag_G} (green) and weighted diffusivities κ_{w_L} (magenta) and κ_{w_G} (cyan) for the experiments: a) *A_incr*, b) *A_decr* and c) *A_oc* with asymmetric initial tracer condition (weighted diffusion overlaid by diagnosed diffusion).

3.2.1 Results of the divergence and the tracer flux methods

In the experiments shown in this section there is only vertical diffusion acting on the tracer. As the divergence and the tracer flux methods are discretised in exactly the same way as done in the model set-up, there is no numerically induced diffusion expected in the results of the diagnosed diffusivity.

The simplest experiment for both initial tracer conditions is experiment *A_const*, where the explicit diffusion coefficient is constant with depth and with time. As expected, the diagnosed diffusivities κ_{diag_L} and κ_{diag_G} and weighted diffusivity κ_{w_L} and κ_{w_G} reflect the exact value of $4\,cm^2/s$ of the homogeneous explicit diffusion coefficient.

Figure 3.4 shows the results for the diagnosed diffusivities κ_{diag_L} (red) and

κ_{diag_G} (green) and for the weighted diffusivities κ_{w_L} (magenta) and κ_{w_G} (cyan) for the experiments A_incr (a), A_decr (b) and A_oc (c), using the symmetric initial tracer condition. This allows a direct comparison between the results of the weighted and the diagnosed diffusivities as well as a comparison between the divergence and the tracer flux method.

For both methods and also for all three experiments, the weighted and the diagnosed diffusivity within one method give almost identical results. This means that the tracer-based methods of diagnosing diapycnal diffusion are not sensitive to the vertical structure of the explicit diffusion coefficient.

A comparison of the diffusivities analysed by the divergence method with the ones analysed by the tracer flux method show substantial differences in the results. Although, the results of both methods decrease with time e.g. in experiment A_incr (Figure 3.4 a), the temporal development is different: κ_{diag_G} decreases with a quicker rate in comparison to κ_{diag_L}. The results of experiment A_decr show the opposite behaviour, where κ_{diag_L} decreases with a quicker rate than κ_{diag_G}. In experiment A_oc, the results for both methods also differ, whereas κ_{diag_G} decreases monotonically, the values of κ_{diag_L} slowly increase after the second month.

Figure 3.5 shows the results of the experiments, A_incr, A_decr and A_oc, where the asymmetric initial tracer condition is used. Again, the results for the diagnosed diffusivity and the weighted diffusivity within one method are consistent. A comparison of the results estimated by the divergence method with the ones estimated by the tracer flux method shows again significant differences in the temporal development.

In summary, both methods can be used for the analysis of diapycnal diffusion. As the weighting over the tracer cloud is different, the results estimated by the divergence method are not consistent with the ones estimated by the tracer flux method. Furthermore, the methods are robust with respect to a depth dependent explicit diffusion coefficient and to the initial tracer condition used.

3.2.2 Results of the variance method

In this section, the analysis of the experiments *A_const*, *A_incr*, *A_decr* and *A_oc* is repeated for both initial tracer conditions using the variance method. Figure 3.6 shows the results for the diagnosed diffusivity κ_{var} (green) and the weighted diffusivity κ_w (blue) for experiment *A_const*, when the symmetric initial tracer condition is used. The weighted diffusivity κ_w is identical to the constant value of $4\,cm^2/s$ of the explicit diffusion coefficient. The diagnosed diffusivity κ_{var} on the other hand shows a $\sim 5\%$ higher value at the beginning and a strong convergence towards the expected value of $4\,cm^2/s$ afterwards.

In contrast to the results of the divergence and the tracer flux method, there is a numerically induced diffusivity in the results of the variance method. This induced diffusivity is a result of the discretisation of the tracer concentration on the vertical model grid and will be discussed in more detail at the end of this section.

A similar behaviour can be seen for experiment *A_incr*, shown in Figure 3.7. The initial difference between the diagnosed diffusivity κ_{var} and the weighted diffusivity κ_w is again about 5%. During the first month the diagnosed diffusivity is strongly converging towards the values of the weighted diffusivity and afterwards the differences are smaller than 1%.

The results of experiment *A_decr* show an even higher difference between κ_{var} and κ_w of $\sim 20\%$ and also a stronger decrease of κ_{var} during the first half of the first month (see also Figure 3.8). After that the difference between κ_{var} and κ_w is again smaller than 1%.

The behaviour of the diagnosed diffusivity κ_{var} in relation to the weighted diffusivity κ_w in experiment *A_oc* is slightly different (Figure 3.9). Note, the explicit diffusion coefficient in this experiment is much smaller compared to the ones used in the previously shown experiments. The diagnosed diffusivity κ_{var} is only $\sim 1\%$ larger than the weighted diffusivity κ_w at the beginning and decreases slowly towards the values of κ_w at a relatively constant rate.

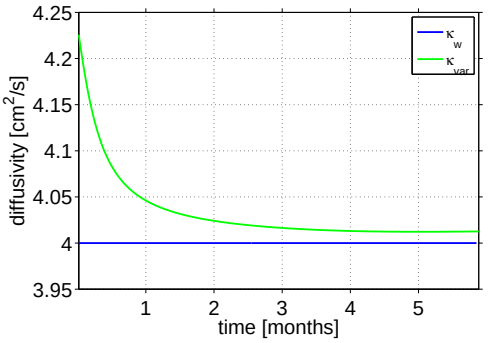

Figure 3.6: κ_{var} (green) and κ_w (blue) with time for experiment *A_const* (symmetric initial tracer condition).

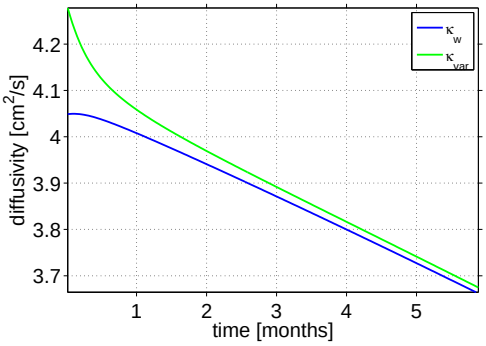

Figure 3.7: κ_{var} (green) and κ_w (blue) with time for experiment *A_incr* (symmetric initial tracer condition).

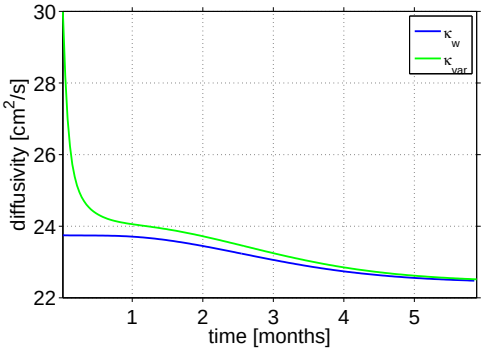

Figure 3.8: κ_{var} (green) and κ_w (blue) with time for experiment *A_decr* (symmetric initial tracer condition).

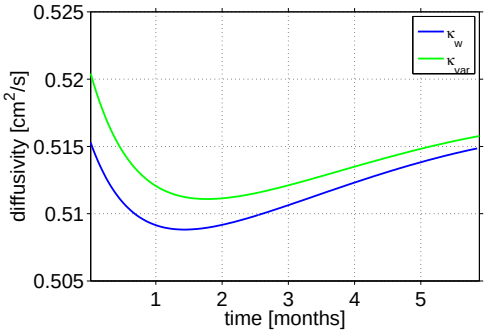

Figure 3.9: κ_{var} (green) and κ_w (blue) with time for experiment *A_oc* (symmetric initial tracer condition).

Using the symmetric initial tracer condition, all experiments show differences between the results of the diagnosed diffusivity κ_{var} and the weighted diffusivity κ_w. Using the asymmetric initial tracer condition, the results (see Figure 3.10 - 3.13) show a smaller difference between κ_{var} and κ_w compared to the analogous experiments using the symmetric initial tracer condition.

Figure 3.10 shows the results for κ_{var} and κ_w of experiment *A_const*. The diagnosed diffusivity κ_{var} at the beginning of the experiment is $\sim 4\%$ larger compared to the weighted diffusivity κ_w. During the first month κ_{var} decreases quickly towards the values of κ_w. In comparison with the

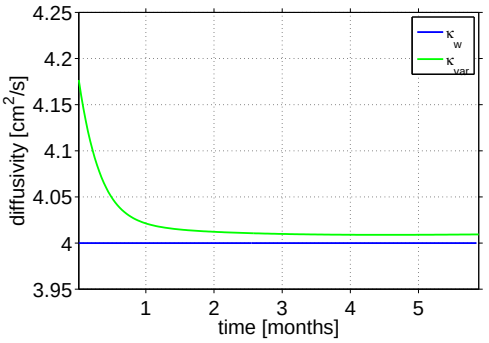

Figure 3.10: κ_{var} (green) and κ_w (blue) with time for experiment A_const (asymmetric initial tracer condition).

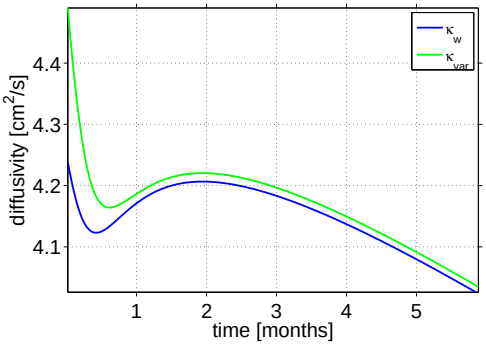

Figure 3.11: κ_{var} (green) and κ_w (blue) with time for experiment A_incr (asymmetric initial tracer condition).

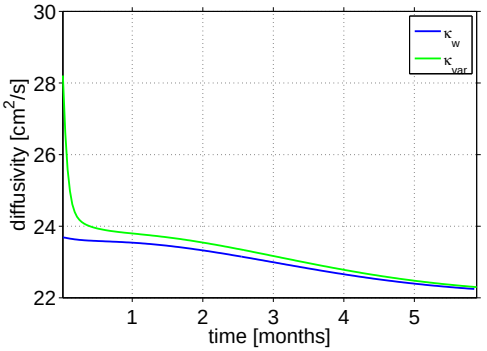

Figure 3.12: κ_{var} (green) and κ_w (blue) with time for experiment A_decr (asymmetric initial tracer condition).

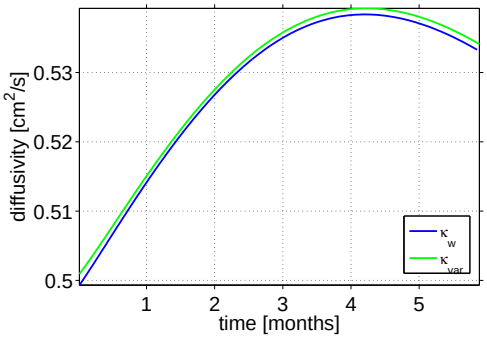

Figure 3.13: κ_{var} (green) and κ_w (blue) with time for experiment A_oc (asymmetric initial tracer condition).

analogous experiment in which the symmetric initial tracer condition is used, there is less induced diffusivity when the asymmetric initial tracer condition is used.

A similar change can be found in experiment A_incr (see Figure 3.11). Again, κ_{var} is $\sim 4\%$ lager than κ_w and after the first month the differences are very small.

Figure 3.12 shows the results for experiment A_decr. The diagnosed diffusivity κ_{var} at the beginning is $\sim 16\%$ larger than κ_w; compared to $\sim 20\%$ in the analogous experiment in which the symmetric initial tracer condition is used. The rapid decrease of the induced diffusivity occurs in

less than half a month and the remaining difference between κ_{var} and κ_w is very small ($<< 1\%$).

Finally the results of experiment *A_oc* are shown in Figure 3.13. There is no significant difference between the diagnosed diffusivity κ_{var} and the weighted diffusivity κ_w during the whole experiment.

The results of the variance method show an induced diffusivity which is not resolved in the results of the divergence and the tracer flux methods. The diagnosed diffusivities analysed by the divergence or the tracer flux method must give the same results compared to the weighted diffusivity, as the fluxes used for the analysis are defined in exactly the same way, as it is done in the model set-up.

In the analytical tracer field the explicit vertical diffusion does not lead to an induced diffusivity in the results of κ_{var}. The explicit diffusion in the model used is implemented with a Eulerian backwards time stepping scheme. This scheme does not conserve the variance and leads in the analysis of the diagnosed diffusivity κ_{var} to an induced diffusion. This effect can be reduced by decreasing the time-step of the model. To give an example, decreasing the time-step by a factor of 5 (1/5 day) leads to an induced diffusivity of only $\sim 1\%$ in κ_{var} at the beginning of the experiment. This is five times smaller compared to the induced diffusivity previously shown. Further reductions of the time-step lead to an even smaller induced diffusivity.

The results show that these effects are pronounced when there is a strong tracer gradient, as it is the case in the beginning of the experiments. These effects are also strong in regions where the explicit diffusion coefficient is large. If the explicit diffusion coefficient is small, as e.g. in experiment *A_oc*, the induced diffusivity is also small, as the changes in the discrete vertical profile of the tracer are small. Additionally, a weaker tracer gradient, as is used for the asymmetric initial tracer condition, results in lower values of the induced diffusivity.

3.3 Experiments with non-equidistant z-levels

Traditionally, most of the OGCMs are set-up with non-equidistant depth-levels in order to better resolve the near-surface layers and the thermocline at low computational costs. In the following, all the experiments shown above for the equidistant depth-grid are repeated with non-equidistant depth-grid in the model set-up instead. Only results for the cases in which the symmetric initial tracer condition is used will be discussed, as the asymmetric initial tracer condition yields similar results.

In Figure 3.14, the results for experiment *A_const* are shown. The weighted diffusivities resolving from the diagnostics of the three methods are identical to the constant value of $4\,cm^2/s$ of the explicit diffusion coefficient. Also, the diagnosed diffusivities κ_{diag_L} (red) and κ_{diag_G} (green), the results of the divergence and the tracer flux methods, are both consistent with the constant explicit diffusion coefficient. Note, as the values for κ_{diag_L}, κ_{w_L}, κ_{diag_G}, κ_{w_G} and κ_w are all the same, the blue line of κ_w overlays the other ones in Figure 3.14. The diagnosed diffusivity κ_{var} (black) analysed by the variance method show a similar behaviour compared to the analogous experiments with equidistant grid, only at the beginning of the experiment the induced diffusion is slightly smaller.

Also the results of experiment *A_incr* (Figure 3.15) show similar results compared to the ones of the analogous experiments with equidistant grid. The diagnosed and the weighted diffusivity analysed by the divergence method show almost identical results, the same can be found for the results of the tracer flux method. Note, in Figure 3.15 the diagnosed diffusivity κ_{diag_G} (green) and the weighted diffusivity κ_{w_G} (cyan) have the same behaviour as the weighted diffusivity κ_w (blue), and therefore κ_{diag_G} and κ_{w_G} can not be seen separately. The same effect can be seen in the figures of the next two experiments.

The results of the weighted diffusivity κ_w analysed by the variance method is, as expected, consistent with the results of the tracer flux method. The

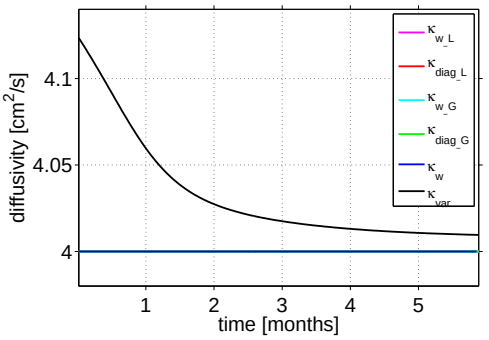

Figure 3.14: Diagnosed and weighted diffusivities for all methods for experiment *A_const* with non-equidistant z-levels (κ_{diag_L}, κ_{w_L}, κ_{diag_G}, κ_{w_G}, κ_w equal to $4\,cm^2/s$).

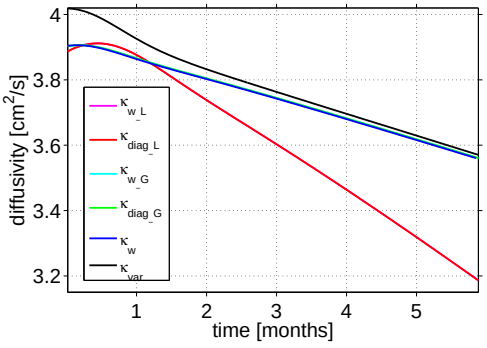

Figure 3.15: Diagnosed and weighted diffusivities for all methods for experiment *A_incr* with non-equidistant z-levels ($\kappa_{diag\_L} = \kappa_{w\_L}$ and $\kappa_{diag\_G} = \kappa_{w\_G} = \kappa_w$).

diagnosed diffusivity κ_{var} on the other hand shows numerically induced diffusion at the beginning of the experiment which decreases afterwards, when κ_{var} converges towards the values of κ_w.

Note, the results using the non-equidistant depth grid are not exactly the same compared to the analogous experiments with the equidistant z-grid. The difference between both experiments is, however, small and and can be ascribed to small differences in the definition of the initial tracer condition used.

Similar results can be found for experiment *A_decr* (Figure 3.16). The results analysed by the divergence or the tracer flux method show almost identical results for the weighted and the diagnosed diffusivities. The weighted diffusivity κ_w, analysed by the variance method, is consistent with the results κ_{diag_G} and κ_{w_G}, as seen in the previous experiments. The diagnosed diffusivity κ_{var} show similar results as the ones of the analogous experiments with equidistant z-levels, with a strong convergence towards the value of κ_w.

Also in the last experiment, *A_oc* (Figure 3.17), the results for the three methods are consistent with the ones of the analogous experiments with equidistant z-grid.

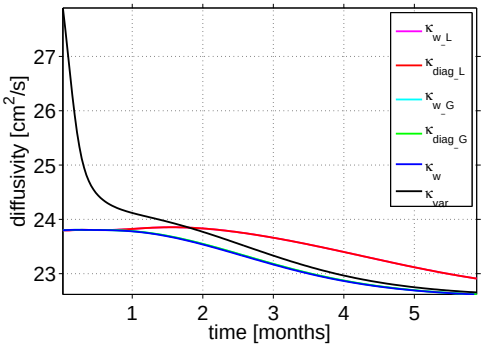

Figure 3.16: Diagnosed and weighted diffusivity using all methods for experiment *A_decr* using non-equidistant z-levels ($\kappa_{diag\_L} = \kappa_{w\_L}$ and $\kappa_{diag\_G} = \kappa_{w\_G} = \kappa_w$).

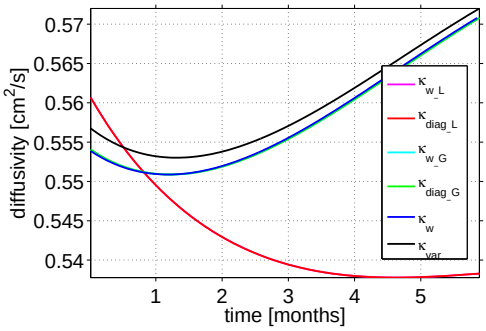

Figure 3.17: Diagnosed and weighted diffusivity using all three methods for experiment *A_oc* using non-equidistant z-levels ($\kappa_{diag\_L} = \kappa_{w\_L}$ and $\kappa_{diag\_G} = \kappa_{w\_G} = \kappa_w$).

In summary it can be said, that the analysis of the divergence and the tracer flux methods is robust with respect to the resolution of the vertical model grid. In consequence of the derivation of these two methods there is no induced diffusivity, as the discretisation of the terms for the diagnosed diffusivity is exactly the same as used for the discetisation of the model. The results of the diagnosed diffusivity analysed by the variance method show a slightly smaller amount of induced diffusion, which can be ascribed to the slight differences in the initial tracer conditions used for the experiments with equidistant z-levels.

3.4 Summary

In these simple 1-dimensional experiments, where diffusion acts on the tracer only, it is possible to use the method described by the observational study of e.g. Ledwell et al. (1998), referred to as divergence method in this study. The diagnosed diffusivity κ_{diag_L} analysed by this method is determined by the discretisation of the temporal derivative and the curvature of the tracer, which is done in exactly the same way as for the discretisation of the explicit diffusion in the model set-up.

Additionally, it is possible to weight the explicit diffusion coefficient in such a way that the difference between the diagnosed diffusivity κ_{diag_L} and the weighted diffusivity κ_{w_L} is the numerically induced diffusivity. In these simple cases, the results for the diagnosed and the weighted diffusivitiy are almost identical, independent of the vertical structure of the explicit diffusion coefficient and the initial tracer condition used and also independent of the z-grid used in the model.

Similar to the approach used in the divergence method, the tracer flux method infers from the cumulative integral of the advection-diffusion equation, similar to the idea of Griffies et al. (2000). The cumulative integral of the advection-diffusion equation says that the change of the total amount of tracer mass above one level is equal to the tracer flux through that level. Similar to the results of the divergence method, the diagnosed diffusivity κ_{diag_G} and the weighted diffusivity κ_{w_G} analysed by the tracer flux method show consistent results independent of the vertical structure of the explicit diffusion coefficient, the initial tracer condition used and the vertical structure of the model grid.

A comparison between the results analysed by the divergence method to the ones analysed by the tracer flux method shows that, although the weighted and the diagnosed diffusivities within each method are consistent, the results for both methods differ. These differences between the methods can be ascribed to the different weighting used in the diagnostics.

The different results for the mean diffusivity of the tracer cloud are leading to the question, which one is now the "correct" diapycnal diffusivity of the tracer. The diffusivity is a value which is defined on each z-level. For an exact analysis, it would be necessary to determine the diagnosed diffusivity on each interface. As the analysis is not appropriate to resolve the vertical behaviour of the diagnosed diffusivity, it is only possible to analyse a mean value. Taking the mean of a depth depending parameter can always be done in different ways; in general it cannot be reduced to only one correct weighting. For the information about the values for the mean diffusivity itself it always has to be taken into account by which weighting the mean values are estimated. For this study, it is of minor interest which weighting

will be used. The important information is the difference between the diagnosed diffusivity and the weighted diffusivity, as this will give evidence about the numerically induced diffusivity. The results show that for this comparison both methods are suitable, at least in the simple experiments just presented.

A more objective analysis is shown by the diagnostics of the variance method, based on the work described by Morales Maqueda and Holloway (2006). In this case the decay of the total tracer variance is estimated and linked to a vertical mean value of the diagnosed diffusivity, which is an analysis independent of the diffusion scheme used.

The diffusion is discretised by a centred differences scheme and implemented into the model as a Eulerian backward time stepping scheme. This time stepping scheme does not conserve the variance and leads to a small amount of induced diffusion in the results of the diagnosed diffusivity κ_{var}, $5 - 1\%$ in the cases shown. A decrease of the time-step leads to a reduction of the numerically induced diffusion. For the analysis of OGCMs, this is of minor importance, as the time-step used is generally chosen to be so small that this effect can be neglected.

Chapter 4

Transformation onto isopycnals

In OGCMs, both advection and diffusion do not act only on passive tracer fields, but also on the fields of temperature and salinity. The mixing in temperature and salinity leads in these cases to a temporal change of the density, which can be interpreted as a vertical movement of the isopycnal layers. In order to diagnose the diapycnal diffusivity, the tracer needs to be transformed onto isopycnal layers. Note, in experiments with more than one dimension, the mapping of the tracer onto isopycnals is also fundamental in experiments, where temperature and salinity are constant with time, in order to diagnose the diapycnal diffusivity, as the isopycnal layers are not necessarily isobaric.

In the following, the mapping scheme used for the further analysis will be introduced. Then, the methods of diagnosing diffusion will be transformed to be applicable in isopycnal coordinates. In the last section, the robustness of the three methods will be tested with respect to the sensitivity of the results according to changes in the transformation axis used.

4.1 Mapping of the tracer

In general, normal interpolation routines, such as linear, spline etc., are not tracer conserving. As the analysis using either of the methods requires tracer conservation, those normal interpolation routines cannot be used. In

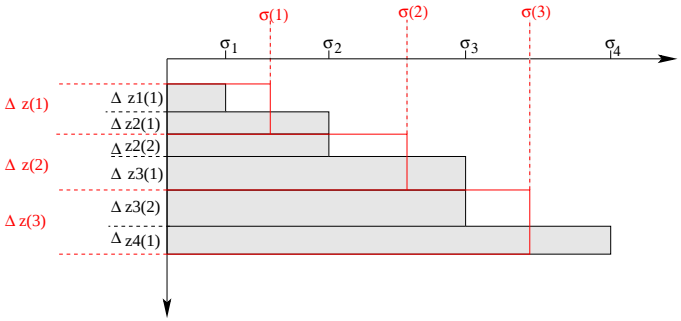

Figure 4.1: Schematics of the transformation of z-grid (red) onto the new σ-axis (black, grey shaded).

the following a discrete mapping scheme will be introduced. This mapping is the only one used for the transformation of the tracer onto isopycnal layers for all different cases shown in this study.

In the following σ_n are the pre-defines isopycnal levels and $\sigma(n)$ are the layers the tracer is transformed to. Figure 4.1 shows the schematics of the tansformation of the tracer concentration (original in red, transformed shaded in grey) for the easiest case in which
$\sigma_n < \sigma(n) < \sigma_{n+1} < \sigma(n+1) < \sigma_{n+2}$; the other cases will be discussed afterwards. Starting at the surface in the first grid box, the tracer has the concentration $C(1)$, the density in that box is homogenous and has a value of $\sigma(1)$ and the thickness of that box is $\Delta z(1)$.

In order to divide the tracer mass $C(1) \times \Delta z(1)$ of the first grid box onto σ_1 and σ_2, the conservation of mass gives:

$$\Delta z(1) \cdot \sigma(1) = \Delta z_1(1) \cdot \sigma_1 + \Delta z_2(1) \cdot \sigma_2$$

where $\Delta z_1(1)$ is the thickness of the tracer volume which goes into the new σ_1-box and $\Delta z_2(1)$ is the thickness of the tracer volume which goes into the new σ_2-box (for the illustration see Figure 4.1). Additionally, the thickness of the first layer is also conserved, which gives:

$$\Delta z(1) = \Delta z_1(1) + \Delta z_2(1)$$

The layer thickness Δz_t of the transformed tracer concentration is then given by

$$\Delta z_t(1) = \Sigma_n \Delta z_1(n)$$
$$\vdots$$
$$\Delta z_t(k) = \Sigma_n \Delta z_k(n), \tag{4.1}$$

where n is the number of sublayers all going into the σ_k layer and $\Delta z_t(k)$ is the thickness of the σ_k layer. In the case shown in Figure 4.1 n is always equal to 2. As the thickness of the σ-layers is known, the transformed tracermass C_m can be calculated as well, following Equation 4.1:

$$C_m(1) = \Delta z_1(1) \cdot C(1)$$
$$C_m(2) = \Delta z_2(1) \cdot C(1) + \Delta z_2(2) \cdot C(2)$$
$$\vdots$$
$$C_m(k) = \sum_n \Delta z_k(n) \cdot C(n) \tag{4.2}$$

This leads to the transformed tracer concentration C_t

$$C_t(1) = \frac{C_m(1)}{\Delta z_t(1)}$$
$$\vdots$$
$$C_t(k) = \frac{C_m(k)}{\Delta z_t(k)} \tag{4.3}$$

With this transformation, the tracer mass is conserved. The distribution of the tracer is not exactly conserved, so the mapping potentially induces diffusion. Note, the transformation of the tracer onto isopycnals using other interpolation routines, e.g. linear, spline, etc., leads to potentially induced diffusion in the results. A linear interpolation of the tracer e.g. results generally in a larger and unpredictable induced diffusivity compared to the one induced by the mapping scheme used in this study.

In the schematics of Figure 4.1 the simplest case of the transformation is shown. Figures 4.2 and 4.3 show two different schematics for the other

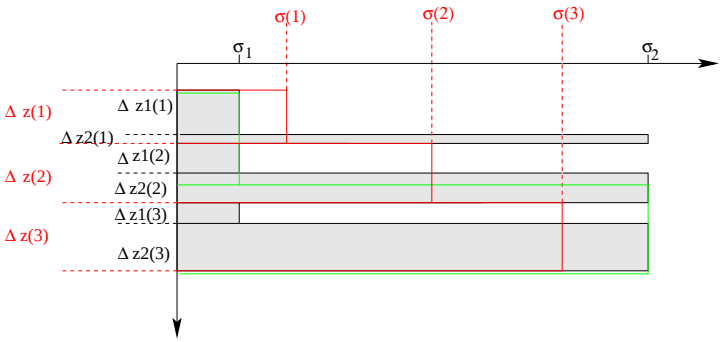

Figure 4.2: Schematics of the transformation of the z-grid (red) onto the new σ-axis (black, grey shaded). The green line shows the layer thickness after the transformation.

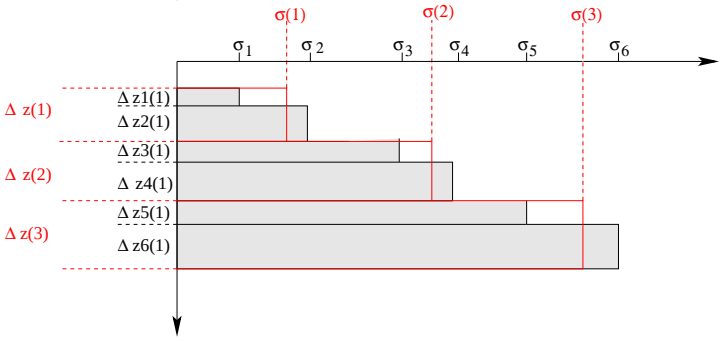

Figure 4.3: Schematics of the transformation of the z-grid (red) onto the new σ-axis (black, grey shaded).

cases occurring dependent on the number of σ-layers used for the transformation. Using about the same amount of σ-layers than there are z-levels in the model, the transformation is straight forward, as already shown in the schematics of Figure 4.1.

More generally, it is also possible that the spacing of the σ-layers of the transformation axis is coarser compared to the spacing of the density profile of the tracer, as shown in Figure 4.2. In such a case, where $\sigma_1 < \sigma(1) < \sigma(2) < \sigma(3) < \sigma_2$, the tracer concentrations of three levels $(\sigma(1-3))$ are divided into two layers (σ_{1-2}). This implies a mixing of the tracer concentration. Whereas increasing the number of layers of the transformation, the thickness of the σ-layers starts to alternate, as shown in Figure 4.3. In this case the noise in the spatial derivatives can get quite large. Increasing the number of layers of the transformation further, the transformation also results in layers with zero thickness.

4.2 Diagnosing diffusion in σ-space

It is necessary to transform the advection-diffusion equation into σ-space, the new coordinate system, for diagnosing diffusion by the divergence or the tracer flux method in experiments where the depths of the isopycnal layers change with time. For the analysis of diagnosing diffusion by the variance method it is not necessary to transform the tracer into σ-space as long as only 1-dimensional experiments are analysed. But it is useful, as a comparison between the variance decay in z-space with the variance decay in σ-coordinates gives evidence about the quality of the transformation with respect to the method used.

4.2.1 Transformation of the advection-diffusion equation onto isopycnals

The advection-diffusion-equation in z-coordinates is given by

$$\frac{\partial C}{\partial t} = \kappa \frac{\partial^2 C}{\partial z^2} - w \frac{\partial C}{\partial z},$$

where C denotes the tracer concentration, κ the vertical diffusivity, w the vertical velocity, z the depth and t the time. The diffusivity κ and the vertical velocity w are taken as depth independent, as it is done in the assumptions of the divergence and the tracer flux methods as well.

In the following, C_t denotes the transformed tracer concentration and z_t the transformed depth in σ-coordinates. The used transformation is given by

$$\frac{\partial}{\partial t}\Big|_z = \frac{\partial}{\partial t}\Big|_\sigma - \frac{\partial z_t}{\partial t}\Big|_\sigma \frac{\partial}{\partial t}\Big|_\sigma.$$

In the continuous case used here the derivatives by ∂z can be directly transformed as

$$\frac{\partial C_t}{\partial z_t} = \frac{\partial C}{\partial z}, \tag{4.4}$$

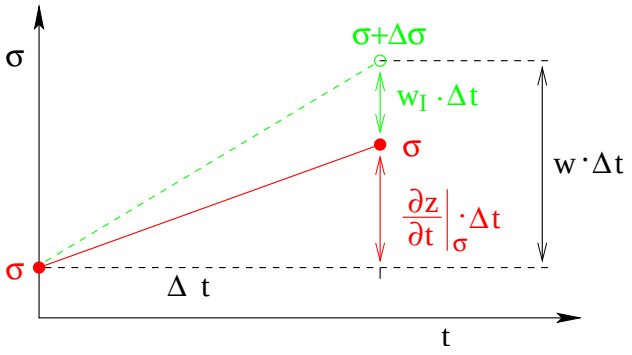

Figure 4.4: Schematics of the components of the vertical velocity of the isopycnal during one time-step Δt.

but the transformation of the temporal change of the tracer is not that easy, as

$$\frac{\partial C_t}{\partial t}\Big|_\sigma \neq \frac{\partial C_t}{\partial t}\Big|_z. \tag{4.5}$$

In order to determine the temporal derivative of the transformed tracer correctly, it is important to take into account the change of the layer thickness with time, which is given by

$$\frac{\partial C_t}{\partial t}\Big|_\sigma = \frac{\partial C}{\partial t}\Big|_z + \frac{\partial z_t}{\partial t}\Big|_\sigma \cdot \frac{\partial C_t}{\partial z_t}. \tag{4.6}$$

As the derivatives by ∂z are not affected by the transformation, the advection-diffusion equation in z-space can be written as follows

$$\frac{\partial C}{\partial t}\Big|_z = \kappa \frac{\partial^2 C_t}{\partial z_t^2} - w \frac{\partial C_t}{\partial z_t}. \tag{4.7}$$

Replacing Equation 4.7 in Equation 4.6 gives

$$\frac{\partial C_t}{\partial t}\Big|_\sigma - \frac{\partial z_t}{\partial t}\Big|_\sigma \cdot \frac{\partial C_t}{\partial z_t} = \kappa \frac{\partial^2 C_t}{\partial z_t^2} - w \frac{\partial C_t}{\partial z_t}. \tag{4.8}$$

The vertical velocity w in equation 4.8 is the total vertical change of the isopycnal layer. This includes the movement of the isopycnal layer due to advection and also due to diffusion. The schematic in Figure 4.4 illustrates the two different components of the vertical velocity w. The advective component can be written as the temporal change of depth, and the interfacial velocity w_I is the diffusive component.

$$w = \frac{\partial z_t}{\partial t}\Big|_\sigma + w_I, \tag{4.9}$$

which is equivalent to

$$\frac{\partial z_t}{\partial t}\Big|_\sigma = w - w_I. \tag{4.10}$$

Now, substituting Equation 4.10 in Equation 4.8 gives

$$\frac{\partial C_t}{\partial t}\Big|_\sigma - (w - w_I) \cdot \frac{\partial C_t}{\partial z_t} = \kappa \frac{\partial^2 C_t}{\partial z_t^2} - w \frac{\partial C_t}{\partial z_t}. \tag{4.11}$$

This can be reduced to

$$\frac{\partial C_t}{\partial t}\Big|_\sigma = \kappa \frac{\partial^2 C_t}{\partial z_t^2} - w_I \frac{\partial C_t}{\partial z_t}. \tag{4.12}$$

As ∂z_t can be written as

$$\partial z_t = \frac{\partial z_t}{\partial \sigma} \cdot \partial \sigma \qquad \rightarrow \qquad \frac{\partial}{\partial z_t} = \frac{1}{\frac{\partial z_t}{\partial \sigma}} \cdot \frac{\partial}{\partial \sigma}, \tag{4.13}$$

and replacing Equation 4.13 in Equation 4.12 gives

$$\frac{\partial z_t}{\partial \sigma}\frac{\partial C_t}{\partial t}\Big|_\sigma = \kappa \frac{\partial}{\partial \sigma}\frac{\partial C_t}{\partial z_t} - w_I \frac{\partial C_t}{\partial \sigma}. \tag{4.14}$$

This equation (4.14) can also be written as

$$\frac{\partial}{\partial t}\left(\frac{\partial z_t}{\partial \sigma} \cdot C_t\right) - \frac{\partial}{\partial t}\Big|_\sigma \left(\frac{\partial z_t}{\partial \sigma}\right) \cdot C_t = \kappa \frac{\partial}{\partial \sigma}\frac{\partial C_t}{\partial z_t} - \frac{\partial}{\partial \sigma}\left(w_I C_t\right) + \frac{\partial w_I}{\partial \sigma} C_t. \tag{4.15}$$

As the temporal derivative is taken at a constant density σ, the second term on the left hand side in Equation 4.15 can be written as

$$\frac{\partial}{\partial t}\Big|_\sigma \left(\frac{\partial z_t}{\partial \sigma}\right) = \frac{\partial}{\partial \sigma}\left(\frac{\partial z_t}{\partial t}\right) = \frac{\partial}{\partial \sigma}\left(w - w_I\right) \tag{4.16}$$

according to Equation 4.10. Now, substituting Equation 4.16 in Equation 4.15 gives

$$\frac{\partial}{\partial t}\left(\frac{\partial z_t}{\partial \sigma}\cdot C_t\right) - \frac{\partial w}{\partial \sigma}\cdot C_t = \kappa \frac{\partial}{\partial \sigma}\frac{\partial C_t}{\partial z_t} - \frac{\partial}{\partial \sigma}\left(w_I C_t\right) \tag{4.17}$$

The change of the vertical velocity with σ is given by $\partial w/\partial \sigma$. As one of the properties of water is its incompressibility, any value of this term different from zero means that there must be an along isopycnal transport. In the analysis of the 1-dimensional experiments, this term must be equal to zero, as in one dimension, there is no along isopycnal flow possible. This leaves the transformed advection-diffusion equation in σ-space, as follows

$$\frac{\partial}{\partial t}\left(\frac{\partial z_t}{\partial \sigma}\cdot C_t\right) = \kappa \frac{\partial}{\partial \sigma}\frac{\partial C_t}{\partial z_t} - \frac{\partial}{\partial \sigma}\left(w_I C_t\right). \tag{4.18}$$

Equation 4.18 needs to be discretised in order to diagnose the diffusion in the model. Therefore we define

$$C_m = \frac{\Delta z_t \cdot C_t}{\Delta \sigma} \tag{4.19}$$

and the tracer gradient

$$C_{grad} = \frac{\Delta C_t}{\Delta z_t}. \tag{4.20}$$

The transformed advection-diffusion equation is given in its discretised form as follows

$$\frac{\Delta C_m}{\Delta t} = \kappa \frac{\Delta C_{grad}}{\Delta \sigma} - \frac{\Delta\left(w_I C_t\right)}{\Delta \sigma} \tag{4.21}$$

For the analysis of the diagnosed diffusion by the divergence and the tracer flux method, both methods do not support the information to analyse a depth dependent interfacial velocity w_I. Similar to the diagnostics of the mean values of κ, Equation 4.21 is solved by the method of the least squares fit and this method is only able to analyse a mean value of w_I.

For the analysis of the diagnosed diffusivity κ_{diag_G}, the cumulative integral of the advection-diffusion equation is used. For the transformed case the cumulative integral of Equation 4.21 gives

$$\sum_{s_1=1}^{s} \frac{\Delta \left(C_{t,s_1} \cdot z_{t,s_1} \right)}{\Delta t} = \kappa \frac{\Delta C_{t,s}}{\Delta z_{t,s}}\Big|_{s+1} - w_I C_{t,s}\Big|_{s+1}, \tag{4.22}$$

where the sum is taken between the first and the density layer s. The form of the integrated advection-diffusion equation in σ-coordinates is very similar to the form of the same equation in z-coordinates. The main difference is that in σ-space, the vertical velocity is reduced to the interfacial velocity w_I. This interfacial velocity is only non-zero in cases, where the isopycnals are moving due to diffusion in temperature and salinity.

4.2.2 Change in the diagnostics

The main changes in the diagnostics occur in the divergence and in the tracer flux methods. These changes infer from the different advection-diffusion equation in σ-layers. The methods are the same, as again the method of the least squares fit is used for the analysis of the diagnosed diffusivity and the diagnosed interfacial velocity. Therefore, the procedure of solving Equation 4.18 and 4.22 will not be shown in more detail.

The interfacial velocity differs only from zero in the cases, where diffusion acts on temperature and salinity. In the cases, where diffusion acts on the tracer only, the interfacial velocity is zero. Therefore, the results of the least squares fit for these cases are shown for the divergence and the tracer flux methods. Note, using the method of the least squares fit in σ-coordinates means that the sum has to be taken over the density layers.

The diagnosed diffusivity $\kappa_{diag\_L,\sigma}$ estimated by the divergence method is given by

$$\kappa_{diag\_L,\sigma} = \frac{\sum_{s=1}^{n} \left(\frac{\Delta C_{m,s}}{\Delta t} \cdot \frac{\Delta C_{grad,s}}{\Delta \sigma_s} \Delta \sigma_s \right)}{\sum_{s=1}^{n} \left(\frac{\Delta C_{grad,s}}{\Delta \sigma_s} \right)^2 \Delta \sigma_s}, \tag{4.23}$$

where C_t is the transformed tracer, C_m as defined in Equation 4.19, C_{grad} the tracer gradient (see Equation 4.20), $\Delta\sigma$ the difference between the density classes, t the time and n the number of layers used for the transformation. The sum is taken over all density classes. The diagnosed diffusivity $\kappa_{diag\_G,\sigma}$ estimated by the tracer flux method is given by

$$\kappa_{diag\_G,\sigma} = \frac{\sum_{s=1}^{n} \left(\left. \frac{\Delta C_t}{\Delta z_t} \right|_{s+1} \cdot \sum_{s_1=1}^{s} \left(\frac{\Delta \left(C_{t,s_1} \cdot \Delta z_{t,s_1} \right)}{\Delta t} \right) \cdot \Delta \sigma_s \right)}{\sum_{s=1}^{n} \left(\left. \frac{\Delta C_t}{\Delta z_t} \right|_{s+1} \right)^2 \Delta \sigma_s}, \tag{4.24}$$

where n is the number of the density classes. In the following experiments, it is always necessary to transform the tracer onto isopycnals, therefore the notation of the diagnosed diffusivities will be reduced to κ_{diag_L} and κ_{diag_G}. In order to be able to compare the diagnosed diffusivity with the weighted one directly, also the weighted diffusivity needs to be transformed into σ-coordinates. Therefore, the explicit diffusion coefficient needs to be transformed onto isopycnals. This is realised by a linear interpolation and the linearly interpolated explicit diffusion coefficient is denoted as $\kappa_{expl,\sigma}$. The term of the explicit diffusive flux $\kappa_{expl,\sigma} \cdot \frac{\Delta C_t}{\Delta z_t}$ is defined as F_{expl} in the following. The weighted diffusivity $\kappa_{w\_L,\sigma}$ estimated by the divergence method is given by

$$\kappa_{w\_L,\sigma} = \frac{\sum_{s=1}^{n} \left(\frac{\Delta F_{expl,s}}{\Delta z_{t,s}} \cdot \frac{\Delta C_{grad,s}}{\Delta z_{t,s}} \cdot \Delta \sigma_s \right)}{\sum_{s=1}^{n} \left(\frac{\Delta C_{grad,s}}{\Delta z_{t,s}} \right)^2 \Delta \sigma_s}. \tag{4.25}$$

Similar the weighted diffusivity $\kappa_{w\_G,\sigma}$ analysed by the tracer flux method in σ-coordinates is given by

$$\kappa_{w\_G,\sigma} = \frac{\sum_{s=1}^{n} \left(F_{expl,s} \cdot \frac{\Delta C_t}{\Delta z_t}\big|_{s+1} \cdot \Delta\sigma_s \right)}{\sum_{s=1}^{n} \left(\frac{\Delta C_t}{\Delta z_t}\big|_{s+1} \right)^2 \cdot \Delta\sigma_s}. \tag{4.26}$$

In the following, the notation of the weighted diffusivity will be also reduced to κ_{w_L} and κ_{w_G}. The sum over $\Delta\sigma$ in the denominator and the numerator in the definitions of the weighted and the diagnosed diffusivities can be interpreted as a weighting of the mean values by the grid of the transformation axis used. In the following the grid is chosen to be equidistant for most of the times.

For the diagnostics of the variance method in 1-dimensional experiments, it is not necessary to transform the tracer onto isopycnals before analysing the diagnosed diffusivity κ_{var}. The variance of the tracer is a depth independent value and as long as the experiments are reduced to one dimension, the tracer does not have to be transformed onto isopycnals.

Nevertheless, it is an interesting aspect how the mapping of the tracer affects the diagnostics of the tracer variance. Therefore, a comparison between the diagnostics of the diffusivity κ_{var} in z -levels and in σ-layers will be included in the following.

4.3 Sensitivity study: variation of the density layers

In the schematics of the tracer transformation in Section 4.1 three different cases are described, which can occur using the introduced way of the tracer mapping. Therefore, it is useful to analyse the influence of the chosen transformation on the results of the diagnosed diffusivities.

The results of Chapter 3 show that only in the experiment in which (i) the explicit diffusion coefficient is constant ($4\,cm^2/s$), (ii) diffusion acts on the tracer only and (iii) the density is stationary, the results for the divergence and the tracer flux methods should be identical. Additionally, there is no numerically induced diffusion in this experiment. This means, differences in

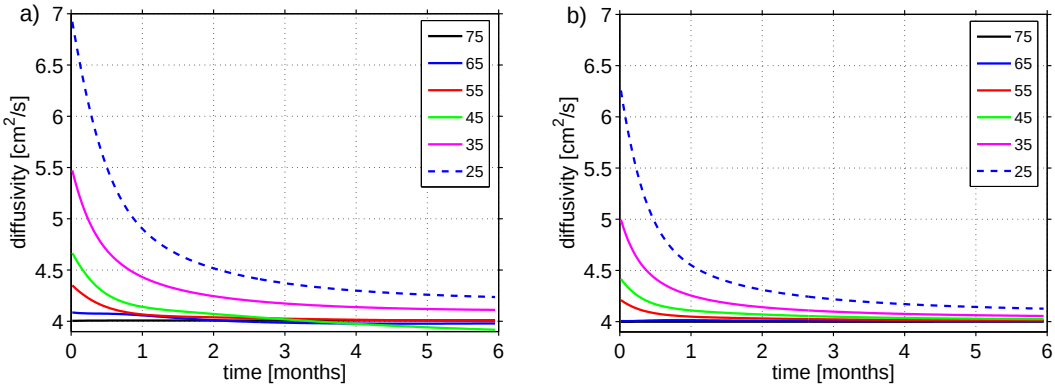

Figure 4.5: Variation of the transformation axis (25 - 75 equidistant σ-levels), a) using the divergence method (κ_{diag_L}) and b) using the tracer flux method (κ_{diag_G}).

the values of the diagnosed diffusivities κ_{diag_G} and κ_{diag_L} to the expected value of $4\,cm^2/s$ are caused by the mapping of the tracer onto isopycnals only.

In the following, two different cases are shown: first, the number of density layers is smaller than in the original model grid and second, the transformation contains more layers than model levels. The used transformation axis always covers the complete density range of the model and is divided into equidistant $\Delta\sigma$. The model used for this experiment has got 75 equidistant z-levels with a thickness of $20\,m$.

Figure 4.5 shows the results for the diagnosed diffusivities κ_{diag_L} (a) and κ_{diag_G} (b) using a smaller number of density layers than z-levels for the transformation. In these cases, the transformation is similar as shown in the schematics of Figure 4.2.

The results show that independent of the method used, the diagnosed diffusivity mainly reacts to the changes in the resolution of the transformation during the first month. This can be ascribed to the relatively narrow tracer distribution close to the beginning of the experiment, which is not necessarily resolved by the transformation axis used. A decrease in the resolution of the transformation results in an overestimation of the diagnosed diffusivities.

Although the main behaviour in Figure 4.5 a) and b) is the same, there are

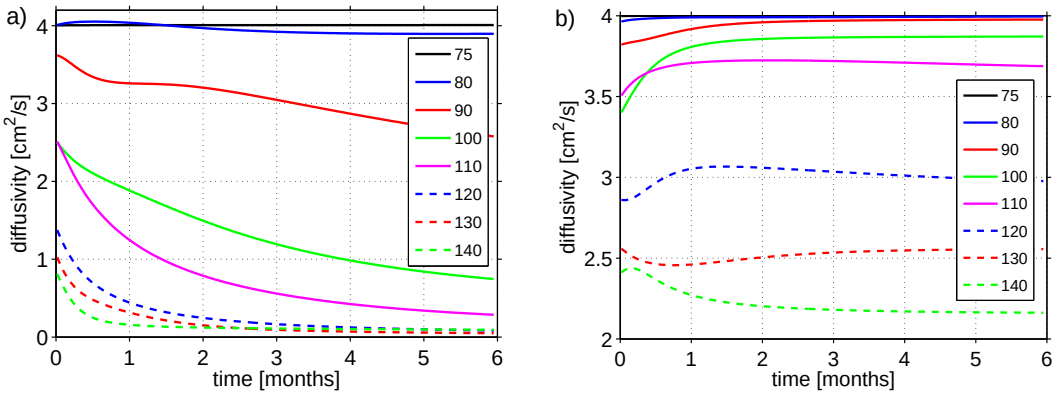

Figure 4.6: Variation of the transformation axis (75 - 140 equidistant σ-levels), a) using the divergence method (κ_{diag_L}) and b) using the tracer flux method (κ_{diag_G}).

some differences in the results of the two different methods. Using the divergence method, the results are more sensitive to the number of density layers used for the mapping. The values of the diagnosed diffusivity κ_{diag_L} are higher compared to the analogous results using the tracer flux method. Additionally, the diagnosed diffusivity κ_{diag_L} is in some cases underestimating the expected constant value of $4\,cm^2/s$, whereas the results of κ_{diag_G} seem to converge towards the level of $4\,cm^2/s$.

Figure 4.6 shows the results for the other case (a, results of the divergence and b, of the tracer flux method), where the number of the density layers used for the mapping are higher than the number of model levels (see also the schematics in Figure 4.3). In these cases, the influence of the used transformation profile and also the difference between the used methods increase.

Using the divergence method, only the cases using 75 and 80 layers for the transformation lead to results close to the expected value. Increasing the number of layers used for the mapping leads to a quick decrease in the diagnosed diffusivity. This can be explained by the effect, that using more layers for the transformation than z-levels, the transformed thickness of the new layers vary strongly. This leads to a very noisy signal in the derivatives, as in some layers the transformed layer thickness is zero or close to zero.

On the other hand, the tracer flux method uses the cumulative sum of the

temporal derivative of the tracer, which is less noisy. But, also in Figure 4.6 b), the diagnosed diffusivity decreases with an increase of the number of layers used for the transformation.

The effect of the decrease in the values of κ_{diag_G} as a result of an increase in the resolution of the transformation can be explained by the definition of κ_{diag_G}, which is given in Equation 4.24 and its discrete form is

$$\kappa_{diag\_G} = \frac{\sum_{s=1}^{n} \left(\frac{\Delta C_t}{\Delta z_t}\Big|_{s+1} \cdot \sum_{s_1=1}^{s} \left(\frac{\Delta (C_t \cdot \Delta z_t)}{\Delta t} \right) \cdot \Delta \sigma_s \right)}{\sum_{s=1}^{n} \left(\left(\frac{\Delta C_t}{\Delta z_t}\Big|_{s+1} \right)^2 \cdot \Delta \sigma_s \right)},$$

where n is the number of layers used for the transformation. Increasing the number of layers used for the transformation mainly has an impact on the gradient of the transformed tracer $\Delta C_t / \Delta z_t|_{s+1}$. The high vertical variation of the tracer concentration and the thickness of the layers do not lead to large variations in the cumulative sum $\sum_{s_1=1}^{s} \frac{\Delta (C_t \cdot dz_t)}{\Delta t}$. This means that the decrease of the diagnosed diffusivity is a result of spurious changes in the spatial derivative of $\Delta C_t / \Delta z_t|_{s+1}$.

As the spatial derivative of the tracer is squared in the denominator, the reduction as a result of the mapping is squared as well. This means that an increase in the number of layers used for the transformation by a factor of 2 leads to an increase of the tracer gradient by the factor of 2 in the numerator and an increase by the factor of 4 in the denominator, which results in a reduction of 2 in the diagnosed diffusivity. And indeed, Figure 4.6 shows, that an increase of the number of layers to 140 (nearly a factor of 2) gives a diagnosed diffusivity of $\sim 2.2\, cm^2/s$, which is consistent with the explanation.

A high resolution in the transformation results in layers with zero thickness which lead to a biased spatial derivative. The cumulative integral of the advection-diffusion equation describes that the change of the tracer mass above an isopycnal layer is equal to the tracer flux through that isopycnal layer. This means that in layers with zero thickness, the total change of the

tracer mass above the isopycnal is equivalent to the total change of the tracer mass above the appropriate z-level. Therefore, it is useful to define the tracer gradient on that isopycnal to be equivalent to the tracer gradient on the appropriate z-level. For layers with a non-zero thickness, the tracer gradient will be linearly interpolated onto the new σ-grid.

Using 75 equidistant layers for the mapping in combination with the linear interpolation of the tracer gradient onto isopycnals, the diagnosed diffusivity κ_{diag_G} is already consistent with the value of the explicit diffusion coefficient and stays consistent by a further increase of the resolution of the transformation. Also decreasing the number of layers to a lower amount z-levels lead to robust results for the diagnosed diffusivity; in this example, the number of layers can be decreased to the amount of 65. For the diagnostics of the tracer flux method, the transformation of the tracer gradient leads to robust results independent of the used transformation, as long as the resolution of the new grid spacing is not getting coarser than the density profiles in the z-grid.

This idea cannot be applied to the divergence method. Inferred from the advection-diffusion equation, the temporal derivative of the tracer and also its curvature need to be estimated for each layer separately. After the mapping, the temporal derivative gets zero in all those layers with a zero thickness, which is not generally the case for each experiment, but for the shown one with the constant explicit diffusion coefficient. The curvature, on the other hand, is biased by the spurious distribution as a result of the tracer mapping. Transforming only the tracer gradient linearly onto isopycnals leads to an imbalance in the advection-diffusion equation.

Although it is not necessary to transform the tracer onto isopycnals for the diagnostics of the variance method in 1-dimensional experiments, the sensitivity of the variance decay with respect to the resolution of the transformation will be analysed in the following. As a reminder, the diagnosed diffusivity κ_{var} estimated by the variance method is given in its discretised form in Equation 2.28

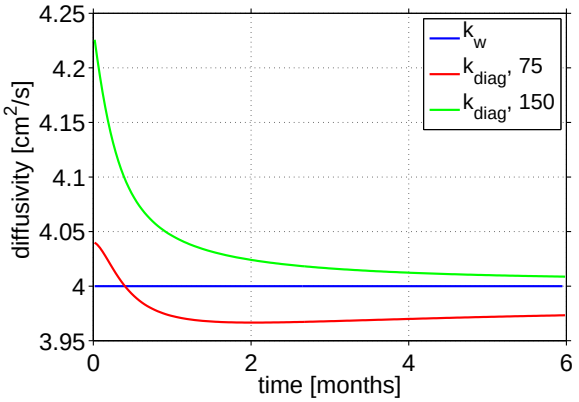

Figure 4.7: Linearly transformed tracer gradient used in the analysis of the variance method of experiment *A_const*: κ_{var} for 75 (red) and 150 (green) equidistant σ-layers, and κ_w (blue).

$$\kappa_{var} = \frac{-\frac{\Delta\sigma^2}{\Delta t}}{\sum_{k=1}^{n}\left(\left(\frac{\Delta C}{\Delta z}\right)^2 \cdot \Delta\tilde{z}_k\right)},$$

where n is the number of z-levels. The variance decay of the tracer is only affected by the mapping, if the transformation leads to a spurious mixing of differing tracer concentrations (as shown in Figure 4.1 and 4.2). Considering a high resolution in the transformation used (Figure 4.3), the variance decay $\Delta\sigma^2/\Delta t$ is not affected by the mapping at all. As the results of the divergence and the tracer flux methods already show, there is a great effect of the mapping on the spatial derivatives. Therefore, the results for the diagnosed diffusivity κ_{var} shown in the following are estimated using the linearly interpolated tracer gradient.

Figure 4.7 shows the diagnosed diffusivity κ_{var} using 75 equidistant σ-layers for the transformation (red) and twice as many layers than levels (green). Compared to the induced diffusivity shown in Section 3.2.2, using the same amount of layers as model levels, the diagnosed diffusivity κ_{var} is underestimated during the whole experimental time. Doubling the number of layers leads to consistent results to the analysis of the diagnosed diffusivity in z-space.

In summary it can be said that the results analysed by the tracer flux method are more stable according to the used transformation axis compared to the divergence method. But although they are more stable as long as the transformation is using the same amount of layers, doubling the number of

layers leads to a reduction of 50% in the values for the diagnosed diffusivity.

The linear transformation of the tracer gradient onto isopycnals leads to stable results for the tracer flux method, which are independent of the transformation axis used. Additionally, the diagnostics of the variance method also lead to stable results in the diagnosed diffusivity κ_{var}, if the resolution of the transformation axis is relatively high.

As the results of the divergence method are highly sensitive with respect to the transformation of the tracer onto isopycnals, the diagnostics in the following chapters will focus on the analysis of the tracer flux and the variance method.

Chapter 5

The role of advection

In the following, the effect of a vertical change of the density layers with time on the diagnostics of the tracer flux and the variance methods will be shown. Therefore, experiments with an implemented vertical advection and no additional explicit diffusion will be analysed. The corresponding effect of the vertical advection acting on temperature and salinity can be interpreted as a vertical movement of the isopycnals.

In general, vertical advection does not lead to an exact parallel movement of the isopycnals but also to small diverging or converging effects. However, in this chapter the easiest case is considered, where the advection generates an exact parallel movement of the isopycnals.

The vertical advection is realised in the model by using the centred differences scheme in space and an Eulerian backwards scheme in time. In order to gain some understanding of the processes by which advection affects the analysis, the discussion will be limited to a basic experiment, where the explicit vertical velocity is constant with depth and time, having a value of $4 \times 10^{-6}\, m/s \approx 0.34\, m/day$ with a downwards direction.

As already mentioned, the advection scheme used is mainly dispersive and only a small amount of numerically induced diffusion is expected. This represents the worst case scenario for the analysis, because the signal which needs to be analysed is relatively small. On the other hand this gives us the possibility to clearly analyse the effect of the parallel movement of the

isopycnals in combination with the tracer mapping on the diagnosed diffusivities. In the current chapter, the focus is on biasing effects that result from the diagnostics. In this respect, it is not necessary to compare the results of different advection schemes.

First, details about the experimental set-up are given. After that the results of the tracer flux and the variance methods will be shown in detail.

5.1 Experiment

The aim of this experiment is to create an exactly parallel movement of the isopycnal layers in the original z-level model. In this case, the divergence or convergence of the isopycnals is eliminated.

In general, the density in the model is a non-linear function depending on temperature and salinity. The corresponding effect of the advection in temperature and salinity in combination with the non-linear density equation does not necessarily lead to a parallel movement of the isopycnal layers. In order to eliminate converging and diverging effects, the density is chosen to be linearly dependent on the temperature. Additionally, the initial temperature profile is chosen to be linear. A perfect advection scheme would result in a parallel movement of the isopycnals, even for a non-linear equation of state. As the isopycnal movement is exactly parallel, the interfacial movement of the isopycnals is zero ($w_I = 0$), which is important for the diagnostics of the tracer flux method.

The temporal change of the isopycnal layers with time is shown in Figure 5.1. The model grid is chosen to be equidistant with a level thickness of $20\,m$ and the initial tracer condition is chosen to be symmetric with depth. Also for this experiment, a relatively long time-step of one day is used, where long is relative to $\frac{\Delta z}{w}$, such that $\frac{w \cdot \Delta t}{\Delta z} = 0.17$. A reduction of the time-step was found to generate an even smaller amount of numerically induced diffusion, similar as shown for the results of the variance method in Section 3.2.2. For the analysis of the robustness of the methods the effect of the time-step on the value of the results is of minor interest.

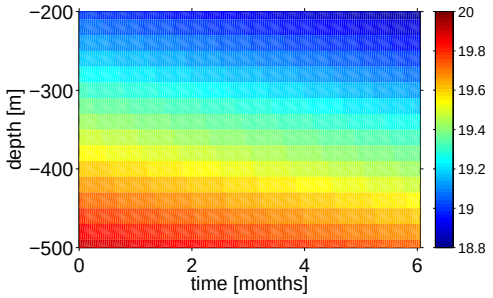

Figure 5.1: Temporal change of the density as a result of a constant vertical advection.

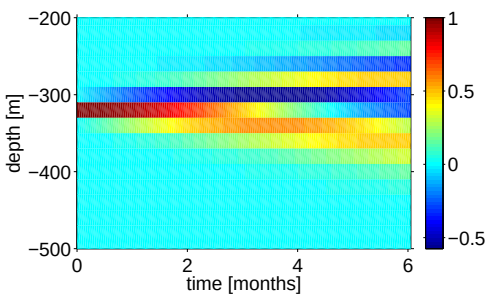

Figure 5.2: Tracer concentration with time as a result of a constant vertical advection.

Similar to the experiments shown in Chapter 3, the tracer is released at a depth of $\sim 300\,m$. The temporal development of the tracer concentration is shown in Figure 5.2, where the large effect of the dispersion generated by the advection scheme is shown. The boundary conditions in the model set-up are closed, which lead to difficulties in the density field close to the boundary (e.g. empty boxes). These effects can be neglected, as the tracer does not reach the surface or bottom boundary region.

5.2 Diagnostics using the tracer flux method

In the diagnostics of the tracer flux method, the interfacial velocity is equal to zero ($w_I = 0$), as the temporal change of the isopycnal layers occur in a parallel way. In order to stay close to the analysis of the z-level experiments in Chapter 3, the initial density profile is used as a transformation axis for the mapping of the tracer onto isopycnal layers.

Figure 5.3 shows the results for the diagnosed diffusivity κ_{diag_G} (red). Note, the transformed tracer is used for the estimate of the spatial derivatives. As there is no explicit diffusion in this experiment, the weighted explicit diffusion coefficient κ_{w_G} (blue) is zero. Surprisingly, the diagnosed diffusivity κ_{diag_G} in Figure 5.3 shows fluctuations with a frequency of about two months and an amplitude of $\pm 0.45\,cm^2/s$. These fluctuations are generated by a combination of the tracer mapping and the

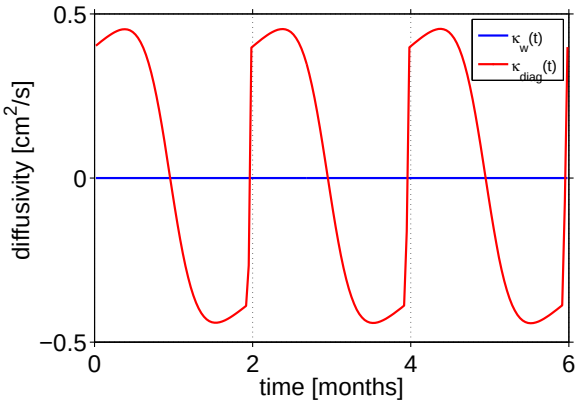

Figure 5.3: Diagnosed diffusivity κ_{diag_G} (red) using initial density profile for the mapping of the tracer; the weighted diffusivity κ_{w_G} (blue) is zero; there is no explicit diffusion in this experiment.

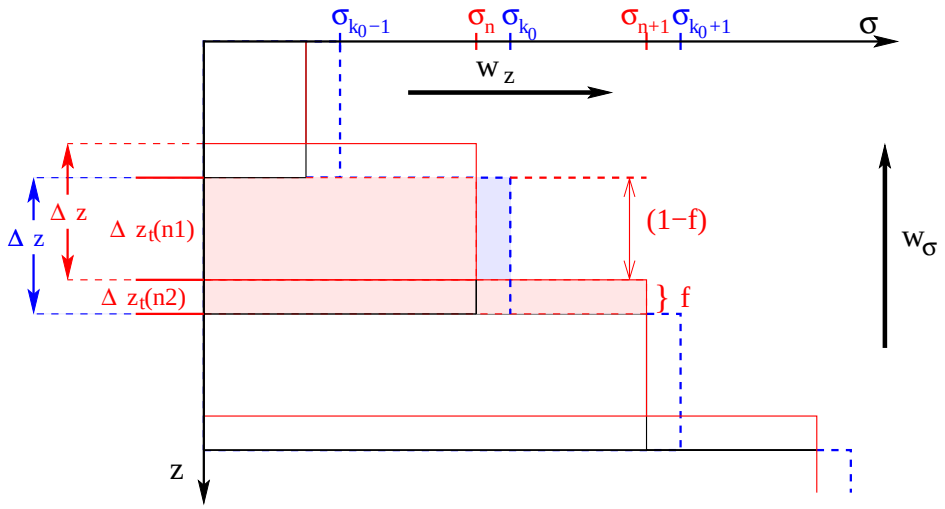

Figure 5.4: Schematics of the tracer mapping for the idealised advection. Black lines show z-grid at time t, blue dashed lines at $t + \Delta t$ and red lines show transformed grid at $t + \Delta t$. Blue shaded region is initial tracer and red shaded the transformed tracer concentration.

vertical movement of the tracer. The transformed tracer concentration needs two months to move from one σ-layer to the next considering the layer thickness of $20\,m$ and the vertical velocity of $4 \times 10^{-6}\,m/s$. Using the density profile at a different time for the mapping of the tracer onto isopycnals, the results show the same behaviour. The only difference is a time shift of the frequency.

In order to explain the combined effect of the mapping and the vertical advection on the diagnostics, we first consider only the effect of remapping the tracer as density is advected. Figure 5.4 shows the schematics of the

mapping for this idealised case. The black lines show the grid at the time-step t. The isopycnal layers σ_n move with the constant vertical velocity w_z towards greater depths. Densities at the z-levels are $\sigma_{k_0}(t)$. Initially at t=0, $\sigma_{k_0}(t) = \sigma_n$. The z-grid at time-step $t + \Delta t$ is visualised by the blue dashed lines, which is the same depth grid, as for time-step t (the black lines). As the advection is highly idealised, the tracer is completely covered by z-box k_0, which has the density σ_{k_0}, here visualised by the blue shaded box. The tracer concentration in this experiment is defined to be $C = 0$ for $k \neq k_0$ and $C = C_0$ for $k = k_0$. Since we assume tracer is not advected, these tracer values do not change as functions of z.

The mapping divides the tracer concentration into the density layers σ_n and σ_{n+1}. The thickness of the $z(k_0)$-level is defined by Δz and the tracer mass is the given by $C_0 \cdot \Delta z$. As the tracer mass is divided into σ_n and σ_{n+1}, a fraction f is defined moving into the layer σ_{n+1}. So, the fraction of the tracer mass C_0 is given by

$$C_0 \cdot \Delta z_t(n2) = f \cdot C_0 \cdot \Delta z.$$

This is the only tracer mass which is added to the layer σ_{n+1}, so the tracer mass in this layer is given by

$$C_t(n+1) \cdot \Delta z = f \cdot C_0 \cdot \Delta z. \tag{5.1}$$

As the fraction f of the tracer mass moves into σ_{n+1}, it leaves the fraction $(1 - f)$ to go into σ_n. Similar to Equation 5.1, the transformed tracer mass in layer σ_n can be written as

$$C_t(n) \cdot \Delta z = (1 - f) \cdot C_0 \cdot \Delta z. \tag{5.2}$$

In this experiment the advection has a constant velocity of w_z. As a result of the transformation, the constant velocity in z-levels is transformed into a constant velocity in σ-layers which is denoted as w_σ in Figure 5.4. The vertical velocity depends only of the rate of change of the fraction f,

$-\frac{\Delta f}{\Delta t}\Delta z = w_\sigma$, so the temporal derivative of the transformed tracer mass $C_t \cdot \Delta z$ is given by

$$\frac{\Delta \left(C_t(n) \cdot \Delta z\right)}{\Delta t} = -w_\sigma \cdot C_0. \tag{5.3}$$

$$\frac{\Delta \left(C_t(n+1) \cdot \Delta z\right)}{\Delta t} = -w_\sigma \cdot C_0. \tag{5.4}$$

There is no change in the tracer on any other layer. As a reminder, the diagnosed diffusivity κ_{diag_G} was given in Section 4.2.2, Equation 4.24, and in its discretised form

$$\kappa_{diag\_G} = \frac{-\sum_{s=1}^{n}\left(\left.\frac{\Delta C_t}{\Delta z_t}\right|_{s+1} \cdot \sum_{s_1=1}^{k}\left(\frac{\Delta (C_t \cdot \Delta z_t)}{\Delta t}\right) \cdot \Delta\sigma_s\right)}{\sum_{s=1}^{n}\left(\left(\left.\frac{\Delta C_t}{\Delta z_t}\right|_{s+1}\right)^2 \cdot \Delta\sigma_s\right)}$$

In the present idealised case, the spatial derivatives can be written as

$$\left.\frac{\Delta C_t}{\Delta z}\right|_{n} = \frac{(1-f)\cdot C_0}{\Delta z} \tag{5.5}$$

$$\left.\frac{\Delta C_t}{\Delta z}\right|_{n+1} = \frac{(1-2f)\cdot C_0}{\Delta z} \tag{5.6}$$

$$\left.\frac{\Delta C_t}{\Delta z}\right|_{n+2} = \frac{f \cdot C_0}{\Delta z} \tag{5.7}$$

That leaves for the diagnostics of κ_{diag_G} using Equation 5.3 and 5.4 to calculate the rate of change of the column-integrated tracer:

$$\kappa_{diag\_G} = \frac{-w_\sigma \cdot (1-2f)\cdot \Delta z}{(1-f)^2 + (1-2f)^2 + f^2} \tag{5.8}$$

As the vertical velocity w_σ and Δz are constant, the diagnosed diffusivity is only a function of the fraction f, which can vary between 0 and 1. The denominator of Equation 5.8 is always positive, the sign of the diagnosed

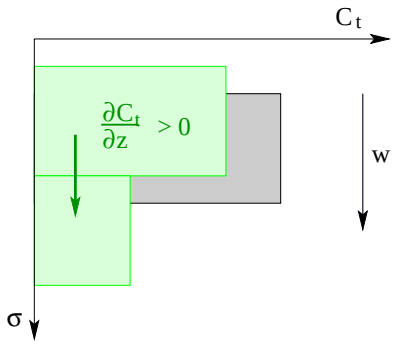

Figure 5.5: Schematics of an idealised tracer (grey) mapped onto the "new" σ-layers (green) during the first month, or generally during the first half of one wavelength.

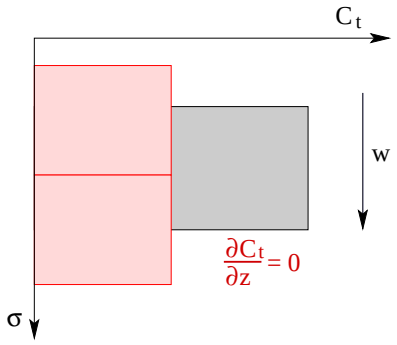

Figure 5.6: Schematics of an idealised tracer (grey) mapped onto the "new" σ-layers at the end of month one (red) , where the tracer maximum is exactly split onto two new layers.

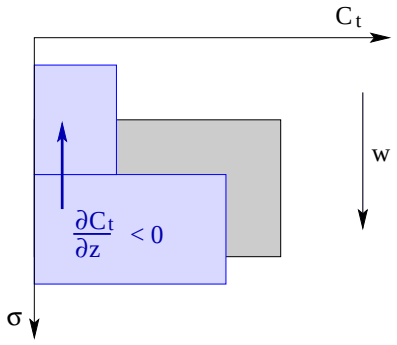

Figure 5.7: Schematics of an idealised tracer (grey) mapped onto the "new" σ-layers (blue) during the second month, or generally during the second half of one wavelength.

diffusivity κ_{diag_G} is determined by the term $(1-2f)$. This means that the values for the diagnosed diffusivity can be divided into three different cases: first, where $(1-2f)$ is positive, second, where $(1-2f)$ is equal to zero and third, where $(1-2f)$ gets negative. These cases are shown in the schematics in the Figures 5.5 - 5.7

In Figure 5.5 the grey shaded region is the tracer concentration in z-levels (before the mapping). The green shaded region is the transformed tracer concentration on the fixed σ-layers. In this case, the fraction f is always greater than 0.5, as the tracer has moved less than half of one model box.

That leaves $(1-2f) > 0$, so the diagnosed diffusivity is always positive.

In the case, where the tracer has moved exactly half of the length of one model box, its mass is divided equally into σ_n and σ_{n+1} and $f = 0.5$ (see Figure 5.6). The denominator is equal to 0.5 and as the numerator is given by $(1-2f) = 0$, the diagnosed diffusivity in this case gets zero.

In the last case (Figure 5.7), the tracer has already moved more than one half model box, so that $f > 0.5$. This means that $(1-2f) < 0$ and the diagnosed diffusivity gets negative.

This mechanism is responsible for the results of the diagnosed diffusivity κ_{diag_G} in the analysis of experiments with implemented advection. This means that the diagnosed diffusivity shown in Figure 5.3 is only a result of the combined effect of the mapping and the vertical movement, but not the result of numerically induced diffusion generated by the advection scheme used.

In Section 4.3, the sensitivity of the mapping to the spatial derivatives and the change of the results in the diagnosed diffusivity have been discussed. In the current case, where the vertical velocity is constant, the linear transformation of the tracer gradient onto isopycnals shows exactly the same dependence on the fraction f, as shown for the derivative of the transformed tracer.

$$\left.\frac{\Delta C_t}{\Delta z}\right|_{s+1} = \left.\frac{\Delta C}{\Delta z}\right|_{k} \cdot \frac{\Delta z_t(n2)}{\Delta z} + \left.\frac{\Delta C}{\Delta z}\right|_{k+1} \cdot \frac{\Delta z_t(n1)}{\Delta z}, \tag{5.9}$$

where s denotes the σ layer and k the z-level. For the idealised case without dispersion the spacial derivative in level k_0 is equal to $-C_0/\Delta z$ and in level $k_0 + 1$ equal to $C_0/\Delta z$. That leaves for the transformed derivative in σ_{n+1}, including the definition of the fraction f (see Figure 5.4)

$$\left.\frac{\Delta C_t}{\Delta z}\right|_{n+1} = -\frac{C_0}{\Delta z} \cdot \frac{f \cdot \Delta z}{\Delta z} + \frac{C_0}{\Delta z} \cdot \frac{(1-f) \cdot \Delta z}{\Delta z} = \frac{(1-2f) \cdot C_0}{\Delta z} \tag{5.10}$$

which is identical to Equation 5.6, the derivative of the transformed tracer.

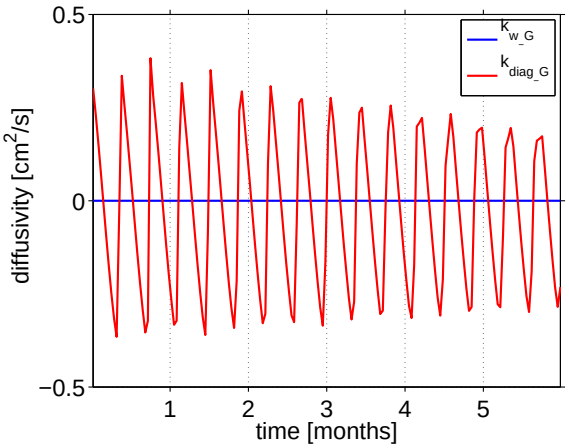

Figure 5.8: Diagnosed diffusivity κ_{diag_G} (red) using 5 times more layers than levels for the tracer mapping; the weighted diffusivity κ_{w_G} (blue) is zero.

The effect of the mapping is very large, but also a longer time mean does not give mapping invariant results for the diagnosed diffusivity κ_{diag_G}. The values of the longer time mean, e.g. a mean over one wavelength, are getting close to zero, but vary slightly from wavelength to wavelength and these values are also sensitive according to the used transformation axis. Using the initial density profile for the transformation axis, the mean of the diagnosed diffusivity κ_{diag_G} is $0.016 cm^2/s$. In Section 5.3, the diagnosed diffusivity analysed by the variance method shows that the numerically induced diffusion in this experiment is about one order of magnitude smaller ($\sim 1.7 \times 10^{-3}\, cm^2/s$).

The sensitivity study (see Section 4.3) of the mapping shows that an increase of the number of σ-layers leads to more robust results. Note, also the tracer is advected. An increase of the number of layers by the factor of e.g. 5 (as shown in Figure 5.8), does not result in a decrease of the amplitude of the spurious fluctuations in the results of the diagnosed diffusivity, but in a decrease of the mean value ($-0.03\, cm^2/s$). A further increase in the resolution of the transformation does not reduce this effect, the mean value of the diagnosed diffusivity decreases further.

The advection scheme used (centred difference in space) is very dispersive, only the implementation into the model by the Eulerian backwards time stepping scheme might result in a small amount of numerically induced diffusion. The diagnosed diffusivity associated with the transformation is larger and masks the amount of numerically induced diffusion.

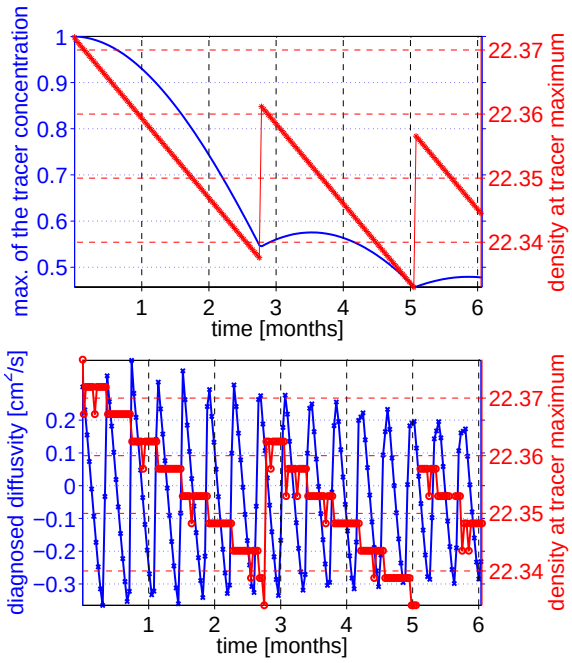

Figure 5.9: Blue: the tracer maximum as a function of time is shown; red: the density σ at the tracer maximum.

Figure 5.10: Diagnosed diffusivity κ_{diag_G} (blue) using 5 times more layers than levels for the mapping and density σ at the maximum of the transformed tracer (red).

In order to give an overview about what happens in the model, Figure 5.9 shows the maximum of the tracer concentration (blue) and the density at the tracer maximum (red). This shows how the layers move and also how the maximum concentration is affected by the vertical advection. Additionally, it shows the linearly decreasing density in the z-level boxes.

Using 5 times more layers than levels for the transformation, the frequency in the fluctuations of the diagnosed diffusivity (Figure 5.10, blue) is directly correlated to the density at the tracer maximum (red). As expected, within one wavelength the tracer maximum is located in the same σ-layer.

In the analytical case, the value of the velocity w_σ (see the schematics in Figure 5.4) should be identical to the explicit vertical velocity w_{expl} used in the advection scheme in the model. The velocity w_σ is equal to the sum of the temporal change of the fraction f and the layer thickness, as follows

$$w_\sigma = \frac{\Delta f}{\Delta t} \cdot \Delta z. \tag{5.11}$$

Using the initial density profile for the tracer mapping, the transformed layer thickness in each layer is constantly $20\,m$ and identical to the level thickness. Figure 5.11 a) shows the fraction f, which is in each layer

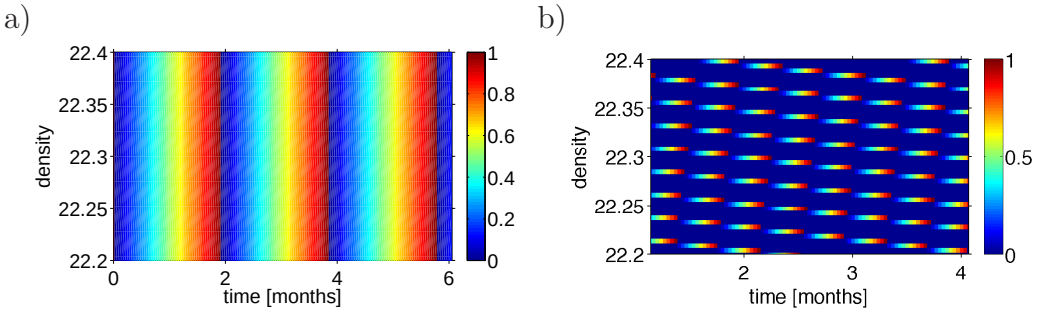

Figure 5.11: Fraction f of the transformation, a) using the initial density profile for the mapping for the mapping, b) using 5 times more layers than levels for the mapping.

constantly increasing. The rate of change of the fraction f is constant ($\partial f/\partial t = const.$). The vertical velocity in that case is also constant with depth and with time, except when f changes from 1 to 0.

An increase in the resolution of the transformation leads to changes in the fraction f. Figure 5.11 b) shows the fraction f where an equidistant transformation axis with 5 times more layers than levels is used. The changes in f do not occur simultaneously in a depth independent way. This means that the velocity w_σ is not constant with depth. Additionally, the temporal change of the fraction f, as long as staying in one layer, is not constant any longer. An increase in the resolution of the transformation leads to a temporal change in the layer thickness. The combination of these effects generates high changes in the velocity w_σ and results also in negative mean values of w_σ. This results in the diagnosed diffusivity in a small decrease of the amplitude of the fluctuations and also in a downwards shift, which leads to negative mean values.

On one hand, the diagnostics of the tracer flux method require a high resolution of the transformation used for the mapping in order to get robust results. On the other hand, the vertical advection causes spurious changes in the diagnosed diffusivity due to a high resolution of the transformation used. Therefore, it might be useful to increase the vertical resolution of the model itself.

In the following, results of experiments will be shown using the same experimental set-up, only the vertical resolution is increased to a level

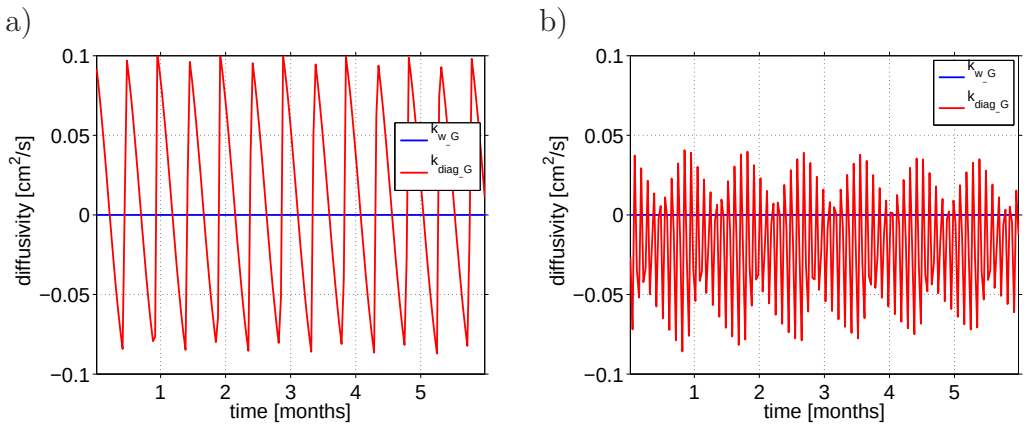

Figure 5.12: Diagnosed diffusivity (red) for model with fine resolved vertical grid (level thickness of $5\,m$): a) using initial density profile for the tracer mapping, b) using 5 times more layers than levels for the transformation. The weighted diffusivity κ_{w_G} (blue) in both Figures is zero.

thickness of $5\,m$. This includes that the initial tracer condition is linearly interpolated onto the new model grid which leads to a decrease in the tracer gradient of the initial tracer condition.

Figure 5.12 a) shows the results for the diagnosed diffusivity κ_{diag_G} , where the initial density profile is used for the tracer mapping onto isopycnals. The amplitude in the diagnosed diffusivity is about 5 times smaller compared to the one of the analogous experiments with the coarser vertical grid, but still of the same order of magnitude as the explicit diffusion coefficient expected in the interior ocean (e.g. in OCCAM, the explicit diffusion coefficient in the region of the NATRE experiments is $0.1\,cm^2/s$). The mean value of the diagnosed diffusivity κ_{diag_G} is $\sim 7.7 \times 10^{-3}\,cm^2/s$. In comparison to the mean induced diffusivity analysed by the variance method ($\sim 5.7 \times 10^{-3}\,cm^2/s$, see Section 5.3), the mean value of κ_{diag_G} is overestimating the numerically induced diffusivity by $\sim 35\%$.

A further increase of the vertical resolution in the model results in a further decrease of the amplitude of the fluctuations in the diagnosed diffusivities. For the realisation in OGCMs a high vertical resolution might lead to mixing problem e.g. at the surface. Note, the amplitude of the diagnosed diffusivity using the initial density profile for the mapping decreases linearly with a decrease of the level thickness in the model set-up.

In Figure 5.12 b) the results for the diagnosed diffusivity κ_{diag_G} (red) using 5 times more layers than levels for the tracer mapping are shown. The amplitude in κ_{diag_G} is much smaller with a negative mean value, although it is very small ($-0.019\,cm^2/s$).

In summary, it can be said that the combination of vertical advection and transformation of the tracer onto isopycnals causes problems in estimating the diagnosed diffusivity using the tracer flux method. A high vertical resolution in the model set-up reduces this effect in such a way that the fluctuations of the spurious diffusivity is reduced, but the mean values are still sensitive with respect to the transformation used. The spurious diffusivity as a combined effect of the mapping and the vertical movement of the tracer is larger than the numerically induced diffusion as a result of the advection scheme used.

5.3 Diagnostics using the tracer variance

The diagnostics of the variance method infer from the analysis of the variance decay. The variance, as defined here, is a depth independent parameter. As the present experiment covers only one dimension, the temporal change of the variance of the total tracer volume can be analysed in z-coordinates. A comparison to the variance decay arising from the transformed tracer in σ-coordinates shows the effect of the tracer mapping on the results of the diagnosed diffusivity.

Figure 5.13 shows the variance of the tracer in z-levels (red) and the variance of the transformed tracer on isopycnals (blue). The tracer variance $\sigma^2(z)$ in z decreases constantly with time at a low rate. Using the initial density profile as a transformation axis for the mapping, the variance $\sigma^2(\sigma)$ of the transformed tracer shows a completely different behaviour with a periodic oscillation. Similar to the diagnosed diffusivity κ_{diag_G} (as shown in section 5.2), the cycle of the variance $\sigma^2(\sigma)$ has a frequency of about 2 months. Estimating the diagnosed diffusivity κ_{var} from the variance in σ-coordinates gives almost identical results compared to the previous one of

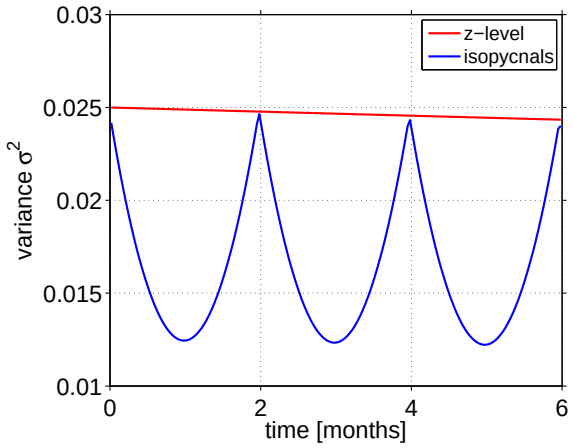

Figure 5.13: Variance of the tracer in z-level (red) and of the transformed tracer (blue) using 75 σ-layers.

the diagnosed diffusivity κ_{diag_G} (see Figure 5.3).

In order to understand the combined effect of the mapping and the vertical movements of the isopycnals on the change of the variance, the same idealised case is considered without dispersion in the tracer concentration. Figure 5.14 shows the similar schematics, as already shown in Section 5.2. The black lines show the grid at the time-step t. The isopycnal layers $\sigma(z)$ move with a constant vertical velocity w_z towards greater depths (σ_n is becoming σ_{k_0}). The z-grid at time-step $t + \Delta t$ is visualised by the blue dashed lines, which is the same depth grid, as for time-step t (the black lines). As the advection is highly idealised, the tracer is completely covered by z-box k_0, which has the density σ_{k_0}, here visualised by the blue shaded box. The tracer concentration in this experiment is defined to be $C = 0$ for $k \neq k_0$ and $C = C_0$ for $k = k_0$.

The mapping divides the tracer mass into the density layers σ_n and σ_{n+1}. The thickness of the $z(k_0)$-level is defined by Δz and the tracer mass is the given by $C_0 \cdot \Delta z$. As the tracer mass will be divided into σ_n and σ_{n+1}, a fraction f is defined moving into the layer σ_{n+1}.

The variance at a given time t is given by

$$\sigma^2(t) = \frac{1}{2} \sum_{n=1}^{s} (C_t(n)^2 \cdot \Delta z), \tag{5.12}$$

where s denotes the number of layers. According to the schematics in

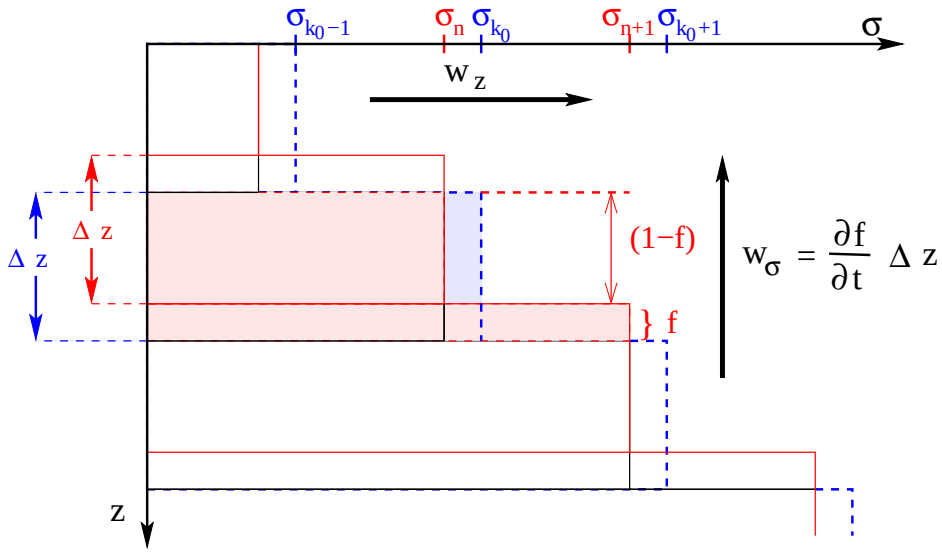

Figure 5.14: Schematics of the tracer mapping for the idealised advection. Black lines show z-grid at time t, blue dashed at $t + \Delta t$ and red lines show transformed grid at $t+\Delta t$. Blue shaded region is initial tracer and red shaded the transformed tracer concentration.

Figure 5.14, the transformed tracer only covers the isopycnal boxes of σ_n and σ_{n+1}. This means that the tracer concentration in those boxes is given by

$$C_t(n,t) = (1-f) \cdot C_0 \tag{5.13}$$

and

$$C_t(n,t) = f \cdot C_0. \tag{5.14}$$

So, the variance can be written as

$$\sigma^2(t) = \frac{1}{2} \cdot ((1-f) \cdot C_0)^2 \cdot \Delta z + \frac{1}{2} \cdot (f \cdot C_0)^2 \cdot \Delta z. \tag{5.15}$$

For the analysis of the diagnosed diffusivity κ_{var}, the temporal change of the variance, given by $\frac{\partial}{\partial t}\sigma^2$, needs to be estimated. In this case, the fraction f is the only time depending parameter in the function of $\sigma^2(t)$. That leads to

$$\frac{\Delta\sigma^2}{\Delta t} = \frac{1}{2} \cdot \frac{\Delta\left[(1-f)^2\right]}{\Delta t} \cdot C_0^2 \cdot \Delta z + \frac{1}{2} \cdot \frac{\Delta\left[f^2\right]}{\Delta t} \cdot C_0^2 \cdot \Delta z, \tag{5.16}$$

which is equivalent to

$$\frac{\Delta\sigma^2}{\Delta t} = \frac{1}{2} \cdot (2f-2)\frac{\Delta f}{\Delta t} \cdot C_0^2 \cdot \Delta z + \frac{1}{2} \cdot 2f\frac{\Delta f}{\Delta t} \cdot C_0^2 \cdot \Delta z$$

$$\frac{\Delta\sigma^2}{\Delta t} = (2f-1)\frac{\Delta f}{\Delta t} \cdot C_0^2 \cdot \Delta z. \tag{5.17}$$

As the vertical velocity w_z is constant, the rate of change of the fraction f can be expressed as a velocity, which is denoted as w_σ in the schematics of Figure 5.14 and can be written as

$$w_\sigma = \frac{\Delta f}{\Delta t} \cdot \Delta z. \tag{5.18}$$

Substituting Equation 5.18 in Equation 5.17, the rate of change of the variance can be expressed as

$$\frac{\Delta\sigma^2}{\Delta t} = (2f-1) \cdot C_0^2 \cdot w_\sigma \tag{5.19}$$

As introduced in Section 2.3, the diagnosed diffusivity κ_{var} is given in Equation 2.28 by

$$\kappa_{var} = \frac{-\frac{\Delta\sigma^2}{\Delta t}}{\sum_k \left[\left(\frac{\Delta C}{\Delta z}\right)^2 \cdot \Delta z\right]} \tag{5.20}$$

In the present example, where the advection is constant, the diagnosed diffusivity can be written as

$$\kappa_{var} = \frac{(1-2f) \cdot C_0^2 \cdot w_\sigma}{\left((1-f)^2 + (1-2f)^2 + f^2\right) \cdot \left(\frac{C_0}{\Delta z}\right)^2 \cdot \Delta z}$$

$$\rightarrow \kappa_{var} = \frac{(1-2f) \cdot w_\sigma \cdot \Delta z}{(1-f)^2 + (1-2f)^2 + f^2} \tag{5.21}$$

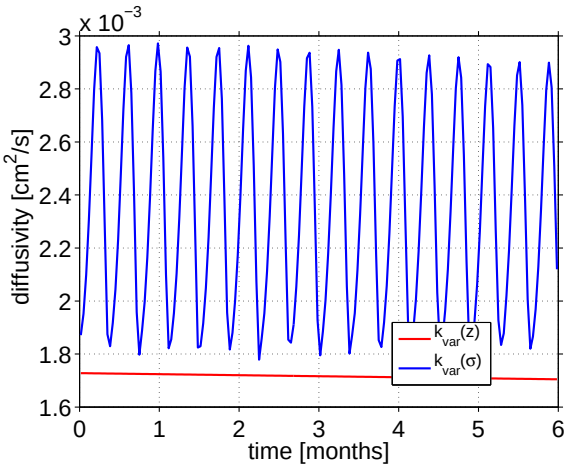

Figure 5.15: Diagnosed diffusivity κ_{var} using the tracer gradient in z (red) and using the transformed tracer gradient in σ (blue), 5 times more layers than z-levels are used for the transformation.

This means that in the idealised case with constant advection, the diagnosed diffusivity κ_{var} is only a function of the rate of change of the fraction f. Additionally, the relation between κ_{var} and f is the same as the relation between the diagnosed diffusivity κ_{diag_G} and f in the diagnostics of the tracer flux method (as shown in Section 5.2).

In Section 4.3, the results showed that an increase in the resolution of the transformation leads to more robust results in the variance decay. By increasing the resolution using 5 times more layers than original z-levels, the variance of the transformed tracer is equal to the variance of the tracer in z-coordinates (same as red line in Figure 5.13).

As the results for the variance are independent of the used grid, either inferring from the tracer concentration in z-levels or from the transformed tracer in σ-layers, the results for the diagnosed diffusivity depend on the values of the tracer gradient. In these 1-dimensional experiments, the tracer gradient can be estimated in z-levels and can be interpolated onto σ-layers.

Figure 5.15 shows the diagnosed diffusivity $\kappa_{var}(z)$ (red), where the variance decay is divided by the tracer gradient in z-levels and the diagnosed diffusivity $\kappa_{var}(\sigma)$ (blue), where the variance decay is divided by the transformed tracer gradient. The diagnosed diffusivity $\kappa_{var}(z)$ has got a nearly constant value of $1.72 \times 10^{-3}\, cm^2/s$. This means that there is a numerically induced diffusion as a result of the Eulerian backwards time stepping scheme.

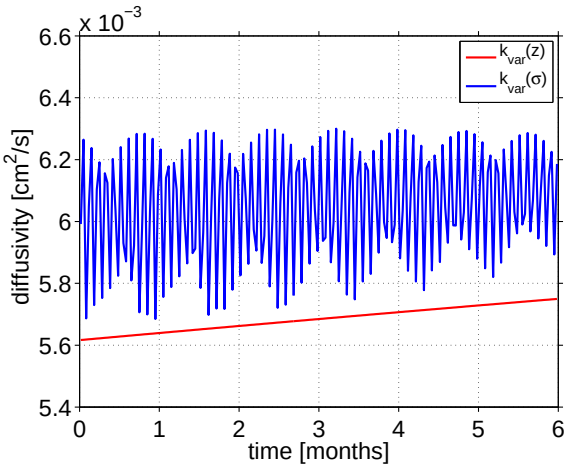

Figure 5.16: High vertical model resolution: diagnosed diffusivity κ_{var} using the tracer gradient in z (red) and using the transformed tracer gradient in σ (blue), using 5 times more layers than z-levels for the transformation.

Using the transformed tracer gradient for the estimation of the diagnosed diffusivity $\kappa_{var}(\sigma)$, the maximum values are twice as high compared to the numerically induced diffusivity $\kappa_{var}(z)$ and the frequency of the fluctuations depend on the number of layers chosen for the transformation.

The results of the tracer flux method show that an increase in the resolution of the vertical model grid leads to a decrease in the amplitude of the spurious fluctuations of the diagnosed diffusivity. In the following the results will be shown using the same experiment with the high vertical resolution and a level thickness of $5\,m$. The initial tracer condition is linearly interpolated onto the new model grid.

Figure 5.16 shows the results for the diagnosed diffusivities $\kappa_{var}(z)$ (red, the tracer gradient is taken in z-levels) and $\kappa_{var}(\sigma)$ (blue, the transformed tracer gradient is taken in σ-layers). Using 5 times more layers than levels for the transformation (as done for the results shown in Figure 5.16), the variance decay is independent if either analysed in z- or in σ-coordinates. The mean values for the diagnosed diffusivities are higher compared to the ones found in the analogous experiment with the coarser vertical resolution.

The results for the diagnosed diffusivity $\kappa_{var}(z)$ using the tracer gradient in z-levels for the analysis increase from a value of $5.6 \times 10^{-3}\,cm^2/s$ to $5.75 \times 10^{-3}\,cm^2/s$. The diagnosed diffusivity $\kappa_{var}(\sigma)$ (the transformed tracer gradient is used here) in Figure 5.16 shows high frequency variations with an amplitude of $\pm 0.2 \times 10^{-3} cm^2/s$. The amplitude of these variations

are smaller compared to the ones in the results of the analogous experiment with the coarse vertical model grid (Figure 5.15). The mean value of $\kappa_{var}(\sigma)$ is with $\sim 6 \times 10^{-3} cm^2/s$ only $\sim 8\%$ higher compared to the values of the diagnosed diffusivity $\kappa_{var}(z)$.

In summary, it can be said that the numerically induced diffusion in this 1-dimensional model, as a result of the vertical advection, can be determined by the variance method. The values of the induced diffusivity for typical velocities, as they are found in the interior ocean, are relatively low with values of about $1.72 \times 10^{-3}\, cm^2/s$ in a model with a level thickness of $20\, m$ and $\sim 5.7 \times 10^{-3}\, cm^2/s$ in a model with a smaller level thickness of $5\, m$. An increase in the vertical resolution of the model results in a smaller difference between the diagnosed diffusivity $\kappa_{var}(z)$ in z-levels and $\kappa_{var}(\sigma)$ analysed after the transformation onto isopycnals.

5.4 Summary

In this chapter, the analysis of the experiment which includes a constant vertical advection is presented. The set-up of the experiment is chosen in such a way that as a result of the constant advection, the isopycnal layers move in a parallel manner. This gives the possibility to analyse the effect of the tracer mapping onto isopycnal layers in combination with a movement of the isopycnals without the effect of diverging or converging isopycnals.

The results of the tracer flux method show a high dependence of the diagnosed diffusivity κ_{diag_G} on the transformation of the tracer onto isopycnals. The values of the diagnosed diffusivity κ_{diag_G} show fluctuations with an amplitude of $\pm 0.45\, cm^2/s$. The frequency of these fluctuations depends on the layer thickness used for the transformation. An increase of the number of layers used for the transformation leads to an increase in the frequency of the fluctuations. The amplitude of these fluctuations depends on the level thickness; therefore an increase in the number of layers used for the tracer mapping does not result in a decrease of the amplitude. Although, the instantaneous effect of the mapping on the diagnosed

diffusivity κ_{diag_G} is very large, the mean values are very small ($o(10^{-2}cm^2/s)$). This is still about one order of magnitude larger than the numerically induced diffusivity.

An increase in the vertical resolution of the model leads to a decrease in the amplitude of the fluctuations in the diagnosed diffusivity. Additionally, using a high number of layers for the tracer mapping, the amplitude of the fluctuations decreases even further without resulting in artificially high negative values. In order to analyse a mean induced diffusivity, it should be possible to use the tracer flux method, as long as the vertical resolution is relatively high.

The approach of the variance method gives the possibility to analyse the diagnosed diffusivity in the original z-coordinates. The results of the diagnosed diffusivity in z-levels show, that there is a small amount of numerically induced diffusion which is generated by the vertical advection scheme used. A finer vertical resolution (to a level thickness of $5m$) leads to an increase in the numerically induced diffusivity, as a result of the different gradients in the initial tracer distribution. The study of Lee et al. (2002) predicts that a finer vertical resolution of the model grid leads to an increase of the numerically induced diffusion, which is consistent with our results although a different advection scheme has been tested. For both experiments (fine and coarse vertical grid) the numerically induced diffusion decreases linearly with a decrease of the time-step used.

Analysing the diagnosed diffusivity on isopycnal layers leads also to a high dependence of the results on the used transformation axis. Different to the results of the tracer flux method, an increase in the number of layers used for the mapping leads to a constant overestimation of the diagnosed diffusivity with a mean value of $\sim 35\%$. An increase in the vertical resolution of the model reduces the difference between the diagnosed diffusivity $\kappa_{var}(z)$, analysed on z-levels, and the diagnosed diffusivity $\kappa_{var}(\sigma)$, analysed on isopycnals, to only $\sim 8\%$.

In the observational studies done by Ledwell et al. (1998), this problem is avoided as they are defining the layers with reference to the layer, where

the tracer was released. With this definition, it doesn't matter, if the isopycnals are moving in a parallel manner, but the problem of diverging and converging isopycnals will be neglected this way.

Chapter 6

The role of diffusion in temperature and salinity

In the previous chapter the tracer flux and the variance methods had been used to analyse the diagnosed diffusivities in experiments with implemented vertical advection. The vertical advection results in that particular case in a parallel movement of the isopycnal layers. In general, the vertical advection does not lead to an exact parallel movement of the isopycnals but also to small diverging and converging effects. The current chapter focuses on the analysis of experiments, where explicit diffusion acts on tracer, temperature and salinity. The corresponding effect in the density can be interpreted as an interfacial movement of the isopycnal layers, which leads to divergence or convergence in the isopycnals.

The results of 1-dimensional experiments with explicit diffusion of the tracer, the temperature and the salinity fields will be shown and discussed. Note, these experiments do not implement explicit vertical velocity ($w_{expl} = 0$). Similar to the previous chapter, the discussion will be divided into the diagnostics of the variance method, and the diagnostics of the tracer flux method.

In order to get an overview of the influence of the diffusion in temperature and salinity, the whole set of experiments (except A_decr) will be repeated, as shown in Chapter 3: (i) A_const, where the explicit diffusion coefficient

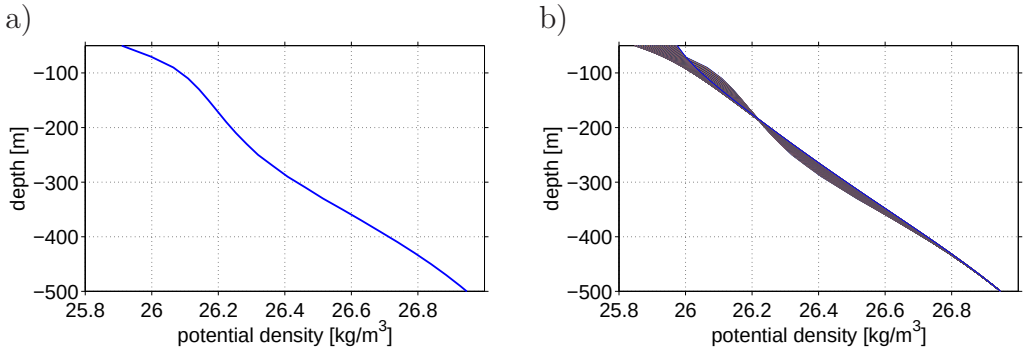

Figure 6.1: a) Initial density profile, b) set of the time series of profiles for experiment A_const.

is constant, (ii) A_incr, where the explicit diffusion coefficient is linearly increasing with depth and (iii) A_oc, where it is non-linear with depth, as is expected in the ocean interior.

The fourth experiment A_decr, with high values in the explicit diffusion coefficient close to the surface, will not be repeated. As in this simple model the boundaries are closed, problems in the surface layers, such as e.g. empty boxes, arise from high explicit diffusion coefficients in this region.

The initial tracer condition is chosen to be symmetric with depth, as the asymmetric initial tracer condition yields similar results. The model grid is again chosen to be equidistant with a level thickness of $20\,m$.

Different from the experiments presented in Chapter 3, the initial density profile is not exactly linear, instead slightly non-linear, as expected in the ocean interior. Figure 6.1 a) shows the initial density profile and b) the set set of the time series of profiles resulting for the experiment A_const, in which the explicit diffusivity is set constant with depth with a value of $4cm^2/s$.

A linear initial density profile would only result in changes starting at the upper and lower boundary slowly moving towards the inner water masses. But in such a case, the tracer would not reach the region in which the isopycnals change with time. Using the non-linear initial density profile, the main changes occur at a depth of $\sim 300\,m$, the depth in which the tracer is released.

6.1 Diagnostics using the variance method

The results presented in Chapter 4 show, that using the variance method (Section 2.3), the diagnosed diffusivity κ_{var} is independent of the transformation of the tracer onto isopycnals. As already seen in the previous chapter, the advection of temperature and salinity has no impact on the temporal change of the tracer variance and therefore also not on the diagnosed diffusivity $\kappa_{var}(z)$, as for the estimation of the variance it is not necessary to map the tracer onto isopycnals. The reason for this was given by the depth independent value of the variance.

The diffusion in temperature and salinity, and their corresponding effect on the density distribution, has no impact on the tracer variance for the same reason. Only the transformation of the tracer onto isopycnals, might change its variance, which is a result only of the mapping itself.

In order to analyse the diagnosed diffusivity $\kappa_{var}(\sigma)$, the variance of the transformed tracer needs to be estimated for each time-step before taking the temporal difference. The sensitivity studies showed, that the variance of the transformed tracer is independent of the chosen transformation, if the resolution of that transformation is high enough. The variance decay of the tracer is independent of the interfacial movement of the isopycnals. For these 1-dimensional experiments, it is not necessary to transform the tracer gradient onto isopycnals, but in terms of analysing higher dimensional models, it is of greater interest to determine the effect of the interfacial velocity on the transformed tracer gradient.

Figure 6.2 shows the results of experiment *A_const* for the weighted diffusivity κ_w (blue), diagnosed diffusivity $\kappa_{var}(z)$ analysed in z-levels (green) and the diagnosed diffusivity $\kappa_{var}(\sigma)$ (red) analysed in σ-layers. In Figure 6.2 a) 75 equidistant layers are used for the transformation (the same amount than z-levels in the model), in b) 150 (twice as many layers than levels) and in c) 750 layers (10 times more layers than model levels). Only the results for the diagnosed diffusivity $\kappa_{var}(\sigma)$ depend on the number of layers used for the mapping.

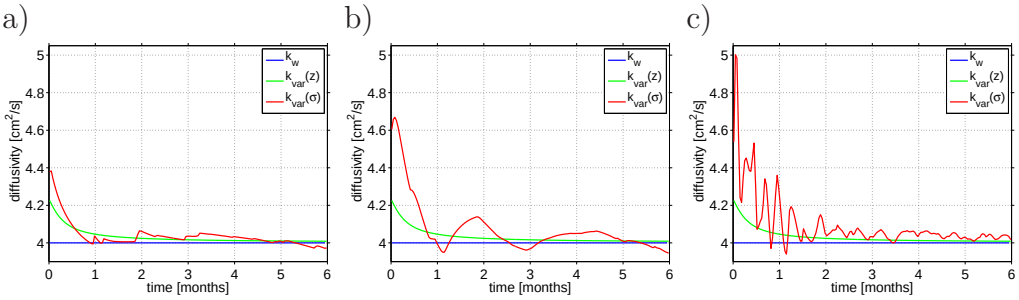

Figure 6.2: Experiment *A_const*, diffusion acts on tracer temperature and salinity: diagnosed diffusivities $\kappa_{var}(z)$ (green) and $\kappa_{var}(\sigma)$ (red) and weighted diffusivity (blue) using (a) 75 layers, (b) 150 layers and (c) 750 layers for the tracer transformation.

As expected, the results for the diagnosed diffusivity $\kappa_{var}(z)$ (green) and the weighted diffusivity κ_w (blue) are identical to the ones shown in Section 3.2.2, where diffusion acts on the tracer only. In all cases shown in Figure 6.2, the variance of the transformed tracer is consistent with the variance of the tracer in z-levels. The difference of diagnosed diffusivity $\kappa_{var}(\sigma)$ (red) to the values of $\kappa_{var}(z)$ (green) are an effect caused by the transformation of the tracer gradient onto isopycnal layers.

In Figure 6.2 a), where 75 layers are used for the mapping, the diagnosed diffusivity $\kappa_{var}(\sigma)$ shows $\sim 5\%$ higher values at the beginning of the experiment. Between the end of the first until the third month the diagnosed diffusivity $\kappa_{var}(\sigma)$ fluctuates around the expected value.

Increasing the number of layers used for the transformation by a factor of two (see Figure 6.2 b.), the amplitude and the frequency of the fluctuation of the diagnosed diffusivity $\kappa_{var}(\sigma)$ increase. The difference between $\kappa_{var}(\sigma)$ and $\kappa_{var}(z)$ at the beginning of the experiment is already $\sim 10\%$. A further increase of the number of layers (750) used for the transformation (see Figure 6.2 c.) leads to a further increase of the frequency of the fluctuations of the diagnosed diffusivity.

These different results for the diagnosed diffusivity $\kappa_{var}(\sigma)$ are only a result of the different number of layers used for the transformation. They show that the transformation of the tracer gradient reacts sensitively to an interfacial velocity, similar to the analysis of the experiment with advection

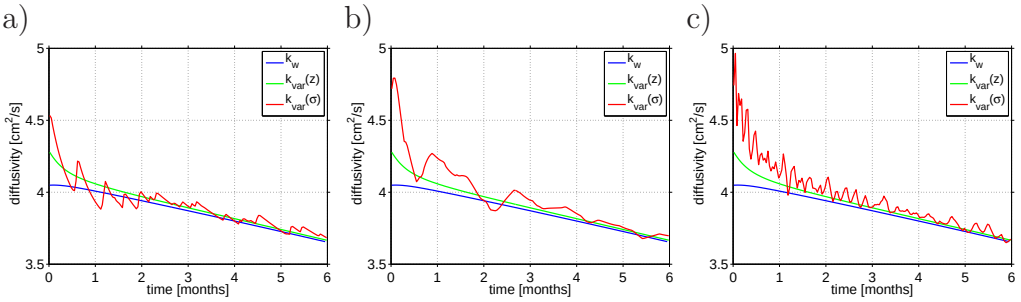

Figure 6.3: Experiment *A_incr*, diffusion acts on tracer temperature and salinity: diagnosed diffusivities $\kappa_{var}(z)$ (green) and $\kappa_{var}(\sigma)$ (red) and weighted diffusivity (blue) using (a) 75 layers, (b) 150 layers and (c) 750 layers for the tracer transformation.

(see Section 5.2).

The results for experiments *A_incr*, as shown in Figure 6.3, are similar. The diagnosed diffusivity $\kappa_{var}(z)$ (green) and the weighted diffusivity κ_w (blue) are not affected by the interfacial movement of the isopycnals and show exactly the same behaviour as in the experiments with stationary isopycnals (see Section 3.2.2).

The diagnosed diffusivities $\kappa_{var}(\sigma)$ (red) are sensitive towards changes of the transformation axis, although in the shown cases the variance of the tracer is not affected by the mapping. In Figure 6.3 a) 75 equidistant layers are used for the mapping of the tracer and the tracer gradient. The diagnosed diffusivity shows high frequency fluctuations $(5 - 1\%)$ around the expected values.

An increase of the number of layers used for the transformation by a factor of two (Figure 6.3 b.) shows an increase of the amplitude of the fluctuations in the diagnosed diffusivity $\kappa_{var}(\sigma)$ (up to 20% at the beginning) associated with a decrease in the frequency. A further increase of the number of layers (750, see Figure 6.3 c.) leads to a further increase in the frequency of the fluctuations. Additionally, the fluctuations are no longer around the expected value of $\kappa_{var}(z)$, but biased highly with a maximal difference of 25% at the beginning of the experiment.

The pattern of the high frequency fluctuations arises from the movement of the tracer maximum in relation to the isopycnal surfaces. So the effect is

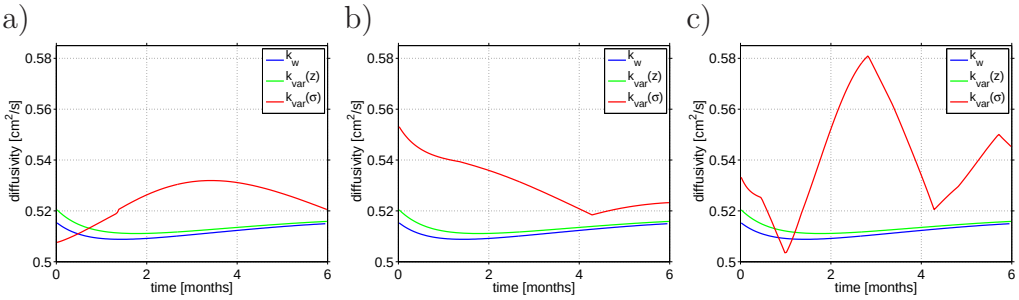

Figure 6.4: Experiment *A_oc*, diffusion acts on tracer temperature and salinity: diagnosed diffusivities $\kappa_{var}(z)$ (green) and $\kappa_{var}(\sigma)$ (red) and weighted diffusivity (blue) using (a) 75 layers, (b) 150 layers and (c) 750 layers for the tracer transformation.

artificially caused by the combination of the mapping and the interfacial movement.

In the last experiment, *A_oc*, the explicit diffusion coefficient is non-linear with depth and much lower compared to the one in the previously shown experiments. The results for the diagnosed diffusivity $\kappa_{var}(z)$ and the weighted diffusivity κ_w, as shown in Figure 6.4, are consistent to the results of the experiments with stationary isopycnals.

A comparison of the diagnosed diffusivity $\kappa_{var}(\sigma)$ varying the number of layers of the transformation axis (Figure 6.4 a. 75, b. 150 and c. 750) shows a wide range in the results. As the diffusion in this experiment is very low, the high frequency pattern, seen in the previous two experiments, cannot be found in this case. This is a result of the low relative movement between the tracer and the isopycnals (the tracer maximum and the maximum of the gradient are not moving from one isopycnal layer to the next one so quickly).

Similar to the results of the experiments including advection, these studies show that the weak point of the diagnostics lays in the transformation of the tracer gradient. As long, as the tracer gradient can be used in its original z-coordinates, the diagnosed diffusivity κ_{var} can be analysed correctly. The relative movement of the isopycnals to the z-grid in combination with the transformation used leads to errors in the diagnostics. In terms of analysing experiments of higher dimensions, the awareness of

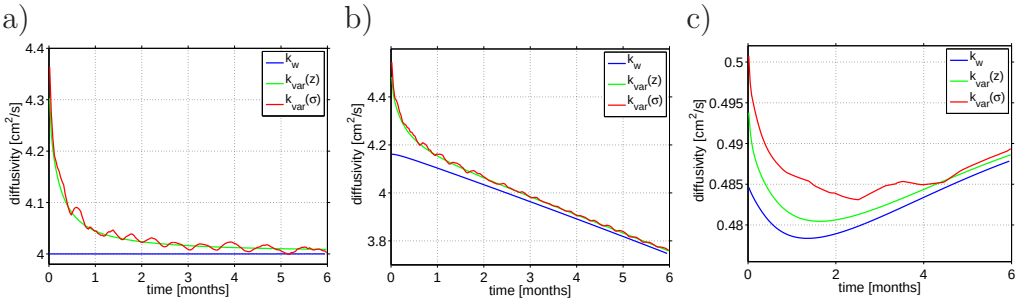

Figure 6.5: Experiments with fine resolved vertical grid (level thickness of $5\,m$) using twice as many layers than levels for the mapping, a)A_const, b) A_incr and c) A_oc.

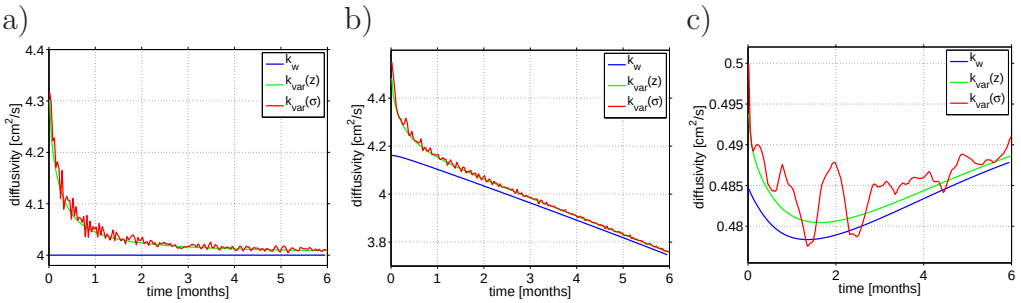

Figure 6.6: Experiments with fine resolved vertical grid (level thickness of $5\,m$) using 10 times as many layers than levels for the mapping, a)A_const, b) A_incr and c) A_oc.

these problems is necessary, as generally, the tracer field has to be transformed onto isopycnals.

The spurious fluctuations in the diagnosed diffusivity $\kappa_{var}(\sigma)$ are caused by the mapping of the tracer gradient onto isopycnals and are always large, if the tracer gradient is strong. In general, OGCMs use an even coarser grid than chosen for the shown experiments, where the z-levels are uniform with a thickness of $20\,m$. The combination of a decrease in the level thickness and the linear interpolation of the initial tracer condition onto the fine resolved grid results in smaller tracer gradients. By choosing z-levels with a thickness of $5\,m$, the error, which is caused by the mapping, gets very small.

Figure 6.5 and 6.6 show the results for all three experiments, a)A_const, b) A_incr and c) A_oc, with the higher resolution of the vertical model grid. In Figure 6.5 twice as many layers then levels (600) are used for the transformation onto isopycnals and 10 times more layers than levels (3000)

are used in Figure 6.6 for the mapping. Note, in this case, the model depth reaches only 1500m, as the tracer reaches no greater depths.

For the experiments, where the explicit diffusion coefficient is relatively high (A_const and A_incr: both times $\sim 4\,cm^2/s$ in the region of interest), the influence of the mapping on the results of the diagnosed diffusivity $\kappa_{var}(\sigma)$ is getting very small (max. of 1% during the first month, else $<< 1\%$). In the experiment A_oc, where the explicit diffusion coefficient is small ($\sim 0.48\,cm^2/s$), the maximal changes in the fluctuations of the diagnosed diffusivity $\kappa_{var}(\sigma)$ are about 1.5%, and different from the results of the coarser model resolutions, the temporal behaviour is similar to the behaviour of the diffusivity $\kappa_{var}(z)$, although there are fluctuations.

In summary, it can be said that an increase in the vertical resolution of the model grid reduces the error in the diagnosed diffusivity, which is caused by the combination of the mapping of the tracer onto isopycnals and the interfacial movement of the isopycnals.

6.2 Diagnostics using the tracer flux method

The results in Chapter 5 already showed that using the diagnostics of the tracer flux method is not an appropriate method for the analysis of models, if isopycnals are not constant in time. Different to the parallel movement of the isopycnals the result of an implemented vertical advection, diffusion in temperature and salinity leads to a rather small rate of change of the isopycnal interface. This vertical movement of the interfaces depends on the used explicit diffusion coefficient and leads to divergence and convergence in the isopycnal layers. Although being aware that divergence and convergence in the isopycnals have an effect on results of the diagnosed diffusivity κ_{diag_G}, the observational studies (Ledwell et al., 1998) neglect these effects in their analysis. In models, these changes in the diagnosed diffusivity due to diverging or converging isopycnals are part of the numerically induced diffusivity. The numerically induced diffusivity includes all different sources which lead to differences between the weighted

and the diagnosed diffusivity, which are a result of the model parameterisation itself.

For the analysis of these experiments, it is necessary to diagnose the interfacial velocity (derivation is shown in section 4.2). To get an idea about the amount and vertical structure of the interfacial velocity, an overview for all three experiments is given before the results for the diagnosed diffusivities are shown. The initial density profile used in the model set-up is slightly non-linear with depth (see Figure 6.1) and the initial tracer distribution is symmetric with depth.

According to the transformation of the advection-diffusion equation (see also Section 4.2), the interfacial velocity w_I is given by

$$w_I = \frac{\frac{\partial \sigma}{\partial t}}{\frac{\partial \sigma}{\partial z}}. \tag{6.1}$$

The total change of the density in z-coordinates, given by the model equation, is the explicit diffusion term of the density, as follows

$$\frac{\partial \sigma}{\partial t} = \frac{\partial}{\partial z}\left(\kappa_{expl}\frac{\partial \sigma}{\partial z}\right). \tag{6.2}$$

Substituting Equation 6.1 in Equation 6.2, the interfacial velocity of the isopycnal layer can be written as a function of z

$$w_I = \frac{\frac{\partial}{\partial z}\left(\kappa_{expl}\frac{\partial \sigma}{\partial z}\right)}{\frac{\partial \sigma}{\partial z}}. \tag{6.3}$$

To give an overview about the values of the interfacial velocity, Figures 6.7 - 6.9 show the interfacial velocity in the depth range of interest for the experiments A_const, A_incr and A_oc.

The interfacial velocity w_I according to Equation 6.3 for experiment A_const, where the explicit diffusion coefficient is constant with depth, between 150 and 550 m depths is shown in Figure 6.7. The maximum values of $\sim 4 \times 10^{-4}\, cm/s$ can be found at the beginning of the experiment

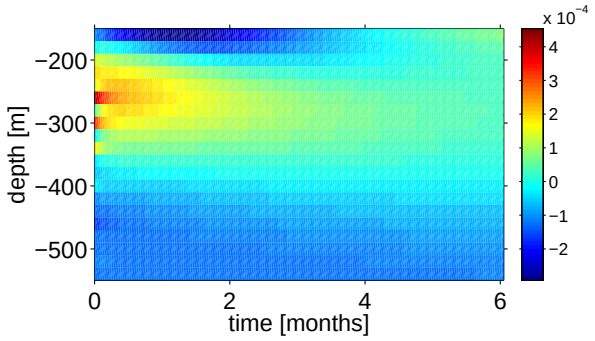

Figure 6.7: Interfacial velocity w_I of the isopycnal layer, estimated by the explicit diffusion coefficient for the experiment A_const.

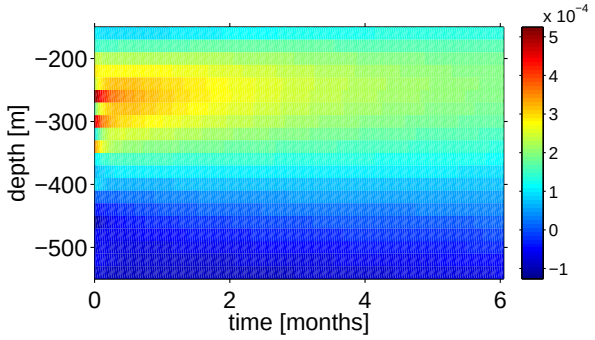

Figure 6.8: Interfacial velocity w_I of the isopycnal layer, estimated by the explicit diffusion coefficient for the experiment A_incr.

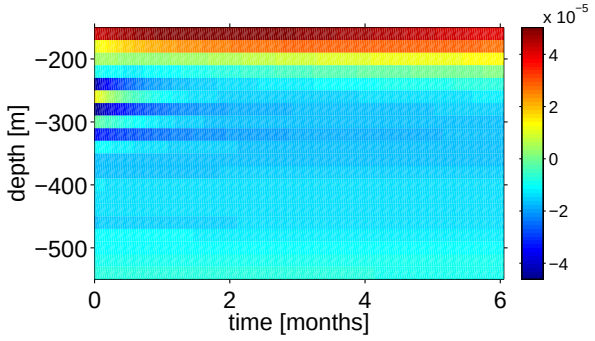

Figure 6.9: Interfacial velocity w_I of the isopycnal layer, estimated by the explicit diffusion coefficient for the experiment A_oc.

at a depth of $\sim 280\,m$. This maximum value decreases with time to values of $\sim 1 \times 10^{-4}\,cm/s$ and the velocity gradients decrease as well.

The results for the interfacial velocity w_I in experiment A_incr are similar (see Figure 6.8) as the values of the explicit diffusivity in the depth of $\sim 300\,m$ are also $\sim 4\,cm^2/s$. The maximum values of w_I are $\sim 5 \times 10^{-4}\,cm/s$, which are slightly higher compared to the previous experiment, however the temporal development is the same. The maximum value decreases also with time to values between $\sim 1 - 2 \times 10^{-4}\,cm/s$ and also the gradients decrease.

Figure 6.9 shows the results for the last experiment, A_oc, where the explicit diffusion coefficient is more than one order of magnitude smaller compared to the explicit diffusion coefficients in A_const and A_incr. In this case, the interfacial velocity w_I shows maximal positive values in the surface regions of $\sim 4 \times 10^{-5}\, cm/s$, but in the region of $300\, m$ depths, where the tracer is released, the values of w_I are negative with values of $\sim -4 \times 10^{-5}\, cm/s$. This can be ascribed to the fact, that the profile of the explicit diffusion coefficient in this experiments is non-linear and decreases strongly in the depth range between $\sim 200 - 350\, m$.

A comparison between the flux which is caused by the interfacial velocity $(w_I \cdot C)$ and the diffusive flux of the tracer $(\kappa_{expl} \cdot \partial C/\partial z)$ shows that the ratio is rather small $(<< 1)$. This means that the analysis of the interfacial velocity has a rather small effect on the diagnostics of the diffusivity. Only at the tracer maximum the ratio is large, which is caused by the very small tracer gradients.

Solving the advection-diffusion equation (in σ-co-ordinates) with the method of the least squares fit can only be done, if the diagnosed diffusivity κ_{diag_G} and the interfacial velocity are taken as depth independent (vertical mean). This diagnosed interfacial velocity will be denoted as $\overline{w_I}$. In the following, the results for the diagnosed diffusivity κ_{diag_G} will be shown and discussed, followed by the results of the diagnosed interfacial velocity $\overline{w_I}$.

Figure 6.10 shows the results of the diagnosed diffusivity κ_{diag_G} (red) for the experiment A_const. Using the same amount of layers as levels (75) for the tracer mapping (see Figure 6.10 a), the values for the diagnosed diffusivity are up to 14% smaller compared to the value of the weighted diffusivity κ_{w_G} (blue), which is $4\, cm^2/s$. Doubling the number of layers (see Figure 6.10 b) does not change the shape of the diagnosed diffusivity, but the values of κ_{diag_G} are slightly higher leading to a maximal difference of $\sim 8\%$ to the expected value κ_{w_G}. Using 10 times more layers than levels (750) for the transformation of the tracer (see Figure 6.10 c), the temporal behaviour of the diagnosed diffusivity gets noisier and differs with a maximum of $\sim 7.5\%$ from the value of the explicit diffusivity.

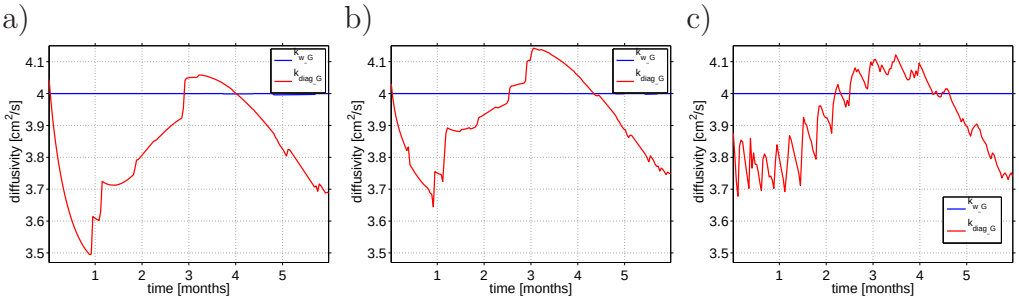

Figure 6.10: Diagnosed diffusivity κ_{diag_G} (red) and weighted diffusivity κ_w (blue) for experiment A_const, using 75 layers (a), 150 (b) and 750 (c) layers for the transformation.

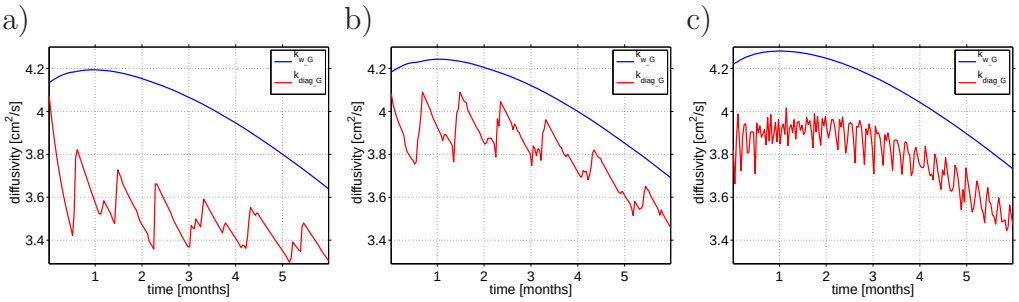

Figure 6.11: Diagnosed diffusivity κ_{diag_G} (red) and weighted diffusivity κ_w (blue) for experiment A_incr, using 75 layers (a), 150 (b) and 750 (c) layers for the transformation.

In Figure 6.11, the results of the diagnosed diffusivities of experiment A_incr are shown. Already in Figure 6.11 a), where 75 layers are used for the transformation, the diagnosed diffusivity κ_{diag_G} shows fluctuations with periods of about one month. The values of κ_{diag_G} are $\sim 15\%$ smaller compared to the values of the weighted diffusivity κ_{w_G}.

Doubling the number of layers (shown in Figure 6.11 b.), the frequency of the fluctuations have still a period of about one month, but the values are slightly higher, now differing about $\sim 10\%$ from the weighted diffusivity. A further increase of the number of layers used for the mapping (see Figure 6.11 c.) results in a higher frequency (about 7 days) and a smaller amplitude, but a longer time mean still gives smaller values ($\sim 10\%$) for the diagnosed diffusivity compared to the values of the weighted diffusivity.

The results for the last experiment, A_oc, are shown in Figure 6.12. Using 75 layers for the transformation (shown in Figure 6.12 a.), the diagnosed

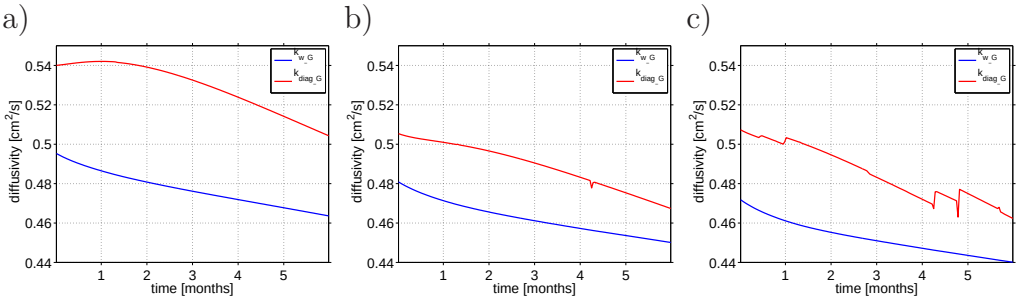

Figure 6.12: Diagnosed diffusivity κ_{diag_G} (red) and weighted diffusivity κ_w (blue) for experiment A_oc, using 75 layers (a), 150 (b) and 750 (c) layers for the transformation.

diffusivity is $\sim 8\%$ higher compared to the values of the weighted diffusivity. Increasing the number of layers by a factor of two (see Figure 6.12 b.), the difference between the weighted and the diagnosed diffusivity decreases to $\sim 5\%$. Note, also the values of the weighted diffusivity decrease if the number of layers used by the transformation is increased. This can be ascribed to the fact that the weighted diffusivity is also analysed in σ-coordinates. Thus the explicit diffusion coefficient needs to be transformed onto isopycnals, realised by a linear interpolation in the same way as introduced for the tracer gradient. An increase in the number of layers is therefore changing the values of the explicit diffusivity which are weighted. Increasing the number of layers further to 750 (see Figure 6.12 c.), the weighted diffusivity decreases by another $\sim 1-2\%$ and the difference to the diagnosed diffusivity is still $\sim 5\%$, but κ_{diag_G} starts getting noisy.

The analysis of the mean interfacial velocity $\overline{w_I}$ is shown in Figure 6.13 a)-c) for all three experiments. The mean interfacial velocity for experiment A_const (see Figure 6.13 a.) using the same amount of layers as levels (as shown in blue) gives values varying between ~ 2.5 and $1.3 \times 10^{-4}\, cm/s$. Increasing the number of layers used for the transformation by the factor of two (red line), the mean interfacial velocity increases also to values between ~ 3.5 and $1.5 \times 10^{-4}\, cm/s$.

From the analysis of the interfacial velocity w_I, estimated by the term of the explicit diffusion, values in the range of $\sim 1-3 \times 10^{-4}\, cm/s$ (compare

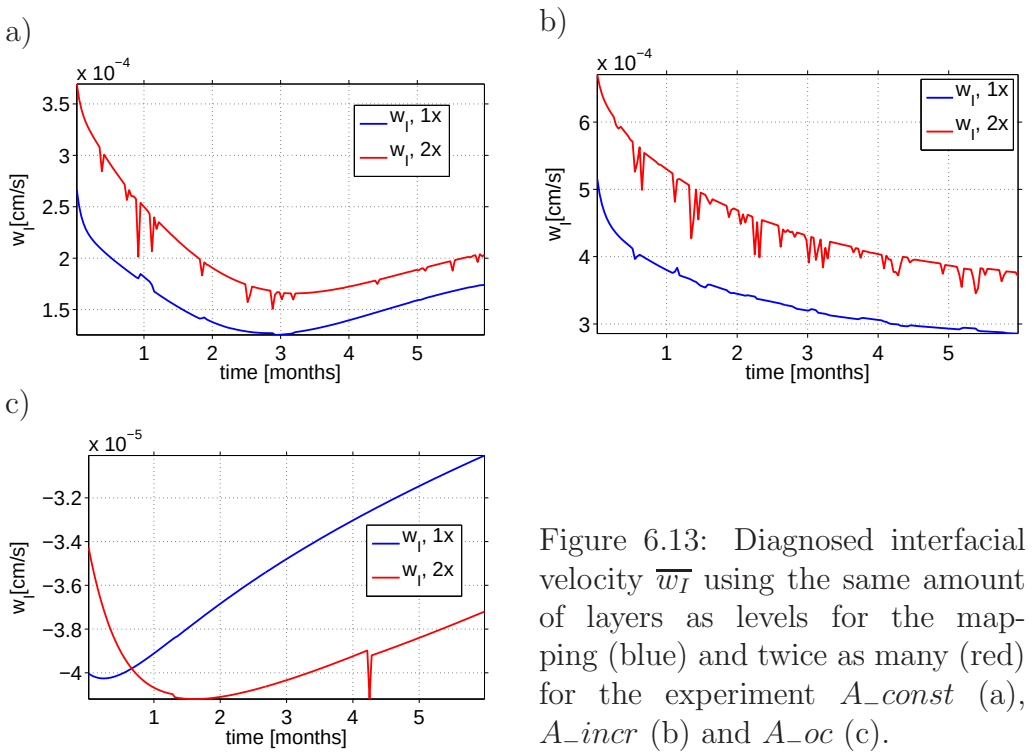

Figure 6.13: Diagnosed interfacial velocity $\overline{w_I}$ using the same amount of layers as levels for the mapping (blue) and twice as many (red) for the experiment A_const (a), A_incr (b) and A_oc (c).

Figure 6.7) would be expected. Although, the results for the two different numbers of layers used for the transformation differ, they are both in the range of the values expected from the analysis of the depth dependent value for the interfacial velocity w_I.

Using 10 times more layers than levels, the mean interfacial velocity $\overline{w_I}$ increases to values of about one order of magnitude higher compared to the expected value; therefore this case is not shown in Figure 6.13 a). Additionally, the mean interfacial velocity is getting noisier with the increase of the number of layers used for the transformation.

Figure 6.13 b) shows the results of the mean interfacial velocity $\overline{w_I}$ for experiment A_incr. The values are about twice as high compared to the previous experiment varying between $\sim 5 - 3 \times 10^{-4}\, cm/s$ using the same number of layers as levels for the mapping (blue line). Using twice as many layers than model levels for the mapping (red line) the values of $\overline{w_I}$ vary between $\sim 6.4 - 3.8 \times 10^{-4}\, cm/s$. This is also consistent with the results of the depth dependent value of the interfacial velocity w_I as shown in Figure 6.8 in the depth region of interest.

Increasing the number of layers used for the mapping by a factor of 10 compared to the number of model levels, the mean interfacial velocity $\overline{w_I}$ is about one order of magnitude higher compared to the expected values, and it also gets very noisy.

For the last experiment, A_oc, the results for the mean interfacial velocity $\overline{w_I}$ are shown in Figure 6.13 c). The values for the velocity, as already mentioned for the analysis of the interfacial velocity w_I, are about one order of magnitude smaller compared to the results of the previous two experiments and do have the opposite sign, with values varying between ~ -4.3 and $-3 \times 10^{-5}\, cm/s$. The temporal behaviour of the mean interfacial velocity $\overline{w_I}$ using the same number of layers as levels for the transformation (blue line) is different from the one using twice as many layers than levels for the mapping (red line), but the range of the values of $\overline{w_I}$ is the same.

Similar to the results of the previous experiments, also the results in this experiment are highly influenced by the transformation of the tracer onto isopycnals, using 10 times more layers than model levels. This is not restricted by a change in the values, also the noise in the mean velocity is increasing.

In order to explain this effect, it is necessary to go back to the origin of the tracer flux method, the cumulative integral of the advection-diffusion-equation in σ-coordinates:

$$\sum_{s_1=1}^{s} \frac{\Delta \left(C_{t,s_1} \cdot \Delta z_{t,s_1} \right)}{\Delta t} = \kappa_{diag\_G} \cdot \frac{\Delta C_{t,s}}{\Delta z_{t,s}}\Big|_{s+1} - \overline{w_I} \cdot C_{t,s}\Big|_{s+1}$$

In the sensitivity studies (see Section 4.3), the analysis of the case with no interfacial velocity ($\overline{w_I} = 0$) showed that the results are sensitive to changes in the transformation axis used. The sensitivity depends on the change of the vertical tracer distribution by the mapping onto isopycnals. This biasing effect was reduced by mapping the tracer gradient onto isopycnals.

In the present case, the tracer gradient is also mapped onto isopycnals, but the tracer distribution is mapped discretely into σ-space. That means, by

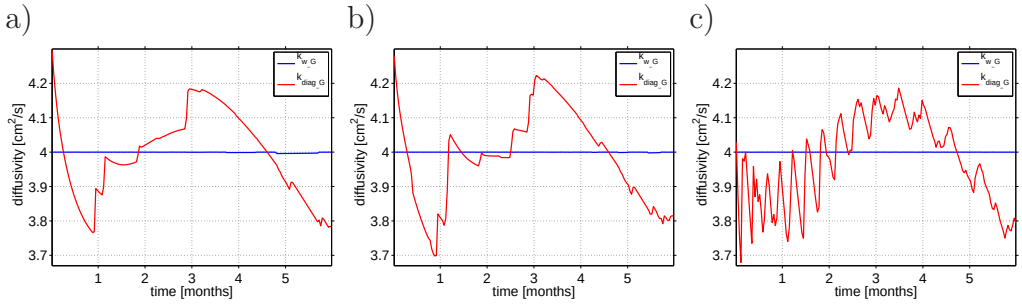

Figure 6.14: Diagnosed diffusivity κ_{diag_G} (red) and weighted diffusivity κ_{w_G} (blue) for experiment A_const, using 75 layers (a), 150 (b) and 750 (c) layers for the transformation, where $\overline{w_I}$ is considered to be zero.

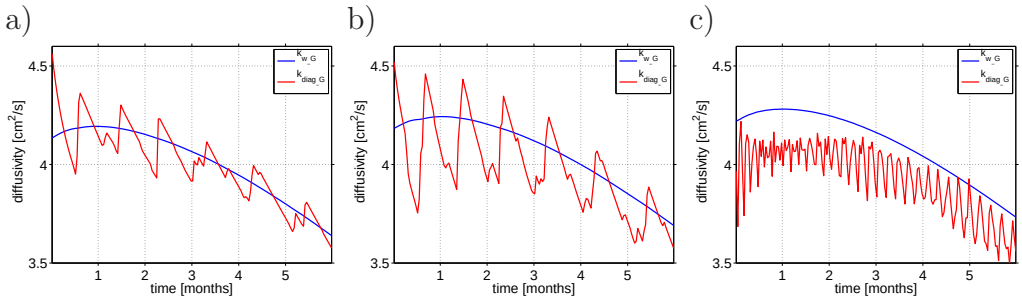

Figure 6.15: Diagnosed diffusivity κ_{diag_G} (red) and weighted diffusivity κ_{w_G} (blue) for experiment A_incr, using 75 layers (a), 150 (b) and 750 (c) layers for the transformation, where $\overline{w_I}$ is considered to be zero.

increasing the number of layers used for the transformation, also the number of layers with a zero thickness increase. As a result the spurious interfacial velocity is quiet large.

As already mentioned, the flux which is caused by the interfacial velocity $(w_I \cdot C)$ is much smaller compared to the diffusive flux of the tracer $(\kappa_{expl} \cdot \partial c/\partial z)$. Thus in the following, the results for the same experiments are shown, but in the analysis the mean interfacial velocity $\overline{w_I}$ is neglected. Assuming $\overline{w_I} = 0$, Figures 6.14 - 6.16 shows the results for the diagnosed diffusivity κ_{diag_G}, using the same number of layers as levels (a), twice as many (b) and 10 times more layers than levels (c).

The results for the diagnosed diffusivity κ_{diag_G} of experiment A_const are shown in Figure 6.14. Independent how many layers are chosen for the transformation, the diagnosed diffusivity varies with $\pm 5 - 6\%$ around the expected value of $4\,cm^2/s$.

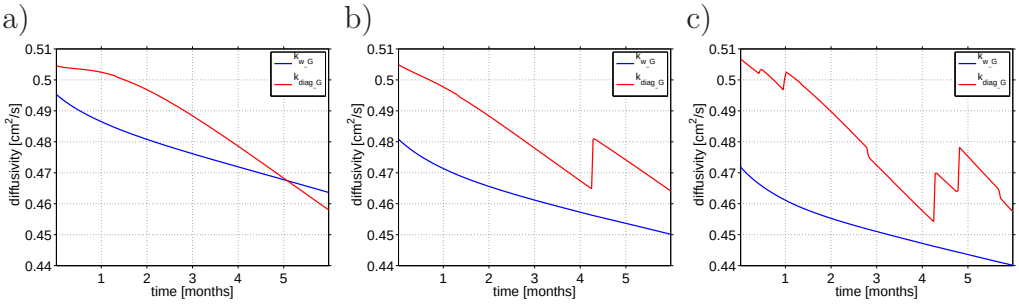

Figure 6.16: Diagnosed diffusivity κ_{diag_G} (red) and weighted diffusivity κ_{w_G} (blue) for experiment A_oc, using 75 layers (a), 150 (b) and 750 (c) layers for the transformation, where $\overline{w_I}$ is considered to be zero.

Using the same number of layers as levels, or twice as many (a, b) does not change neither the frequency, which has a wavelength of about 6 months, nor the noise in the diagnosed diffusivity. Increasing the number of layers further (10 times as many than levels), there is still a longer time change with a wavelength of ~ 6 months, but this change is overlaid by fluctuations with a much higher frequency. Different to the results, where the diagnostic of the interfacial velocity was included, the variation of the diagnosed diffusivity κ_{diag_G} is now centred around the value of the weighted explicit diffusion coefficient κ_{w_G} (blue).

Similar results can be found for the experiment A_incr in Figure 6.15. Using the same number of layers as model levels (Figure 6.15 a), there is a $\sim 10\%$ variation around the expected values of the weighted diffusivity. Increasing the number of layers by a factor of two, the amplitude of the fluctuations also increases to maximal 12%. A further increase of the number of layers used for the transformation (Figure 6.15 c), does not lead to a further increase in the amplitude, only the frequency of the variations increases.

Similar to the previous results, the variations of the diagnosed diffusivity are centred around the weighted explicit diffusion coefficient. In comparison to the analysis including the approximation of the mean interfacial velocity, the amplitude of the variations in the diagnosed diffusivity is higher, the frequency is about the same, but the mean values are much closer to the value of the weighted explicit diffusion coefficient.

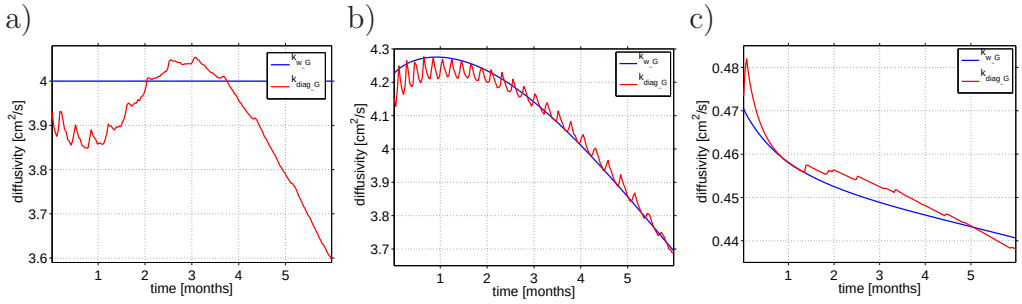

Figure 6.17: Diagnosed diffusivity κ_{diag_G} (red) and weighted diffusivity κ_{w_G} (blue) for experiments with fine resolved vertical grid (level thickness of $5\,m$) using twice as many layers than levels for the mapping: a) A_const, b) A_incr and c) A_oc.

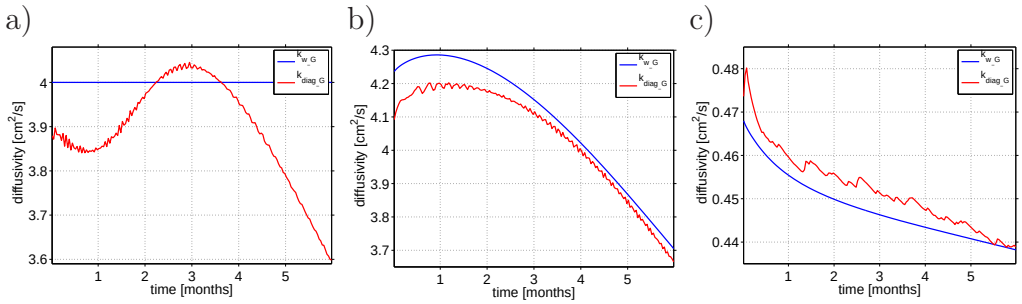

Figure 6.18: Diagnosed diffusivity κ_{diag_G} (red) and weighted diffusivity κ_{w_G} (blue) for experiments with fine resolved vertical grid (level thickness of $5\,m$) using 10 times as many layers than levels for the mapping: a) A_const, b) A_incr and c) A_oc.

In the last experiment, A_oc, the results of the diagnosed diffusivity are slightly different (Figure 6.15). The diffusive spreading of the tracer is so slow, that although, the transformation uses 10 times more layers than levels (Figure 6.15 c), the diagnosed diffusivity does not show high frequency fluctuations. The diagnosed diffusivity gives in all three cases close results compared to the weighted diffusivity, with a maximal difference of $\sim 5\%$.

These results show, in line with the analysis from Chapter 5, that the combination of the transformation of the tracer gradient and the diffusive movement of the isopycnals leads to spurious diffusion in the results. The symptoms in the results are the same compared to the ones found in the results of the experiments including vertical advection: the stability of the fluctuations and the decrease of the wavelength initiated by an increase in

the resolution of the transformation axis. In Chapter 5 the results showed, that the spurious diffusivity can be reduced by an increase in the vertical resolution of the model grid. Thus, the analysis of the diagnosed diffusivity will be repeated using a level thickness of $5\,m$ in the model set-up.

Figure 6.17 and 6.18 show the results of the diagnosed diffusivity κ_{diag_G} for a) experiment A_const, b) experiment A_incr and c) experiment A_oc. Twice as many layers than levels are used for the mapping in Figure 6.17 and 10 times more layers than levels in Figure 6.18.

The diagnosed diffusivity in experiment A_const does not differ much from the results of the experiments using the coarser vertical model resolution. The main difference between the results of the two model resolutions is the much smaller amplitude of the high frequency fluctuations. This suggest the possibility that the results show the induced diffusivity, which is caused by the divergence and convergence of the isopycnals.

Note that the definition of the tracer flux method infers on a comparison between the flux of the tracer through one isopycnal layer and the total change of the tracer above that layer. The diffusion of temperature and salinity leads to convergences and divergences of density fluxes. The density fluxes can be interpreted as isopycnals moving upwards or downwards, which in turn can lead to changes in the total amount of tracer above the isopycnal layer. This effect can cause an induced diffusivity, which only will be analysed by the diagnosed diffusivity κ_{diag_G}.

Figure 6.19 a) shows the temporal change of the density for experiment A_const. In this experiment, the isopycnals are converging, e.g. in the depth between 200 and $300\,m$, and at different depth diverging, e.g. after the second month above $200\,m$. This change in the direction of the isopycnal movement might result in an induced positive or negative diffusivity.

In the next two experiments, A_incr and A_oc, the results of the diagnosed diffusivity κ_{diag_G} are very close to the weighted explicit diffusivity coefficient κ_{w_G}. Similar to the results of the first experiment, the amplitude of the high frequency fluctuations are very small. That means,

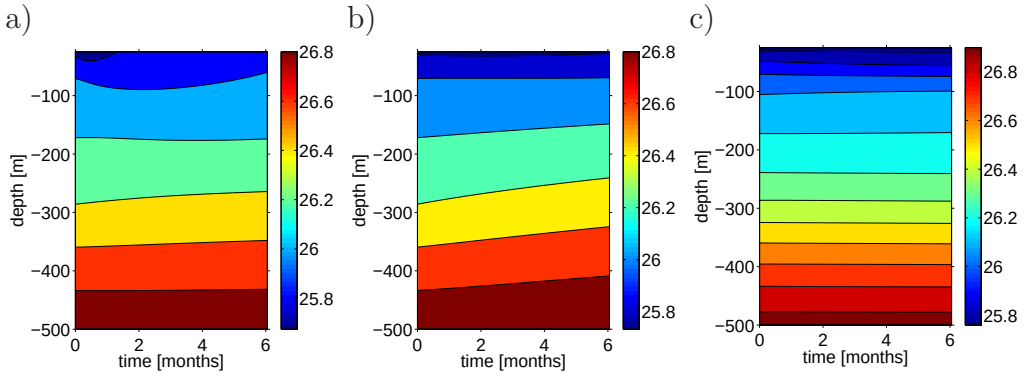

Figure 6.19: Density with time for the model set-up using a fine resolved vertical grid with a level thickness of $5m$: a) A_const, b) A_incr and c) A_oc.

there is only a very small amount of induced diffusivity in these experiments.

In order to link the difference between the diagnosed diffusivity κ_{diag_G} and the weighted explicit diffusivity coefficient κ_{w_G} to the time dependent change of the isopycnals, Figure 6.19 b) shows the density for experiment A_incr. At the beginning of the experiment, there is a slight convergence of the isopycnals in the region between 300 and 200 m depth, which is getting smaller with time. This can be linked to the slightly smaller diagnosed diffusivity during the first two months. The main feature in the behaviour of the isopycnals is the very strong nearly parallel movement of the isopycnals between 300 and 500 m, which might be the reason for the small amount of induced diffusivity.

In experiment A_oc, the vertical movement of the isopycnals is so slow, that one cannot say if and where the isopycnals are diverging and converging. This is consistent with the small difference between the weighted and the diagnosed diffusivity. Although, the uncertainty of the method might cause similar changes in the diagnosed diffusivity, which might be the reason for the difference between both values.

Note, in the analysis using the higher vertical model resolution, the effect of neglecting the mean interfacial velocity $\overline{w_I}$ in the diagnostics is of minor importance. The effect on the results of the diagnosed diffusivity is $< 0.1\%$.

Thus in the following of the thesis, the mean interfacial velocity is assumed to be zero ($\overline{w_I} = 0$).

In summary, it can be said that in these experiments the effect of the diffusive density on the tracer mapping leads to uncertainties in the results of $5 - 10\%$, depending on the value of the explicit diffusion coefficient. The diagnostics of the mean interfacial velocity in combination with a high number of layers used for the mapping leads to a sensitivity according to the mapping. Therefore, it is useful to neglect the analysis of the mean interfacial velocity.

An increase of the number of z-levels in the model, still shows high frequency fluctuations in the results of the diagnosed diffusivity, but the amplitude is very small. This indicates that the difference between the diagnosed and the weighted diffusivity is the amount of induced diffusivity, which is caused by the divergence and convergence of the isopycnal layers.

In the analysis described by Ledwell et al. (1998), the diagnosed diffusivity is estimated by neglecting the effect of the temporal diverging or converging isopycnals. They find errors of $\sim 11 - 17\%$, which they address mainly to the assumption of neglecting the effect that the isopycnals may diverge and converge. In the simple 1-dimensional model, using the coarser vertical resolution, the errors are slightly smaller, which occur here by the combination of the tracer mapping and the diverging and converging isopycnals.

6.3 Summary

In this chapter the analysis of the diagnosed diffusivity, using the variance and the tracer flux method, has been given for experiments in which tracer, temperature and salinity are diffusive. The diffusion in temperature and salinity leads to an interfacial movement of the isopycnal layers and results in a diverging or converging behaviour.

For the analysis of the diagnosed diffusivity using the variance method it is not necessary to transform the tracer onto isopycnals. The difference

between the diagnosed diffusivity $\kappa_{var}(z)$, analysed in z-levels, and the diagnosed diffusivity $\kappa_{var}(\sigma)$ is the artificial effect of the mapping on the diagnostics. As long as the model resolution is relatively coarse (level thickness of $20\,m$), the diagnosed diffusivity $\kappa_{var}(\sigma)$ shows high frequency fluctuations and the longer time mean is slightly larger compared to the results of $\kappa_{var}(z)$. An increase in the vertical resolution of the model (level thickness of $5\,m$) leads to a decrease in the fluctuations of $\kappa_{var}(\sigma)$ and the values for the longer time mean are consistent with the values of $\kappa_{var}(z)$.

The difference between $\kappa_{var}(z)$ and $\kappa_{var}(\sigma)$ is large, when the tracer gradient is strong. This is the case, when the model resolution is coarse and the tracer distribution is still narrow.

In the diagnostics of the tracer flux method the divergence or convergence of the isopycnal layers with time lead to changes in the temporal derivative of the total amount of tracer above an isopycnal. This can result in an artificially induced diffusion. For these experiments, the analysis of the mean interfacial velocity $\overline{w_I}$ is required. However, the effect of the tracer transformation onto isopycnals leads to major errors in the values for the diagnosed interfacial velocity. Therefore, it is useful to neglect the diagnosed interfacial velocity in the diagnostics.

The diagnosed diffusivity κ_{diag_G} in the experiment with the coarse vertical resolution shows changes with an amplitude of $\sim 8 - 10\%$, although a high number of layers is used for the transformation. An increase in the vertical model resolution leads to high frequency fluctuations with a very small amplitude. Additionally, the effect of the diagnosed interfacial velocity on the results of the κ_{diag_G} is smaller than 0.1%. Therefore, the diagnostics of the interfacial velocity can be neglected in the analysis of the tracer flux method.

Chapter 7

Summary: Part I

In this part, three different methods to analyse diagnosed diffusivities in one-dimensional models have been introduced. The divergence method and the tracer flux method both start from the advection-diffusion equation. The different approach of the variance method based on the variance decay of the tracer field.

Divergence method Analysing the diagnosed diffusivity by the divergence method tests in how far this method, which is introduced and used in a similar way by observationalists (Ledwell et al., 1993, 1998), can be used for the analysis of z-levels models. It turns out that as long as the diffusion acts on the tracer only, the values for the diagnosed and the weighted diffusivities are identical. The results are consistent independent of the definition of the vertical shape of the explicit diffusion coefficient in the model set-up and also independent of the z-level grid, either uniform or non-uniform.

For the analysis of diapycnal mixing in experiments, when the isopycnal layers are not constant with time, the transformation of the diagnostics from z-space into σ-space is necessary. The results of the diagnosed diffusivity are very sensitive with respect to changes in the resolution of the transformation, as shown in the sensitivity studies. It is not possible to modify the divergence method in order to get robust results.

In the analysis of the diapycnal diffusivity as introduced and used in the work of Ledwell et al. (1998), the tracer data reflect only a part of the injected tracer and therefore, it is necessary to inter- and extrapolate the tracer field onto the known isopycnal field. In the observational studies, the density structure of local profiles are well known with a high vertical resolution. The temporal change of the tracer concentration is analysed as a function of height above the target density surface, which is the density surface, where the tracer was initialised. With this transformation of the advection-diffusion equation effects caused by the parallel movement of the isopycnals are eliminated. For a model study, such a definition is not suitable, as the combination of the discrete and coarse model grid and the interpolation of the tracer field onto a high resolved density field lead to spurious changes in the vertical structure of the tracer, which are larger than changes inferring from the model integration itself.

The process neglected in the observational study (Ledwell et al., 1998) is the effect of diverging and converging isopycnals, which is found to be the main error source in their analysis. The results of the 1-dimensional case studies show, that converging or diverging isopycnals can result in a numerically induced diffusion.

Tracer flux method The diagnostics of the tracer flux method based on the analysis of the basin wide average value for the diagnosed diffusivity by Griffies et al. (2000), but is modified in such a way that the mean diffusivity of a tracer field is diagnosed. The results of experiments where diffusion acts on the tracer only showed consistent values for the diagnosed and the weighted diffusivities. Although the results are consistent within the tracer flux method itself, they cannot be directly compared to the results of the divergence method as the weighting of both methods differs. This means in general that for the comparison of different methods, it is always necessary to take into account how the values are weighted.

For the analysis of the diagnosed diffusivity in experiments where the isopycnals are not constant in time the tracer flux method also requires a transformation of the tracer onto σ-coordinates. The sensitivity studies

showed that a modification of the tracer flux method is necessary in order to get robust results with respect to changes in the resolution of the transformation. This modification is realised by the linear transformation of the tracer gradient onto isopycnal layers. As long as the transformation is not getting coarser than the density profiles in the model, the tracer flux method leads to robust results independent of the transformation axis used.

In order to analyse the effect of a parallel movement of the isopycnal layers on the robustness of the tracer flux method, experiments with an implemented constant vertical advection were shown. In these experiments, the density equation was chosen to be linear, in order to eliminate any diverging or converging effects in the temporal change of the isopycnal layers. The advection scheme used in this model is a centred differences scheme in space and a Eulerian backwards scheme in time. This is mainly dispersive, but might generate a small amount of numerically induced diffusivity as a result of the discretisation in time. However, the results show that the combination of the mapping and the vertical movement of the isopycnals lead to high changes in the diagnosed diffusivities. These changes depend linearly on the movement of the transformed tracer from one layer to the next one. The amplitude of these fluctuations decreases by an increase in the vertical resolution of the model grid. Considering mean values of these fluctuations over at least one wavelength, the values are of the order of $O(10^{-2}\,cm^2/s)$, which is about one order of magnitude larger than the numerically induced diffusion in this experiment. An increase in the vertical resolution of the model grid leads to a reduction of the mean values ($O(10^{-3}\,cm^2/s)$), which is still masking the numerically induced diffusion.

The effect of diverging or converging isopycnals on the results of the diagnosed diffusivity is even larger. An increase in the vertical resolution of the model grid to a level thickness of $5\,m$ leads to robust results with respect to changes in the resolution of the transformation used. The results suggest that diverging isopycnals lead to negative induced diffusivities and converging isopycnals to positive induced diffusivities.

In principle, it is also possible, analogue to the studies of Griffies et al.

(2000), to analyse the vertical behaviour (and only horizontal mean values) of the diapycnal diffusion by the tracer flux method. In the analysis described by GRIFFIES ET AL. (2000), a different transformation of the tracer onto isopycnals has been used.

In the study performed by GRIFFIES ET AL. (2000), the diapycnal diffusion of the density is analysed. Therefore the density is sorted to a reference density profile by keeping the information of both the density and the volume of each water parcel during the sorting. This leads to a significant amount of small scale structure as a result of the sorting map which interleaves the horizontal and the vertical stratification of the unsorted fluid. As a result, the analysed diapycnal diffusivity is extremely noisy. In order to avoid the influence of the mapping, vertical mean values for the density and also for the gradient are taken for the analysis in order to smooth out the fine vertical steps. Using the mapping introduced in the current study the analysis done by GRIFFIES ET AL. (2000) can be done without restrictions.

Variance method The diagnostics of the variance method are based on the analysis of the variance decay. The variance of the tracer, as defined here, is a depth independent value and depends only on the tracer concentration in each model box. This is a different approach compared to the one of the previous two methods, where the diffusive flux is the determining process for the analysis of the diagnosed diffusivity.

The Eulerian backwards time stepping scheme, which is used in this model to implement the explicit diffusion and the vertical advection, does not conserve the variance. The leads in the diagnosed diffusivities of the experiments in which diffusion acts on the tracer only to a numerically induced diffusivity, which depends on the time-step used. A decrease of the time-step results in a smaller amount of numerically induced diffusion. The vertical advection also generated a small amount of numerically induced diffusion ($\sim 1.7 \times 10^{-3}\, cm^2/s$ in the specific case shown). Diffusion in temperature and salinity do not generate changes in the tracer variance.

As in Part II of this thesis, diapycnal diffusivities in 2-dimensional case

studies will be analysed, it is useful to examine the effect of the tracer mapping on the robustness of the variance method. It turns out, that similar to the results of the tracer flux method, a constant vertical advection (also with the restriction, that the isopycnals are moving in an exactly parallel manner) leads to spurious fluctuations in the diagnosed diffusivities. This effect can be ascribed to the combination of the mapping and the vertical movement of the isopycnals. The diagnosed diffusivity depends linearly on the movement of the tracer concentration from one layer to the next one. The values are always larger than the values of diagnosed diffusivity analysed in z-levels.

An increase in the vertical resolution leads to a decrease of these spurious differences in the diagnosed diffusivities. However, the diagnosed diffusivity $\kappa_{var}(\sigma)$ shows high frequency fluctuations, but using a level thickness of $5\,m$, $\kappa_{var}(\sigma)$ is only $\sim 8\%$ larger than the exact value $\kappa_{var}(z)$. The combined effect the transformation into σ-coordinates and the vertical movement of the isopycnals, lead to spurious fluctuations in the diagnosed diffusivities analysed in σ-layers. However, these spurious fluctuations are very small ($< 1\%$).

Conclusion The diagnostics of the tracer flux and the variance method show that a fine resolved vertical grid is necessary in order to get robust results with respect to changes in the resolution of the tracer transformation. In these simple case studies the levels thickness is chosen to be $5\,m$. This is a value, which can be realised in OGCMs, as a higher vertical resolution might lead to problems in the surface circulation.

The 1-dimensional case studies show, that the results of the tracer flux method are very sensitive to the resolution of the transformations used as a result of the combined effect of the tracer mapping onto isopycnals and the movement of the isopycnal interfaces. The difficulties in applying this method in z-level models arise from these transformations. In isopycnal-coordinate models, the same approach can be used without restrictions, as there it is not necessary to transform the tracer onto isopycnals. The problem which arises from the transformation of the tracer

onto isopycnal layers also affects the other methods tested here to quantify diapycnal diffusion in a z-level model. Despite the difficulties in evaluating it, and its crudity as a measure of mixing, it is a familiar concept, whose values are immediately meaningful.

In general, the diapycnal diffusivity, in this study estimated by the diagnosed diffusivity, is the sum of the explicit diffusivity and the numerically induced diffusivity, a result of e.g. the discretisation of advection or an effect of converging and diverging isopycnals. The diagnosed vertical diffusivity is equal to the (suitably weighted) explicit diffusivity only where there is not numerically induced diffusivity, e.g. in the experiments in which the only process is vertical diffusion.

In the following the diagnostics of 2-dimensional case studies will be shown, where the experiments are restricted to the fine resolved vertical grid.

Part II

2-dimensional Experiments

Chapter 8

2-dimensional case studies: Diagnostics using the variance method

The results of the 1-dimensional case studies showed that it is possible to link the variance decay to a diapycnal diffusivity. In order to analyse OGCMs, the variance method introduced in Chapter 2 needs to be applied and tested in idealised experiments of higher dimensions. In this chapter, all the different cases shown in Part I of this thesis for the 1-dimensional experiments will be repeated for 2-dimensional experiments, including changes in the diagnostics that account for the additional dimension.

The analysis of 3-dimensional experiments is similar to that of 2-dimensional experiments. Thus, the results of the 2-dimensional experiments already gives an idea about what to expect for the analysis of OGCMs.

First, the variance method for the analysis of 2-dimensional case studies will be introduced. Second, the results using horizontal isopycnals will be shown and after that the same experiments will be repeated using a non-horizontal initial density field.

8.1 Changes in the method

Before it is possible to diagnose diffusivities in models with two dimensions, the method needs to be adapted. In general, the physics in higher dimensional experiments allow the tracer not only to move in the diapycnal direction, but more likely along the isopycnals. Therefore, it is necessary to separate the diapycnal mixing from the mixing along the isopycnals. This was not necessary for the analysis of the 1-dimensional experiments, as the diffusivity estimated by the variance decay was equivalent to the diapycnal diffusivity.

Diagnosed diffusivity In order to get an overview about the applicability of the variance method in 2-dimensional experiments, three different ways of analysing the variance decay will be introduced. In experiments with only vertical diffusion or vertical advection, the diagnosed diffusivity can be estimated from the decay of the sum of the variance in z-coordinates. This assumption is not suitable for a general analysis, as in this case, the variance decay caused by diapycnal mixing is not separated from the one caused by along isopycnal mixing. Therefore, the tracer will first be integrated along the isopycnal layers before estimating its variance. This step includes the transformation of the tracer onto isopycnals and the along isopycnal integration of the tracer, both potential sources of spurious mixing. Therefore, the effect of the tracer transformation onto isopycnals on the results will be shown separately, as well as the effect of the along isopycnal integration of the tracer.

First case In the first case, the diagnosed diffusivity is analysed by the decay of the integrated variance. In the 2-dimensional experiments, the variance σ^2 of the total tracer is given by

$$\sigma^2 = \frac{1}{2}\sum_{i=1}^{m}\left(\left(\sum_{k=1}^{n} C(i,k)^2 \Delta z(k)\right)\cdot \Delta x(i)\right), \tag{8.1}$$

where C is the tracer concentration in z-levels, Δz is the thickness and Δx

the horizontal width of each model box, n denotes the number of model levels and m the number of columns. Note, the temporal change of the variance σ^2, as given in Equation 8.1, is not separating between changes caused by diapycnal mixing and those due to along isopycnal mixing. The diagnosed diffusivity $\kappa_{var,z}$ in z-coordinates is defined as follows

$$\kappa_{var,z} = \frac{-\frac{\Delta\sigma^2}{\Delta t}}{\sum_{i=1}^{m}\left(\sum_{k=1}^{n}\left(\left(\frac{\Delta C(i,k)}{\Delta z(k)}\right)^2 \cdot \Delta z(k)\right) \cdot \Delta x(i)\right)}. \tag{8.2}$$

Note, this diagnosed diffusivity $\kappa_{var,z}$ will only be used as a reference value for the sensitivity studies with horizontal isopycnals (see Section 8.2).

Second case In the second case, the analysis of the diagnosed diffusivity is modified in such a way, that changes in the results are only an effect of the tracer mapping. The variance σ_s^2 of the transformed tracer is given in σ-coordinates by

$$\sigma_s^2 = \frac{1}{2}\sum_{i=1}^{m}\left(\left(\sum_{s=1}^{l} C_t(i,s)^2 \cdot \Delta z_t(i,s)\right) \cdot \Delta x(i)\right), \tag{8.3}$$

where C_t denotes the transformed tracer, Δz_t is the layer thickness of the density class and Δx the horizontal width of each model box, l denotes the number of layers of the used transformation and m the number of columns. The diagnosed diffusivity $\kappa_{var,\sigma}$ is then given by

$$\kappa_{var,\sigma} = \frac{-\frac{\Delta\sigma_s^2}{\Delta t}}{\sum_{i=1}^{m}\left(\sum_{s=1}^{l}\left(\left(\frac{\Delta C_t(i,s)}{\Delta z_t(i,s)}\right)^2 \cdot \Delta z_t(i,s)\right) \cdot \Delta x(i)\right)}. \tag{8.4}$$

Note, the difference between $\kappa_{var,z}$ and $\kappa_{var,\sigma}$ gives only evidence about the effect of the tracer transformation into σ-coordinates in the diagnostics, but is still not separating between diapycnal and isopycnal diffusivities.

The separation between the diapycnal and the isopycnal diffusivity is mainly important for the analysis of OGCMs, as the along isopycnal

diffusivity of the tracer is at least one order of magnitude larger compared to the diapycnal diffusivity and will therefore always mask that signal.

Third case In the third case, the analysis of the diagnosed diffusivity will be modified further in order to separate the diapycnal from the isopycnal component of the diagnosed diffusivity. For the realisation, the idea from the analysis done by LEDWELL ET AL. (1998) is used. This is basically a reduction of the, in this case, 2-dimensional tracer field to a 1-dimensional one, by averaging the tracer along the isopycnals, before the diagnosed diffusivity is estimated.

For the along isopycnal average, the mean tracer concentration C_{int} is defined as follows

$$C_{int}(s) = \frac{\sum_{i=1}^{m}(C_t(i,s) \cdot \Delta z_t(i,s) \cdot \Delta x(i))}{\sum_{i=1}^{m}(\Delta z_t(i,s) \cdot \Delta x(i))}, \tag{8.5}$$

where C_t denotes the transformed tracer, Δz_t is the layer thickness of the density class and Δx the horizontal width of each model box, m the number of columns and s denotes number of density classes used for the transformation. The variance σ^2_{int} of the averaged tracer is given by

$$\sigma^2_{int} = \frac{1}{2}\sum_{s=1}^{l}\left(C_{int}(s)^2 \cdot \Delta z_{int}(s)\right), \tag{8.6}$$

where $\Delta z_{int}(s) = \sum_{i=1}^{m}(\Delta z_t(i,s) \cdot \Delta x(i))$ denotes the integrated layer thickness.

When the tracer concentration is not spread equally along the isopycnal layer, the along isopycnal average of the tracer leads to a spurious mixing, as the tracer mass of different concentrations are mixed together. This spurious mixing might result in an artificial change of the variance decay.

For the diagnostics of the variance method, also the diapycnal tracer gradient needs to be determined. For the 2-dimensional case studies, it is necessary to average the transformed tracer along the isopycnal layers before estimating its diapycnal gradient. The sensitivity study of the

1-dimensional experiments showed (see Section 4.3) that the results are very sensitive to the mapping by analysing the gradient of the transformed tracer. This can be reduced by linearly interpolating the tracer gradient into σ-space.

To avoid these problems in the analysis of the 2-dimensional experiments, a similar assumption to that employed previously for the analysis of the 1-dimensional experiments is made. Instead of analysing the gradient of the integrated tracer concentration, the isopycnal mean value of the linearly (vertically) interpolated tracer gradient is taken. The averaged tracer gradient is denoted as $\overline{\Delta C_t/\Delta z_t}$.

This means that the diagnosed diffusivity $\kappa_{var\_int,\sigma}$ of the integrated tracer is given by

$$\kappa_{var\_int,\sigma} = \frac{-\frac{\Delta\sigma^2_{int}}{\Delta t}}{\sum_{s=1}^{l}\left(\left(\frac{\overline{\Delta C_t}}{\Delta z_t}\right)^2 \cdot \Delta z_{int}(s)\right)}, \tag{8.7}$$

where σ^2_{int} is the variance of the averaged tracer C_t, Δz_{int} is the horizontally integrated layer thickness and $\overline{\Delta C_t/\Delta z_t}$ is the isopycnal mean of the linearly transformed tracer gradient. Additionally to the analysis of the diagnosed diffusivity, it is necessary to compute the weighting of the explicit diffusion coefficient on the 2-dimensional grid in order to allow a comparison of the weighted diffusivity with the diagnosed one.

Weighted diffusivity The weighted diffusivity can be estimated in two different ways: first in z-coordinates, which is a useful way, as long as the isopycnals are horizontal. Second in σ-coordinates, which is the weighting used for the more general analysis.

The variance decay of the total tracer, which is given by the term of the explicit diffusivity in 2-dimensional experiments is given by

$$\frac{\Delta\sigma^2}{\Delta t} = \sum_{i=1}^{m}\left(\sum_{k=1}^{n}\left(\kappa_{expl}(i,k)\cdot\left(\frac{\Delta C(i,k)}{\Delta z(k)}\right)^2 \cdot \Delta z(k)\right)\cdot \Delta x(i)\right), \tag{8.8}$$

where C is the tracer concentration (in z-levels), Δz is the level thickness and Δx the horizontal width of each model box, n the number of model levels and m the number of horizontal units. By substituting Equation 8.8 into Equation 8.2, the weighted diffusivity $\kappa_{w,z}$ in z-coordinates is given by

$$\kappa_{w,z} = \frac{\sum_{i=1}^{m}\left(\sum_{k=1}^{n}\left(\kappa_{expl}(i,k)\cdot\left(\frac{\Delta C(i,k)}{\Delta z(k)}\right)^2\cdot\Delta z(k)\right)\cdot\Delta x(i)\right)}{\sum_{i=1}^{m}\left(\sum_{k=1}^{n}\left(\left(\frac{\Delta C(i,k)}{\Delta z(k)}\right)^2\cdot\Delta z(k)\right)\cdot\Delta x(i)\right)}. \tag{8.9}$$

In order to estimate the explicit diapycnal flux of the tracer in σ-coordinates, the explicit diffusion coefficient needs to be interpolated onto isopycnals. The linear interpolated explicit diffusion coefficient will be denoted as $\kappa_{expl,\sigma}$ in the following. The tracer gradient is invariant to a transformation from z- space into σ-space. Thus, the weighted diffusivity $\kappa_{w,\sigma}$ is given by

$$\kappa_{w,\sigma} = \frac{\sum_{i=1}^{m}\left(\sum_{s=1}^{l}\left(\kappa_{expl,\sigma}(i,s)\cdot\left(\frac{\Delta C_t(i,s)}{\Delta z_t(i,s)}\right)^2\cdot\Delta z_t(i,s)\right)\cdot\Delta x(i)\right)}{\sum_{i=1}^{m}\left(\sum_{s=1}^{l}\left(\left(\frac{\Delta C_t(i,s)}{\Delta z_t(i,s)}\right)^2\cdot\Delta z_t(i,s)\right)\cdot\Delta x(i)\right)}, \tag{8.10}$$

where C_t is the transformed tracer concentration and z_t the transformed depth. The difference between the weighted diffusivity $\kappa_{w,\sigma}$ and the diagnosed diffusivity $\kappa_{var\_int,\sigma}$ is the amount of induced diffusivity caused by the artefacts of the model discretisation, only if the tracer mapping and the along isopycnal integration do not lead to an additional spurious diffusivity in the results.

In the following, first, results of the experiments with horizontal isopycnals will be shown including the analysis of the sensitivity of the transformation onto isopycnals. The results will focus on a comparison of the different diagnosed diffusivities, as this gives evidence about the influence of the transformation on the method and the along isopycnal integration of the

tracer concentration. Second, the analysis for the same experiments will be repeated using an initial density field with non-horizontal isopycnals, as it is expected in the interior ocean in coarse resolution OGCMs.

8.2 Results: horizontal isopycnals

In this section, experiments with horizontal isopycnals will be analysed. A sensitivity study of the dependence of the results on the number of layers used for the tracer mapping gives evidence about the robustness of the analysis. Additionally, the effect caused by the additional mixing due to the along isopycnal integration of the tracer will be shown. This will be realised by two different initial tracer conditions.

As long as the isopycnals are horizontal, the weighted diffusivity $\kappa_{w,z}$ analysed in z-coordinates gives the same results as the weighted diffusivity $\kappa_{w,\sigma}$ analysed in σ-coordinates; therefore only the results of $\kappa_{w,z}$ will be shown in this section. In the following, it will be focused on possible sources of spurious mixing in the analysis of $\kappa_{var\_int,\sigma}$.

The structure of the following section is similar to the analysis of the 1-dimensional case studies. First, experiments are shown in which only the tracer is diffusive. Second, the effect of vertical advection is analysed. Finally, results for the experiments including diffusion in tracer, temperature and salinity are shown. But before this, an overview of the model configuration and the experimental set-up will be given in more detail.

8.2.1 Model configuration and experiments

The results of the 1-dimensional experiments showed, that a high vertical resolution of the model leads to more robust results. This was especially the case in experiments with implemented vertical advection or with additional diffusion in temperature and salinity. Therefore, the

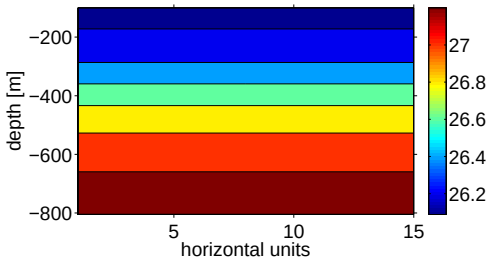

Figure 8.1: Initial density field for the 2-dimensional case studies with horizontal isopycnals.

2-dimensional experiments are limited to the model set-up using a high vertical resolution with a level thickness of $5\,m$.

The horizontal grid is chosen to be equidistant and has an arbitrary number of 15 equidistant horizontal boxes. The width of the horizontal boxes is defined to be equal to 1.

The diffusion and later the advection scheme in the 2-dimensional model are implemented as a Eulerian backwards scheme, the same as used in the 1-dimensional configuration. The diffusion and advection are both realised in the model with a centred differences scheme. Note, that the experiments are only used to test the robustness of the methods of diagnosing diffusion and weighting the explicit diffusion coefficient in a more dimensional model and to see the influence of the used density regime.

The initial density condition is shown in Figure 8.1, where the isopycnals are horizontal. Note, the density is not linearly increasing with depth, which is different to the configuration of the 1-dimensional experiments, but is a closer realisation for a comparison with the non-horizontal initial density field used in Section 8.3 (non-horizontal isopycnals in the initial density field).

In general, mimicking the tracer release experiments described by Ledwell et al. (1998) in OGCMs, the tracer must be initialised in the model in one single model box. As a results of advection and diffusion, the tracer spreads along the isopycnal layers and also in a diapycnal manner. In the idealised 2-dimensional case studies, there is no horizontal movement of the tracer included. This means that initialising the tracer in one model box leads to exactly the same results as shown for the 1-dimensional experiments.

Shortly after releasing the tracer in the ocean (similar in OGCMs), the

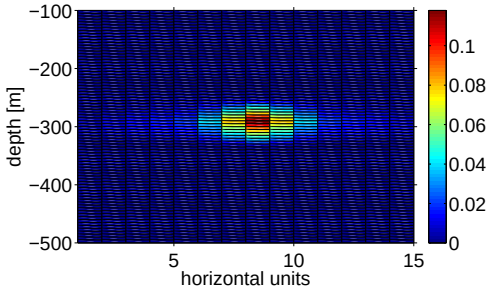

Figure 8.2: Initial tracer field, with a tracer maximum in the middle and fading concentration towards the outer sides; isopycnals are horizontal.

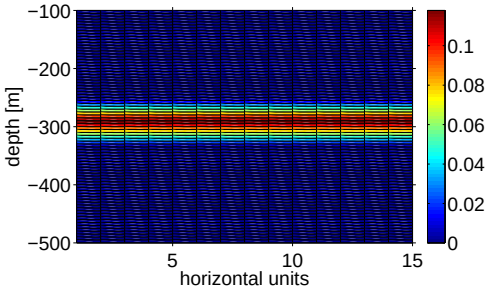

Figure 8.3: Initial tracer field, where the tracer is equally labelled along one isopycnal layer; isopycnals are horizontal.

tracer is concentrated at its releasing position with areas of low concentration around that maximum. After some time, the tracer maximum is less sharp and the concentration is spread more equally on the isopycnal layers. To mimic these two different distribution in the idealised 2-dimensional case studies, two initial tracer conditions are defined.

In Figure 8.2, the idealisation of the first case is shown. The tracer maximum is concentrated in the middle of the horizontal field with a fading concentration towards the outer sides; which is denoted as horizontally varying initial tracer condition. Figure 8.3 shows the idealisation of the second case, where the tracer mass is equally spread along the isopycnal layer, which is denoted as equally labelled initial tracer condition in the following.

This model set-up will be used to repeat the same experiments as discussed for the 1-dimensional model: first, experiments in which diffusion acts on the tracer only, second, where vertical advection is added and third, experiments in which diffusion acts on tracer, temperature and salinity. In the experiments including only vertical diffusion, either in the tracer field or additionally in the temperature and salinity fields, a variation of the explicit diffusion coefficient is used (analogous to the 1-dimensional case studies):
(i) A_const with a constant explicit diffusion coefficient ($4\,cm^2/s$),
(ii) A_incr where the explicit diffusion coefficient is linearly increasing

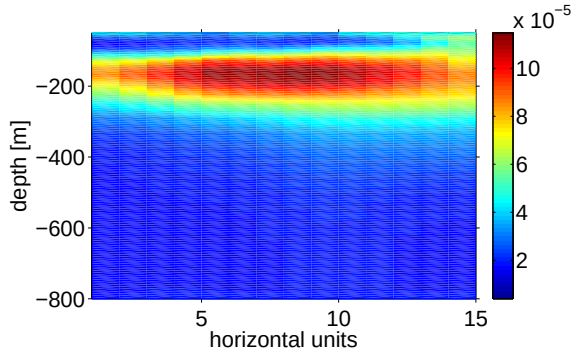

Figure 8.4: Field of the non-linear explicit diffusion coefficient as used in experiment *A_oc*; isopycnals are horizontal.

Experiment	explicit diffusion coefficient
A_const	constant with x and z
A_incr	linearly increasing with σ,constant with x
A_horiz	linearly decreasing with x, constant with depth
A_oc	non-linear in both dimensions

Table 8.1: Experiments of the 2-dimensional case studies.

with sigma and

(iii) *A_oc* where the explicit diffusion coefficient is non-linear with depth and also along the horizontal unit (Figure 8.4).

Note, the explicit diffusion coefficient in experiment *A_incr* is defined to be constant along the isopycnals, so it is linearly increasing with the density.

In 2-dimensional experiments, it is also possible to vary the explicit diffusion coefficient along the horizontal direction. Therefore, results of a fourth experiment, *A_horiz*, will be shown, where the explicit diffusion coefficient decreases linearly from 3.1 to $0.2\,cm^2/s$ along the horizontal direction and stays constant with depth. Table 8.1 gives an overview of all four experiments.

8.2.2 Diffusion acts on the tracer only

For the experiments shown in this section, it is not necessary to transform the tracer onto isopycnals or to diagnose the diffusivity of the along isopycnal integrated tracer, as the isopycnals are horizontal and the vertical

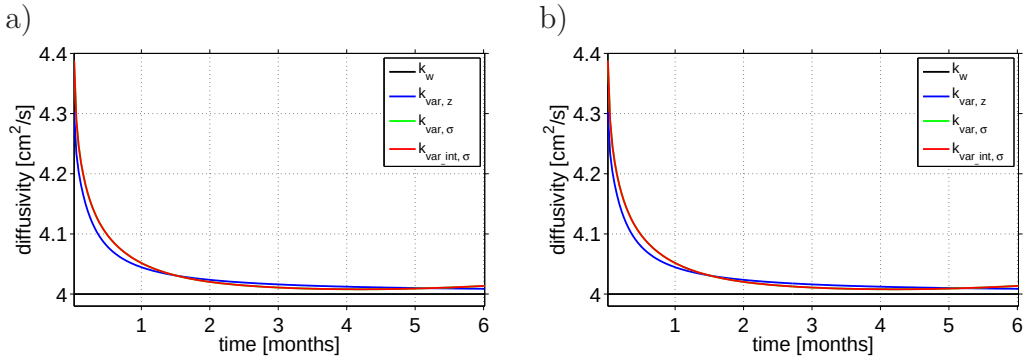

Figure 8.5: Diffusivities for experiment *A_const* (2-dimensional), diffusion acts on tracer, isopycnals are horizontal: a) horizontally varying initial tracer condition, b) initial tracer is equally labelled along one isopycnal.

diffusion acts on the tracer only. Therefore, the following experiments will be taken as sensitivity studies to analyse the effect of the tracer mapping onto isopycnals and the along isopycnal integration of the tracer on the results of the diagnosed diffusivity.

The effect of the transformation of the tracer onto σ-coordinates on the results of the weighted diffusivity $\kappa_{w,\sigma}$ is very small ($\sim 0.3\%$). The focus in this section is the comparison of the diagnosed diffusivities. Thus only the results of $\kappa_{w,z}$ will be shown in this section and the notation is reduced to κ_w.

As long as the resolution of the transformation is chosen to be coarser than the density profiles in the model, the results are robust (maximal changes of 1%) according to changes in the resolution of the transformation axis used. For the results shown in the following, twice as many layers than model levels are used for the transformation of the tracer and the tracer gradient.

Figure 8.5 shows the results for the diagnosed and the weighted diffusivities in experiment *A_const*. The results are independent of the initial tracer condition used. The values for the weighted diffusivity $\kappa_{var,z}$ are identical with the constant value of $4\,cm^2/s$ of the explicit diffusion coefficient.

The diagnosed diffusivity $\kappa_{var,z}$ (blue) essentially gives the exact value for the diffusivity in this experiment, without any error caused by the mapping or the interpolation of the tracer. The values for the diagnosed diffusivities

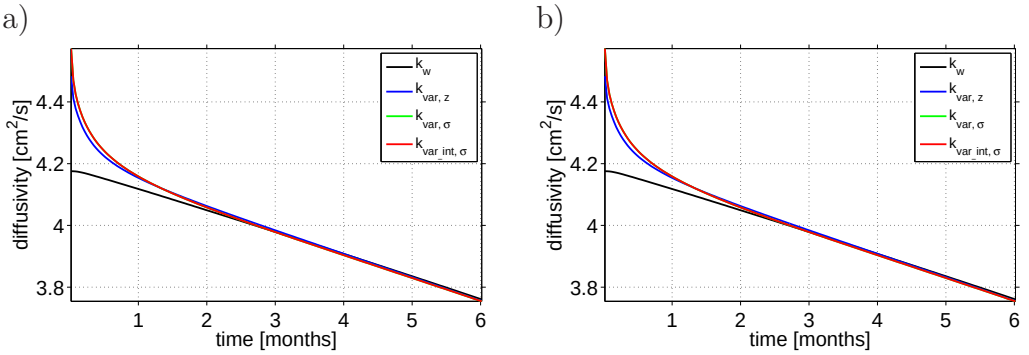

Figure 8.6: Diffusivities for experiment *A_incr* (2-dimensional), diffusion acts on tracer, isopycnals are horizontal: a) horizontally varying initial tracer condition, b) initial tracer is equally labelled along one isopycnal.

$\kappa_{var,\sigma}$ (green) and $\kappa_{var\_int,\sigma}$ (red) are identical, therefore $\kappa_{var,\sigma}$ cannot be seen separately in Figure 8.5. This means that there are no differences resulting from the along isopycnal integration of the tracer. The only differences ($< 1\%$) are caused by the interpolation of the tracer and the tracer gradient onto isopycnals. An increase in the number of layers used for the mapping is reducing this effect.

Similar to the results of the previous experiment, the results for the diagnosed and weighted diffusivities of experiment *A_incr* (Figure 8.6) are independent of the initial tracer condition used. At the beginning of the experiment, the difference between κ_w and $\kappa_{var,z}$ shows, that the amount of numerically induced diffusion is similar to the one in the analogous 1-dimensional experiment. The results for the diagnosed diffusivities $\kappa_{var,\sigma}$ and $\kappa_{var\_int,\sigma}$ are identical, and very similar to the ones of $\kappa_{var,z}$. The effect of the mapping is small ($< 1\%$) and decreases further with an increase in the resolution of the transformation.

For the two shown experiments, *A_const* and *A_incr*, the results are independent of the initial tracer condition used. The explicit diffusion in both experiments is defined to be constant along the isopycnals and as both initial tracers are released in the same isopycnal layer, the values for the diagnosed diffusivities have to be identical.

As long as the explicit diffusion stays constant along the isopycnals, the mean tracer gradient is changed in exactly the same way, as the

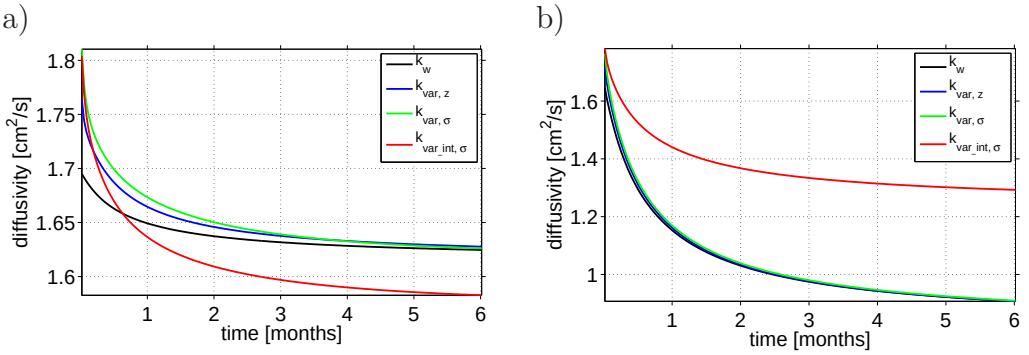

Figure 8.7: Diffusivities for experiment *A_horiz* (2-dimensional), diffusion acts on tracer, isopycnals are horizontal: a) horizontally varying initial tracer condition, b) initial tracer is equally labelled along one isopycnal.

concentration is mixed along the isopycnals. Therefore, the results for $\kappa_{var,\sigma}$ and $\kappa_{var\_int,\sigma}$ have to be identical as shown in the results.

In experiment *A_horiz* (Figure 8.7) the explicit diffusion coefficient is linearly decreasing along the horizontal distance and stays constant with depth. Different to the results of the previous two experiments, the diagnosed and the weighted diffusivities differ with respect to the used initial tracer condition, which can be ascribed to the along isopycnal variation of the explicit diffusion coefficient used.

Using the horizontally varying initial tracer condition (Figure 8.7 a), the difference between κ_w (black) and $\kappa_{var,z}$ (blue) is $\sim 3\%$ at the beginning with a converging behaviour during the experiment. The effect of the tracer mapping leads to a slightly larger diffusivity $\kappa_{var,\sigma}$ ($\sim 0.6\%$) during the first half of the experiment and the results are consistent with the values of $\kappa_{var,z}$ during the rest of the experiment. The along isopycnal integration of the tracer has a large effect on the results. Although the values of $\kappa_{var\_int,\sigma}$ are very similar to the ones of $\kappa_{var,\sigma}$ at the beginning of the experiment, towards the end $\kappa_{var\_int,\sigma}$ is $\sim 3\%$ smaller than $\kappa_{var,\sigma}$.

Using the equally labelled initial tracer condition (Figure 8.7 b), the results for the diagnosed diffusivities $\kappa_{var,z}$ and $\kappa_{var,\sigma}$ are almost identical with the ones of the weighted diffusivity κ_w. This means that there is no numerically induced diffusivity in this experiment and the tracer mapping does not lead to a spurious diffusivity in $\kappa_{var,\sigma}$. The along isopycnal integration of the

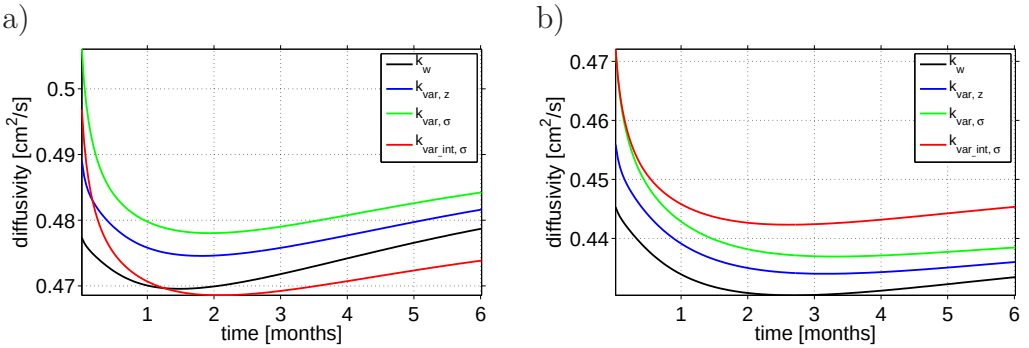

Figure 8.8: Diffusivities for experiment *A_oc* (2-dimensional), diffusion acts on tracer, isopycnals are horizontal: a) horizontally varying initial tracer condition, b) initial tracer is equally labelled along one isopycnal.

tracer leads to a maximum difference of $\sim 40\%$ between $\kappa_{var\_int,\sigma}$ and $\kappa_{var,\sigma}$ at the end of the experiment.

The variation of the explicit diffusivion along the isopycnals leads to spurious changes in the diagnosed diffusivity $\kappa_{var\_int,\sigma}$. The spurious mixing of the tracer concentration leads to artificial changes in the variance decay different to the spurious changes in the mean tracer gradient.

In the last experiment, *A_oc* (Figure 8.8), the explicit diffusion coefficient is changing with depth and additionally along the horizontal distance. Therefore, the results are expected to show the effects caused by the vertical variation of the explicit diffusivity as well as the effects by the horizontal variation.

Using the horizontally varying initial tracer condition (Figure 8.8 a), the numerically induced diffusivity, given by the difference between κ_w (black) and $\kappa_{var,z}$ (blue), is $\sim 2\%$ at the beginning decreasing to $\sim 0.6\%$. The effect of transforming the tracer into σ-coordinates, given by the difference between $\kappa_{var,z}$ and $\kappa_{var,\sigma}$, leads to a further increase of the diagnosed diffusivity of 0.6%. The along isopycnal integration of the tracer leads to $\sim 2\%$ smaller values for the results of $\kappa_{var\_int,\sigma}$ towards the end of the experiment, whereas at the beginning this effect is nearly zero. The spurious mixing caused by the transformation and the along isopycnal integration of the tracer is larger than the numerically induced diffusivity and masking its signal.

Using the equally labelled initial tracer condition (Figure 8.8 b), the difference between κ_w, $\kappa_{var,z}$ and $\kappa_{var,\sigma}$ is slightly smaller compared to the ones shown for the horizontally varying initial tracer condition. The along isopycnal integration of the tracer leads to an increase of the diagnosed diffusivity of $\sim 2\%$ towards the end of the experiment, whereas at the beginning there is no difference between the values of $\kappa_{var,\sigma}$ and $\kappa_{var\_int,\sigma}$.

In summary, it can be said that the effect of the tracer mapping on its own on the results is very small (1%). By increasing the number of layers used for the transformation, this small effect can be reduced further.

As long as the explicit diffusion is constant along the isopycnal layers, the along isopycnal integration of the tracer does not lead to any spurious diffusion in the results, $\kappa_{var,\sigma}$ and $\kappa_{var\_int,\sigma}$ are identical. Whereas the along isopycnal integration of the tracer field leads to a spurious diffusivity which is larger than the numerically induced diffusivity. In these cases it is not possible to draw conclusions about the numerically induced diffusivity from the values of $\kappa_{var\_int,\sigma}$.

For the analysis of OGCMs this means that in general it is not possible to separate the diapycnal and the isopycnal mixing by integrating the tracer isopycnally before estimating its variance decay. Only in the special case, where the vertical diffusion is constant along the isopycnals it seems possible. As the isopycnals are restricted to be horizontal and there is only vertical diffusion implemented in these experiments, further experiments need to be done in order to get more general results.

8.2.3 The effect of vertical advection

In this section, experiments will be analysed where vertical advection is implemented in the model with a centred differences scheme in space and a Eulerian backwards scheme in time. The vertical velocity is constant with a value of $4 \times 10^{-6}\, m/s \approx 0.35\, m/day$ with a downwards direction, the same as chosen in the analogous 1-dimensional experiments shown in Chapter 5.

The implemented advection acts on temperature and salinity and the

corresponding effect in density can be interpreted as a vertical movement of the isopycnal layers. In order to restrict this movement to be exactly parallel, it is necessary to define the density to be a linear function of e.g. the temperature. Additionally, the temperature in this case is chosen to be linear as well. Firstly, results will be shown, where the vertical movement of the isopycnals is parallel, without converging and diverging effects. Secondly, the same experiment will be repeated using the non-linear density equation as it is done for the analysis of OGCMs, in order to be able to compare the results with the ones of the analogous experiment using non-horizontal isopycnals. In the second case, temperature and salinity are not restricted to be linear with depth.

As the isopycnals are defined to be horizontal in this section, the implemented advection leads in both cases to a horizontally uniform change in the isopycnal layers. This means that the along isopycnal integration of the tracer does not lead to a spurious diffusivity in the results. Therefore, only the results for $\kappa_{var,z}$ and $\kappa_{var\_int,\sigma}$ will be compared, the difference is the spurious diffusivity caused by the tracer transformation into σ-space.

The results in the previous section showed that as long as the explicit diffusion coefficient is constant along the isopycnals the results are indifferent to the initial tracer condition used. The same effect can be seen in the results of the experiment with vertical advection. The diagnostics for both initial tracer conditions give exactly the same results, therefore only one Figure will be shown.

In Figure 8.9 a) the results for the diagnosed diffusivity $\kappa_{var,z}$ (blue) and $\kappa_{var\_int,\sigma}$ (red), where twice as many layers than levels are used for the transformation, are shown for the experiment using the linear density equation. The differences between $\kappa_{var,z}$ and $\kappa_{var\_int,\sigma}$ are small ($\sim 3\%$) and similar to the ones shown for the 1-dimensional experiments. A further increase in the number of layers used for the transformation leads to an increase in the frequency of the fluctuations in $\kappa_{var\_int,\sigma}$, but not to a further reduction of the amplitude.

In the second experiment (8.9 b), the chosen density equation is non-linear.

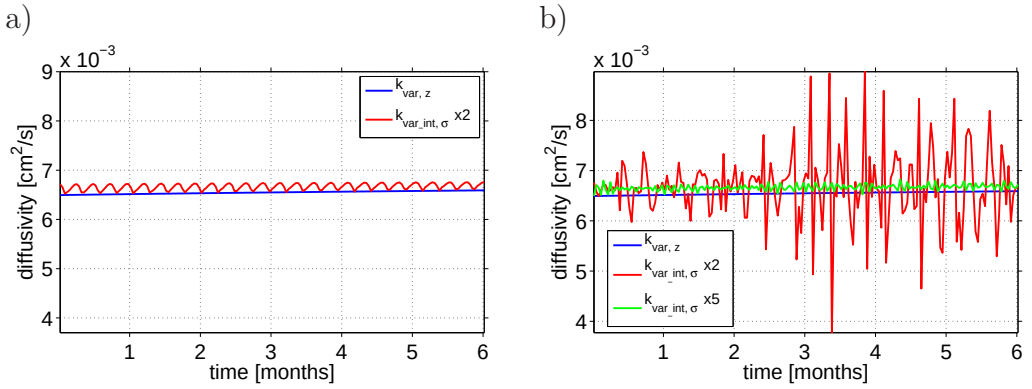

Figure 8.9: 2-dimensional experiment including vertical advection (horizontal isopycnals): diagnosed diffusivity $\kappa_{var,z}$ (blue) and $\kappa_{var\_int,\sigma}$ using twice as many layers than levels (red) and 5 times more than levels (green), a) linear density equation and b) realistic density estimation.

The vertical movement of the isopycnal layers in this case is not restricted to be exactly parallel, but can also have slightly converging and diverging components. The values for the diagnosed diffusivity $\kappa_{var,z}$ are consistent with the ones using the linear equation in the density.

Using twice as many layers than model levels for the mapping, the diagnosed diffusivity $\kappa_{var\_int,\sigma}$ (red) shows variations with an amplitude of $\pm 3.5 \times 10^{-3}\, cm^2/s$, which is about one order of magnitude larger compared to results in Figure 8.9 a) where the linear density equation has been used. An increase in the resolution of the transformation axis by using 5 times more layers than levels for the mapping reduces this effect. The amplitude decreases to $\pm 0.15 \times 10^{-3}\, cm^2/s$, which is similar to the results shown in Figure 8.9 a). A further increase in the number of layers used for the mapping does not lead to a further reduction in the amplitude of the high frequency fluctuations in $\kappa_{var\_int,\sigma}$.

The high amplitude in the fluctuations of $\kappa_{var\_int,\sigma}$ in the case where twice as many layers than levels are used for the mapping, can be ascribed to the fact that although the number of layers of the transformation axis are the same, the resolution in the region of interest is coarser compared to the analogous case, where the density is chosen to be linear. This coarser resolution leads to a spurious mixing as a result of the tracer mapping.

The mean values of the diagnosed diffusivity $\kappa_{var\_int,\sigma}$ give only a very small variation of maximal 0.5% with respect to the changes in the resolution of the transformation axis. More generally, the mean values of $\kappa_{var\_int,\sigma}$ are overestimating the diagnosed diffusivity $\kappa_{var,z}$ by $\sim 3\%$.

In summary, the results for the weighted and the diagnosed diffusivities are independent of the used initial tracer condition. Additionally, the interpolation of the tracer does not cause spurious changes in the results. Using the linear density equation, the results for the diagnosed diffusivities $\kappa_{var,z}$ and $\kappa_{var\_int,\sigma}$ are consistent with the results of the analogous 1-dimensional experiments. A change in the density assumptions leads to a major increase in the amplitude of the diagnosed diffusivity $\kappa_{var\_int,\sigma}$ when twice as many layers than levels are used for the transformation. An increase in the resolution of the transformation axis reduces this effect and leads to a consistency in the values of κ_{var} when the density is chosen to be linear.

For the analysis of the diapycnal diffusion in σ-space, the resolution of the transformation needs to be higher than the resolution of the density profiles in the model, similar as seen in the diagnosed diffusivities of the 1-dimensional experiments in Chapter 5.

8.2.4 Diffusion acts on tracer, temperature and salinity

In the experiments shown in this section not only the tracer but also temperature and salinity are diffusive. The corresponding effect in the density can be interpreted as an interfacial movement of the isopycnal layers. As in the current section, the analysis is restricted to experiments with horizontal isopycnals, only the results of the experiments *A_const* and *A_incr* will be shown. In *A_oc* and *A_horiz* the explicit diffusivity coefficient does not stay constant along the isopycnals, which leads to non-horizontal layers.

In the following, twice as many layers than levels are used for the tracer

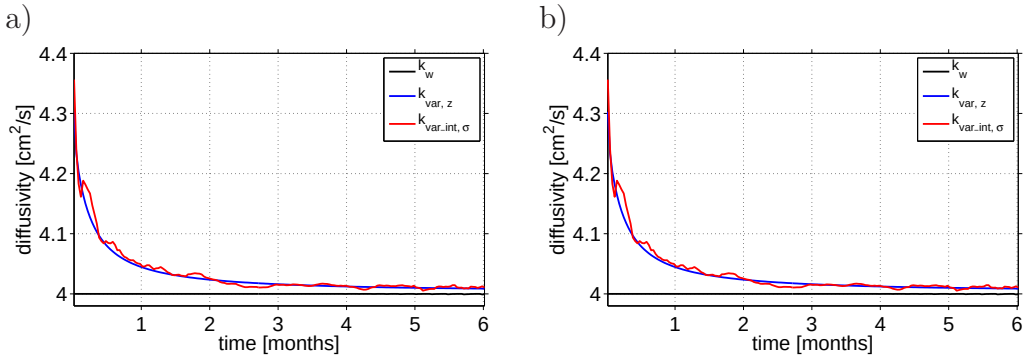

Figure 8.10: Diffusivities for experiment *A_const* (2-dimensional), diffusion acts on tracer, temperature and salinity, isopycnals are horizontal: a) horizontally varying initial tracer condition, b) initial tracer is equally labelled along one isopycnal.

mapping. An increase in the number of layers used for the mapping leads to an increase of the frequency of the fluctuations, but only to a small decrease in the amplitude.

As the variance of the tracer is not affected by the interfacial movement of the isopycnals, the results for the diagnosed diffusivities $\kappa_{var,z}$ and the weighted diffusivity κ_w are identical to the ones shown for the experiments where only the tracer was diffusive (see also Section 8.2.2). Additionally, as seen in Section 8.2.2, the results for the diagnosed diffusivities $\kappa_{var,\sigma}$ and $\kappa_{var\_int,\sigma}$ are identical as long as the explicit diffusion coefficient stays constant along the isopycnal layers, which is the case in the following experiments. Therefore, the results of $\kappa_{var\_int,\sigma}$ will be compared with the ones of $\kappa_{var,z}$ and the difference is the spurious diffusivity which results from the tracer mapping.

The results of experiment *A_const* (Figure 8.10) are independent of the used initial tracer condition, as the explicit diffusion coefficient is constant along the horizontal distance. The weighting of a constant diffusivity is always consistent with the value of that diffusivity, thus the results for the weighted diffusivities $\kappa_{w,z}$ and $\kappa_{w,\sigma}$ are identical and equal $4\,cm^2/s$. In Figure 8.10, the weighted diffusion is shown by κ_w (black).

As expected, the results for the diagnosed diffusivity $\kappa_{var,z}$ are consistent with the ones of the analogous experiments where the diffusion acts on the

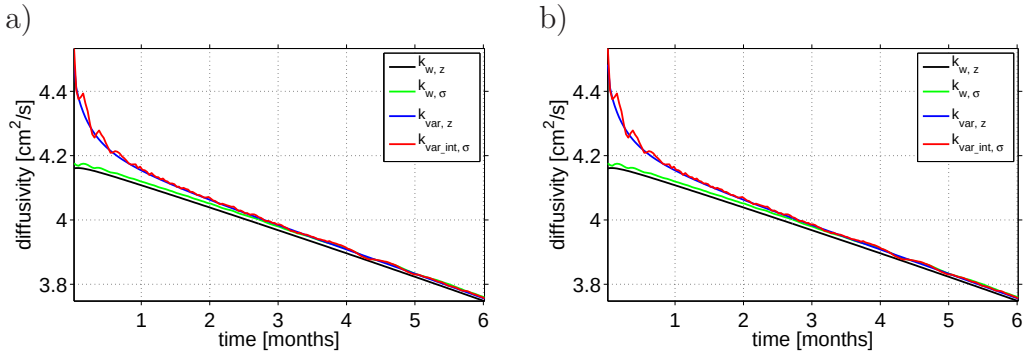

Figure 8.11: Diffusivities for experiment *A_incr* (2-dimensional), diffusion acts on tracer, temperature and salinity, isopycnals are horizontal: a) horizontally varying initial tracer condition, b) initial tracer is equally labelled along one isopycnal.

tracer only. The tracer mapping into σ-space leads to small scale fluctuations in the values for $\kappa_{var\_int,\sigma}$ around the values of $\kappa_{var,\sigma}$. The spurious diffusivity generated by the tracer mapping is much smaller than the numerically induced diffusivity.

In experiment *A_incr*, the results for the weighted and the diagnosed diffusivity are also independent of the initial tracer condition used (Figure 8.11). The diagnosed diffusivitiy $\kappa_{var\_int,\sigma}$ shows small scale fluctuations around the values of $\kappa_{var,z}$. An increase in the number of layers used for the transformation results in an increase of the frequency, but there are no significant changes in the amplitude of the fluctuations in $\kappa_{var\_int,\sigma}$.

For the analysis of the experiments with non-horizontal isopycnals, the weighted diffusivity will be analysed with respect to the isopycnal layers. To test the robustness of the mapping, the results of $\kappa_w(z)$ and $\kappa_w(\sigma)$ are both given in Figure 8.11. The difference between the weighted diffusivities $\kappa_w(z)$ and $\kappa_{w,\sigma}$ are very small ($\sim 0.3\%$), with an off-set like character. Although it is not resolved in Figure 8.11, the weighted diffusivity $\kappa_{w,\sigma}$ shows fluctuations with a similar frequency as seen for $\kappa_{var\_int,\sigma}$ and a very small amplitude.

Similar to the results of the 1-dimensional experiments, diffusion in temperature and salinity does not lead to changes in the diagnosed diffusivities analysed by the variance method. As an effect of the tracer

mapping, the results of the diagnosed diffusivity $\kappa_{var\_int,\sigma}$ show small scale fluctuations around the values of $\kappa_{var,z}$. This means, that it is possible to analyse the diapycnal diffusivity by integrating the tracer along the isopycnals before estimating its variance decay. Note, this result is restricted to experiments where the explicit diffusivity is constant along the isopycnal layers.

The effect of the transformation on the results of the weighted diffusivity $\kappa_{w,\sigma}$ is so small that in the following analysis only the results of $\kappa_{w,\sigma}$ will be shown for the values of the weighted diffusivity.

8.3 Results: isopycnals as in the ocean interior

In this section, the same experiments as shown in Section 8.2 will be repeated using a non-horizontal initial density field in the model set-up. As the isopycnals in this section are not horizontal any longer, the initial tracer conditions need to be redefined on the new isopycnal field, which will be shown in the next section. In the following, the diagnosed and the weighted diffusivity will be analysed in σ-coordinates only. The difference between $\kappa_{var,\sigma}$ and $\kappa_{var\_int,\sigma}$ gives evidence about the effect of the along isopycnal integration of the tracer.

8.3.1 Changes in the initial conditions

The model configuration is the same as described in Section 8.2.1, except the initial density and the initial tracer conditions are chosen to be different. The initial density field is shown in Figure 8.12, which is similar to the one expected in a low resolution OGCM (e.g. 4/3°). Note, in the interior the isopycnals are not parallel, the horizontal gradient is small in comparison to the vertical one and they also slightly diverge along the horizontal direction.

Figure 8.13 shows the initial tracer condition where the tracer maximum is located in the middle of the isopycnal layer and the concentration is fading

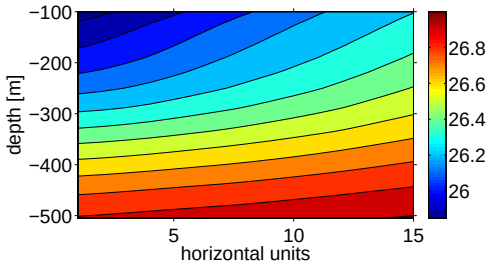

Figure 8.12: Initial density field for the 2-dimensional case studies using non-horizontal isopycnals.

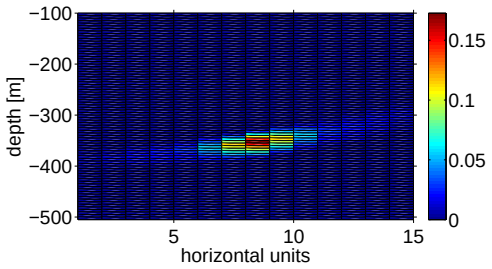

Figure 8.13: Isopycnally varying initial tracer condition: initial tracer field, with a tracer maximum in the middle and fading concentration towards the outer sides; isopycnals are non-horizontal.

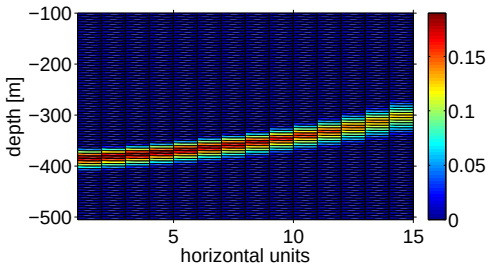

Figure 8.14: Equally labelled initial tracer condition: the tracer is equally labelled along one isopycnal layer; isopycnals are non-horizontal.

towards the outer sides of that isopycnal layer; also denoted as isopycnally varying initial tracer condition. The second initial tracer condition is shown in Figure 8.14. There the tracer mass is spread equally along the isopycnal layer; thus it is also denoted as equally labelled initial tracer condition. As the isopycnals diverge towards the western side, the equal spreading of the initial tracer mass leads to a decrease in its concentration.

In the following, first results of experiments in which the vertical diffusion acts on the tracer only will be presented including a comparison of the different ways of analysing the diagnosed diffusivity. Second, the effect of the vertical advection is analysed followed by the diagnostics of experiments where the vertical diffusion acts also on temperature and salinity.

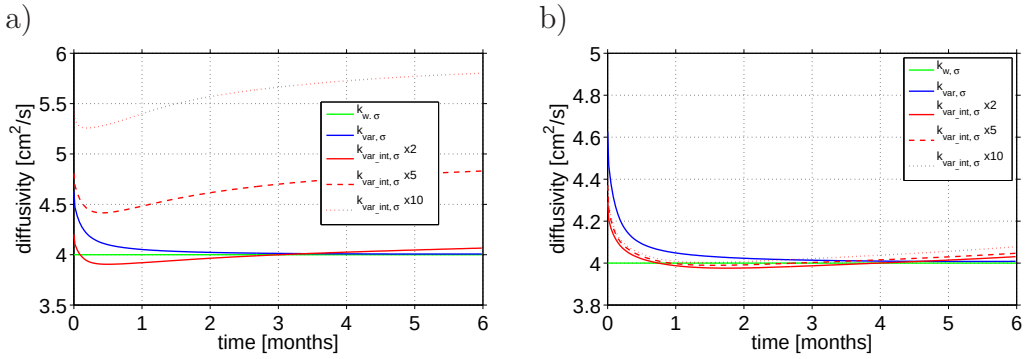

Figure 8.15: Weighted diffusivity $\kappa_{w,\sigma}$ (green) and diagnosed diffusivities $\kappa_{var,\sigma}$ (bue) and $\kappa_{var\_int,\sigma}$ (red) using 2× (solid), 5× (dashed) and 10× (dotted) more layers than levels for the mapping for A_const (2-dimensional), a) isopycnally varying initial tracer condition and b) equally labelled along one isopycnal (diffusion acts on tracer, isopycnals are non-linear).

8.3.2 Diffusion acts on the tracer only

In the experiments shown in this section the vertical diffusion acts on the tracer only, temperature and salinity are both stationary. This will give evidence about the direct effect of the slightly sloping isopycnals on the results of the variance method. For the diagnosed diffusivity $\kappa_{var\_int,\sigma}$, results using twice as many layer, 5 times and 10 times more layers than levels for the transformation will be shown. For the diagnostics of $\kappa_{var,\sigma}$, the change in the number of layers used for the mapping on the results is rather small ($< 1\%$), therefore only results using twice as many layers than levels will be shown.

The results for the diagnosed diffusivity $\kappa_{var,\sigma}$ and the weighted diffusivity $\kappa_{w,\sigma}$ in experiment A_const are independent of the used initial tracer condition (Figure 8.15). The results for the weighted diffusivity $\kappa_{w,\sigma}$ are identical to the constant value of $4\,cm^2/s$ of the explicit diffusion coefficient. The diagnosed diffusivity $\kappa_{var,\sigma}$ shows an induced diffusivity of $\sim 10\%$ at the beginning of the experiment with a strong decrease during the first month. After that, the values for $\kappa_{w,\sigma}$ and $\kappa_{var,\sigma}$ are very similar.

The results for the diagnosed diffusivity $\kappa_{var\_int,\sigma}$ are highly dependent on the initial tracer condition used. First, the results for $\kappa_{var\_int,\sigma}$ are shown for both initial tracer conditions and then an explanation for the differences

will be given.

Using the isopycnally varying initial tracer condition (Figure 8.15 a), the results for the diagnosed diffusivity $\kappa_{var\_int,\sigma}$ are highly dependent on the number of layers used for the transformation of the tracer onto isopycnals. Using twice as many layers than model levels for the transformation (red, solid line), $\kappa_{var\_int,\sigma}$ is underestimating the values of $\kappa_{var,\sigma}$ during the first two months ($\sim 10\%$) and gives close results from the second month onwards. Using 5 times more layers than levels for the mapping, the values of the diagnosed diffusivity $\kappa_{var\_int,\sigma}$ (red, dashed line) are about $10 - 20\%$ larger after the second month compared to the reference values of $\kappa_{var,\sigma}$, with a slow diverging behaviour. Increasing the number of layers by using 10 times more layers than levels leads to a further increase in the diagnosed diffusivity $\kappa_{var\_int,\sigma}$ (red dotted line, $\sim 45\%$ larger).

Using the equally labelled initial tracer condition (Figure 8.15 b), the results for $\kappa_{var\_int,\sigma}$ are independent on the resolution of the transformation axis used. There is a maximum difference between $\kappa_{var,\sigma}$ and $\kappa_{var\_int,\sigma}$ of 5% at the beginning of the experiment.

The high influence of the transformation only occurs in the analysis of $\kappa_{var\_int,\sigma}$ for the experiments with the isopycnally varying initial tracer condition. This mean that the combination of the mapping and the along isopycnal integration of the isopycnally varying tracer concentration leads to a spurious diffusivity which is highly sensitive to the resolution of the transformation used and masks the signal of the numerically induced diffusivity. This spurious diffusivity is denoted as mapping-integration error in the following.

In order to explain, why the mapping-integration error occurs only in the experiments where the isopycnally varying initial tracer condition is used, first an example of the transformed tracer will be given for both initial tracer conditions. Second, profiles of the along isopycnal integrated tracer for different resolutions of the transformation used will be shown.

Figure 8.16 shows the tracer mass after the transformation of the tracer using twice as many layers than levels at the end of experiment *A_const*.

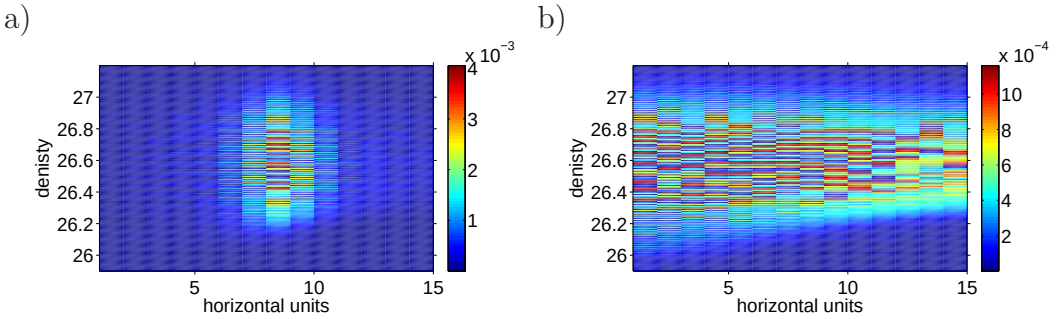

Figure 8.16: Tracer mass after mapping (2× more layers than levels), for *A_const*, a) isopycnally varying initial tracer condition and b) equally labelled one.

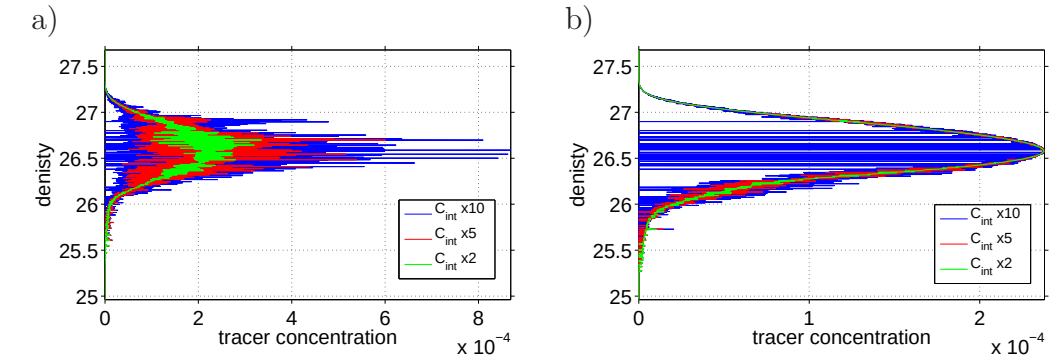

Figure 8.17: Profile of the along isopycnal integrated tracer at the end of experiment *A_const*, a) isopycnally varying initial tracer condition and b) equally labelled along one isopycnal.

Irrespective which initial tracer condition is used, in each profile of the transformed tracer, there are layers with no tracer mass.

In the following, only the density range where the tracer is initialised is considered. Using the isopycnally varying initial tracer condition (Figure 8.16 a), it is more likely that tracer with a low concentration is mixed into layers with no concentration by the along isopycnal integration of the tracer. This leads to an increase in the vertical variation of the integrated tracer concentration, as is will be shown in the following. When on the other hand the equally labelled initial tracer condition is used (Figure 8.16 b), it is more likely that tracer with a high concentration is mixed into layers with no concentration by the along isopycnal integration of the tracer.

The difference can be seen in the profiles of the along isopycnal integrated

tracer as a function of σ at the end of experiment *A_const* (Figure 8.17), using twice as many layers than levels (green), 5 times (red) and 10 times (blue) more layers than levels. By increasing the number of layers used for the transformation in the experiment where the isopycnally varying initial tracer condition is used (Figure 8.17 a), the fluctuations of the vertical profiles of the along isopycnal integrated tracer increase as well. These high vertical variations of the tracer profiles are caused by a combination of the transformation and the along isopycnal integration and lead to changes in the variance decay of the integrated tracer and therefore in the results of $\kappa_{var\_int,\sigma}$.

When on the other hand the equally labelled initial tracer condition is used (Figure 8.17 b), the profile of the integrated tracer using twice as many layers than levels (green) show very small variations in the vertical profile. An increase in the number of layers used for the tracer mapping leads also to an increase of the variance of the integrated tracer profile. The main effect can be found by increasing the number of layers used for the transformation by a factor of 10, as there are layers with no tracer concentration, which does not lead to a change in the variance decay of the integrated tracer.

The sensitivity studies of the 1-dimensional experiments showed (Section 4.3) that using a transformation axis with a coarse resolution for the tracer mapping, the diagnosed diffusivities are artificially too small. A high resolution in the transformation was necessary in order to get robust results. For the analysis of the 2-dimensional experiments, this means that there are two effects working in opposite directions (especially using the isopycnally varying initial tracer condition): First a relatively high number of layers is needed for the transformation in order to get a robust analysis, as spurious mixing leads to a decrease in the diagnosed diffusivity. Second, the high resolution of the transformation leads to a high mapping-integration error, which is much larger than the numerically induced diffusivity.

In experiment *A_incr* (Figure 8.18), the results for the diagnosed diffusivity $\kappa_{var,\sigma}$ and the weighted diffusivity $\kappa_{w,\sigma}$ are independent of the initial tracer condition used and consistent with the results of the analogous

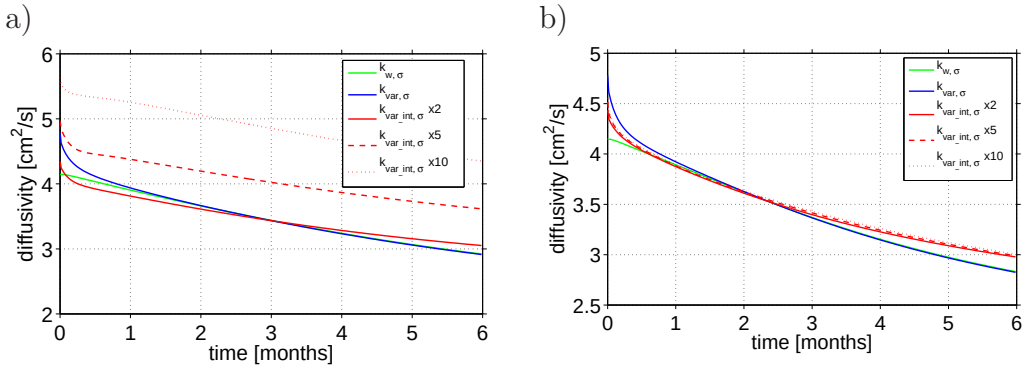

Figure 8.18: Weighted diffusivity $\kappa_{w,\sigma}$ (green) and diagnosed diffusivities $\kappa_{var,\sigma}$ (bue) and $\kappa_{var\_int,\sigma}$ (red) using 2× (solid), 5× (dashed) and 10× (dotted) more layers than levels for the mapping for A_incr (2-dimensional), a) isopycnally varying initial tracer condition and b) equally labelled along one isopycnal (diffusion acts on tracer, isopycnals are non-linear).

experiment using horizontal isopycnals.

Using the isopycnally varying initial tracer condition (Figure 8.18 a), the diagnosed diffusivity $\kappa_{var,\sigma}$, using twice as many layers than model levels for the mapping, is slightly smaller than $\kappa_{var,\sigma}$ during the first two months and larger with a diverging tendency afterwards. Increasing the number of layers used for the transformation leads to an increase of the mapping-integration error in the results of the diagnosed diffusivity $\kappa_{var,\sigma}$, similar as seen in the results of A_const.

Using the equally labelled initial tracer condition (Figure 8.18 b), the results for the diagnosed diffusivity $\kappa_{var\_int,\sigma}$ are indifferent to the resolution of the transformation used. The maximal difference between $\kappa_{var,\sigma}$ and $\kappa_{var\_int,\sigma}$ is $\sim 5\%$ and similar as in the result of A_const.

The diagnosed diffusivity $\kappa_{var,\sigma}$ and the weighted diffusivity $\kappa_{w,\sigma}$ of experiment A_horiz (Figure 8.19) are consistent with the results of the analogous experiment using horizontal isopycnals. Using the isopycnally varying initial tracer condition (Figure 8.19 a), the diagnosed diffusivity $\kappa_{var\_int,\sigma}$ shows the similar dependency on the transformation used as in the previous two experiments. Whereas, using the equally labelled initial tracer condition (Figure 8.19 b), the values of $\kappa_{var\_int,\sigma}$ are independent of the number of layers used for the transformation. The differences between

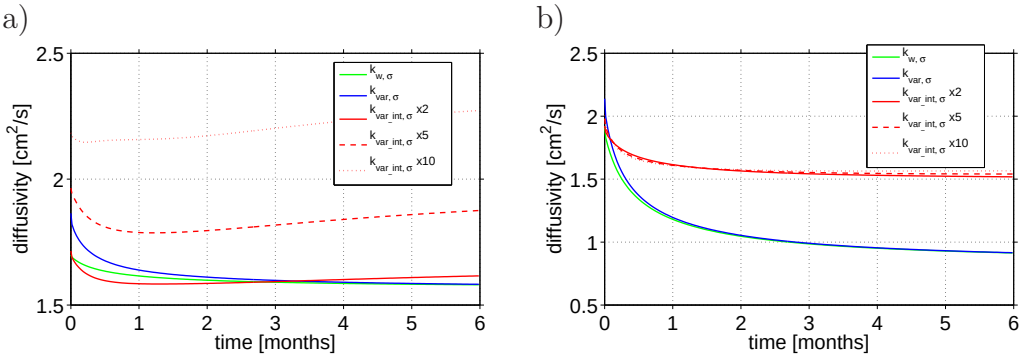

Figure 8.19: Weighted diffusivity $\kappa_{w,\sigma}$ (green) and diagnosed diffusivities $\kappa_{var,\sigma}$ (bue) and $\kappa_{var\_int,\sigma}$ (red) using 2× (solid), 5× (dashed) and 10× (dotted) more layers than levels for the mapping for A_horiz (2-dimensional), a) isopycnally varying initial tracer condition and b) equally labelled along one isopycnal (diffusion acts on tracer, isopycnals are non-linear).

the diagnosed diffusivities $\kappa_{var,\sigma}$ and $\kappa_{var\_int,\sigma}$ are the result of the mapping-integration error.

The results for the last experiment, A_oc, are shown in Figure 8.20. Using the isopycnally varying initial tracer condition (Figure 8.20 a), the difference between the weighted diffusivity $\kappa_{w,\sigma}$ and the diagnosed diffusivity $\kappa_{var,\sigma}$ is $\sim 5\%$ at the beginning with a converging tendency. The diagnosed diffusivity $\kappa_{var\_int,\sigma}$ using twice as many layers than model levels start at a $\sim 8\%$ lower value than $\kappa_{var,\sigma}$. An increase in the number of layers used for the transformation also leads to an increase in the values of the diagnosed diffusivity $\kappa_{var\_int,\sigma}$.

Using the equally labelled initial tracer condition (Figure 8.20 b), the differences between the weighted diffusivity $\kappa_{w,\sigma}$ and the diagnosed diffusivity $\kappa_{var,\sigma}$ are $\sim 4\%$ at the beginning and decrease towards the end of the experiment. The values for the diagnosed diffusivity $\kappa_{var\_int,\sigma}$ are smaller compared to ones of $\kappa_{var,\sigma}$. Although it seems that the differences of $\kappa_{var\_int,\sigma}$ are relatively high and depend on the number of layers used for the mapping, due to the small range in the y-axis, there is only a variation of $\sim 1\%$ in the values for $\kappa_{var\_int,\sigma}$.

Already in these simple experiments, a slight slope of the isopycnals leads to an increase of the difference between the diagnosed diffusivities $\kappa_{var,\sigma}$

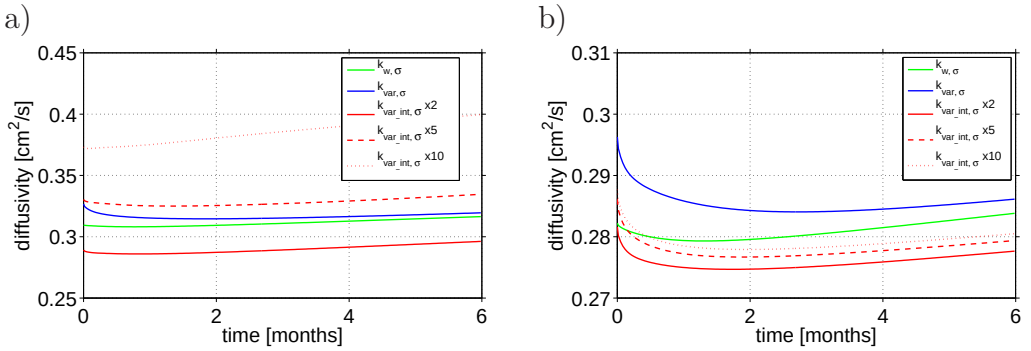

Figure 8.20: Weighted diffusivity $\kappa_{w,\sigma}$ (green) and diagnosed diffusivities $\kappa_{var,\sigma}$ (bue) and $\kappa_{var\_int,\sigma}$ (red) using 2× (solid), 5× (dashed) and 10× (dotted) more layers than levels for the mapping for A_oc (2-dimensional), a) isopycnally varying initial tracer condition and b) equally labelled along one isopycnal (diffusion acts on tracer, isopycnals are non-linear).

and $\kappa_{var\_int,\sigma}$ in the experiments using the isopycnally varying initial tracer condition. For these cases, the results of the diagnosed diffusivity $\kappa_{var\_int,\sigma}$ are highly sensitive to the number of layers used for the mapping of the tracer onto isopycnals. A high number of layers results in a high variation in the vertical profile of the integrated tracer. This high vertical variation causes a spurious change in the variance decay of the integrated tracer, which was denoted as mapping-integration error, and leads to an increase in the diagnosed diffusivity $\kappa_{var\_int,\sigma}$. The effect of the mapping-integration error on the results of the diagnosed diffusivity $\kappa_{var\_int,\sigma}$ is larger than the numerically induced diffusivity itself.

When on the other hand the equally labelled initial tracer condition is used, the mapping-integration error is very small ($< 1\%$). Similar to the results of the analogous experiments with horizontal isopycnals, only an explicit diffusivity which varies along the isopycnal layers leads to a spurious diffusivity in the results of $\kappa_{var\_int,\sigma}$, which masks the numerically induced diffusivity.

8.3.3 The effect of vertical advection

In this section, the analysis of the experiment with implemented vertical advection is repeated for the 2-dimensional case with non-horizontal

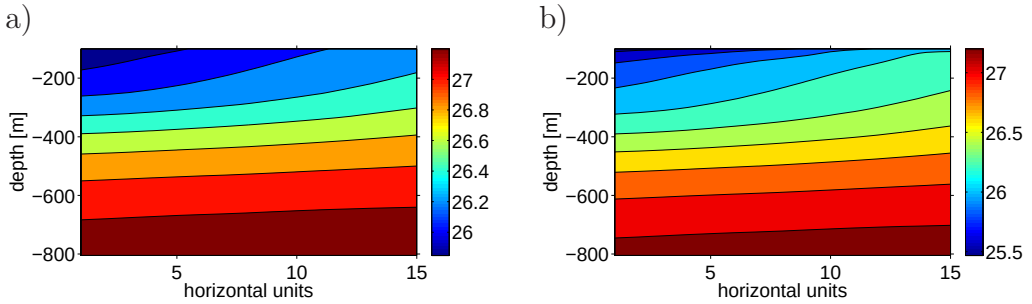

Figure 8.21: a) Density field at the beginning of the experiment with implemented advection and b) after six months of model integration.

isopycnals. The vertical velocity is constant with a value of $4 \times 10^{-6}\, m/s \approx 0.35\, m/day$ and a downwards direction. The experimental set-up is not limited to a purely parallel movement of the isopycnals, as the density equation is non-linear and the gradients in temperature and salinity vary along the isopycnal layers.

To give an overview, Figure 8.21 a) shows the initial density field and b) the density field at the end of the experiment. For the assumed temperature and salinity profiles the effects of the non-linear density equation are larger towards the surface layers and smaller towards greater depth.

The analysis in the previous section showed, that in the experiments with non-horizontal isopycnals a high number of layers used for the mapping might result in an overestimated diagnosed diffusivity $\kappa_{var\_int,\sigma}$ due to the mapping-integration error. Therefore, the diagnosed diffusivities $\kappa_{var,\sigma}$ and $\kappa_{var\_int,\sigma}$ are analysed first by using the same amount of layers as there are model levels and second by using twice as many layers than levels.

In Figure 8.22 the results for the diagnosed diffusivities $\kappa_{var,\sigma}$ (blue) and $\kappa_{var\_int,\sigma}$ (red) are shown using the same amount of layers as model levels for the mapping. For both initial tracer conditions, the diagnosed diffusivities $\kappa_{var,\sigma}$ and $\kappa_{var\_int,\sigma}$ show the same frequency in the fluctuations.

Using the isopycnally varying initial tracer condition (Figure 8.22 a), the amplitude of the variations in the diagnosed diffusivities $\kappa_{var,\sigma}$ is slightly larger ($\pm 0.014\, cm^2/s$) compared to the amplitude in $\kappa_{var\_int,\sigma}$ ($\pm 0.008\, cm^2/s$). The mean value for the diagnosed diffusivity $\kappa_{var,\sigma}$ is

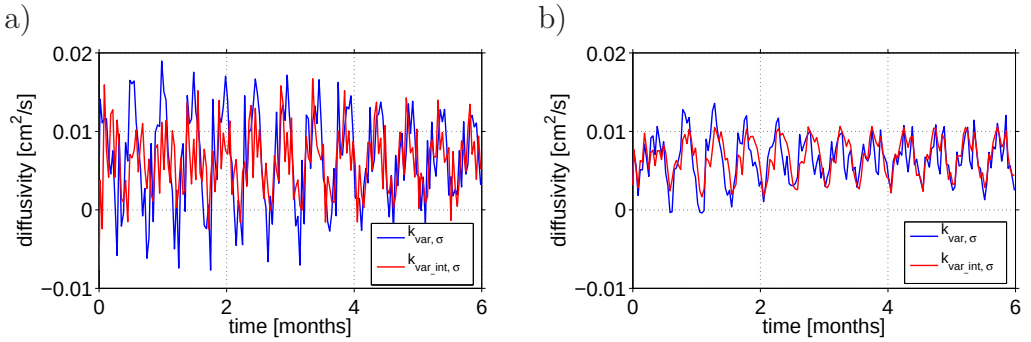

Figure 8.22: Diagnosed diffusivity $\kappa_{var\_int,\sigma}$ (blue) and $\kappa_{var\_int,\sigma}$ (red) for the experiment including a constant advection using the same amount of layers than levels for the mapping, a) isopycnally varying initial tracer condition and b) equally labelled along one isopycnal (isopycnals are non-horizontal).

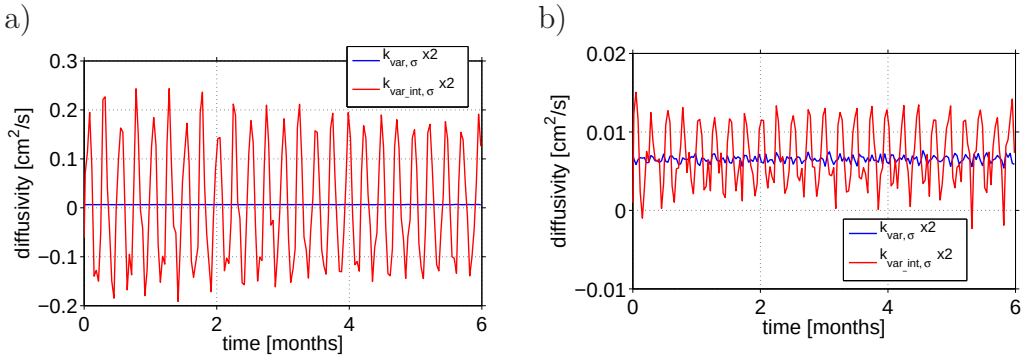

Figure 8.23: Diagnosed diffusivity $\kappa_{var\_int,\sigma}$ (blue) and $\kappa_{var\_int,\sigma}$ (red) for the experiment including a constant advection using twice as many layers as levels for the tracer mapping, a) isopycnally varying initial tracer condition and b) equally labelled along one isopycnal (isopycnals are non-horizontal).

$6.6 \times 10^{-3}\, cm^2/s$ and also slightly larger compared to the mean value of $\kappa_{var\_int,\sigma}$ $(6.1 \times 10^{-3}\, cm^2/s)$.

Using the equally labelled initial tracer condition (Figure 8.22 b), the diagnosed diffusivities $\kappa_{var,\sigma}$ and $\kappa_{var\_int,\sigma}$ are very similar, except for the beginning when the amplitude of $\kappa_{var\_int,\sigma}$ is slightly smaller than the one of $\kappa_{var,\sigma}$. The amplitude for both values is much smaller $(\pm 0.007\, cm^2/s)$ compared to the one using the isopycnally varying initial tracer condition. The mean values for the diagnosed diffusivity $\kappa_{var,\sigma}$ is $\sim 6.4 \times 10^{-3}\, cm^2/s$ and slightly smaller compared to the one of $\kappa_{var\_int,\sigma}$ $(\sim 6.9 \times 10^{-3}\, cm^2/s)$.

Increasing the number of layers used for the transformation by a factor of

two, the diagnosed diffusivities $\kappa_{var,\sigma}$ and $\kappa_{var\_int,\sigma}$ are not similar any longer (Figure 8.23). Note, the limits of the y-axis in Figure 8.23 a) and b) differ by about one order of magnitude.

Using the isopycnally varying initial tracer condition (Figure 8.23 a), the amplitude of the diagnosed diffusivity $\kappa_{var,\sigma}$ is, as expected, much smaller compared to the previously shown results. The mean value of $\kappa_{var,\sigma}$ is $6.5 \times 10^{-3}\, cm^2/s$ and similar to the previous results. For the analysis of $\kappa_{var,\sigma}$ the variance of the tracer is estimated for each of the horizontal profiles and an increase in the number of layers used for the mapping leads to a reduction of the spurious diffusivity which is causd by the mapping itself, as already shown in the 1-dimensional experiment (Chapter 5).

The amplitude of the fluctuations in the diagnosed diffusivity $\kappa_{var\_int,\sigma}$ is much larger compared to the amplitude of the fluctuations using the lower number of layers for the transformation and also the mean value is larger ($\sim 8.6 \times 10^{-3}\, cm^2/s$). The effect of the high amplitude in the fluctuations of the diagnosed diffusivity $\kappa_{var\_int,\sigma}$ is a result of the mapping-integration error.

When on the other hand the equally labelled initial tracer condition is used (Figure 8.23 b.), the amplitude of the diagnosed diffusivity $\kappa_{var,\sigma}$ decreases when the number of layers used for the tracer mapping is increased. The mean value ($\overline{\kappa_{var,\sigma}} = 6.5 \times 10^{-3}\, cm^2/s$) does not change. The amplitude of the fluctuations in the diagnosed diffusivity $\kappa_{var\_int,\sigma}$ is similar compared to the previous ones (Figure 8.22 b). Also the mean value of $\kappa_{var\_int,\sigma}$ is similar to the previous one with a value of $\sim 7.0 \times 10^{-3}\, cm^2/s$.

Similar to the experiments, where the diffusion acts on the tracer only, there are two different mechanisms, which cause problems in the analysis. First, using a low number of layers for the transformation, the mapping itself generates a spurious mixing, which leads to changes in the variance decay. Second, an increase in the number of layers used for the tracer transformation leads to high variations in the profiles of the integrated tracer, which is caused by the combination of the mapping and the along isopycnal integration and leads to an increase of the mapping-integration

error. This second effect only affects the diagnosed diffusivity $\kappa_{var\_int,\sigma}$ in experiments where the isopycnally varying initial tracer condition is used. The effect of the mapping-integration error on $\kappa_{var\_int,\sigma}$ is so large that also the mean values are masked and overestimate the numerically induced diffusivity (by $\sim 30\%$).

The results of the 2-dimensional experiments with implemented vertical advection show that it is not possible to analyse the diapycnal diffusion for each time-step. Whereas, it is possible to analyse time mean values of the numerically induced diffusion, which are taken at least over one wavelength. Different to the results of the equally labelled initial tracer condition, using the isopycnally varying one it is only possible to analyse mean values of $\kappa_{var\_int,\sigma}$ when the mapping-integration error is low. Therefore, it is necessary to choose a relatively coarse resolution for the transformation, e.g. where the same number of layers as model levels are used.

8.3.4 Diffusion acts on tracer, temperature and salinity

In the last section of this chapter, experiments where the vertical diffusion acts on tracer, temperature and salinity will be analysed. The corresponding effect of diffusion in temperature and salinity can be interpreted as an interfacial movement of the density. As an interfacial movement of the isopycnals does not lead to changes in the variance decay, the results for the diagnosed diffusivity $\kappa_{var,\sigma}$ are expected to be identical with the results of the analogous experiments in which diffusion acts on the tracer only (Section 8.3.2).

It is also expected that the combination of the tracer mapping using a high resolution in the transformation axis and the along isopycnal integration of the tracer will lead to high values of spurious diffusivity, the mapping-integration error, in the results of $\kappa_{var\_int,\sigma}$ in experiments that use the isopycnally varying initial tracer condition. First, results are shown using the same amount of layers as model levels and second, using twice as many layers than levels.

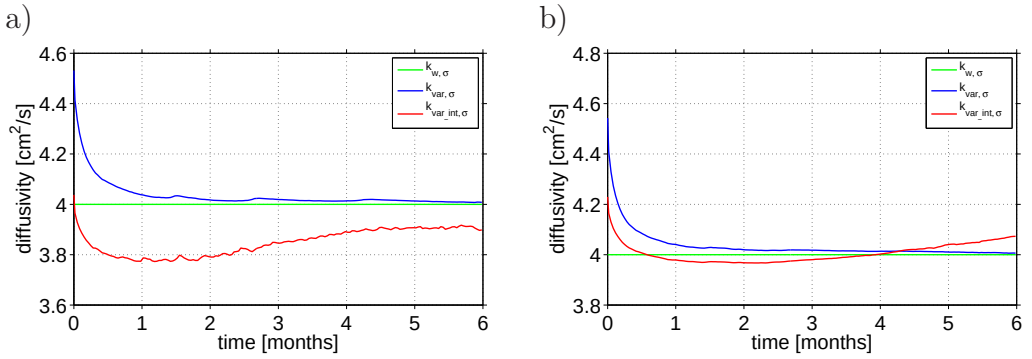

Figure 8.24: Weighted diffusivity $\kappa_{w,\sigma}$ (green) and diagnosed diffusivities $\kappa_{var,\sigma}$ and $\kappa_{var\_int,\sigma}$ using the same number of layers as levels for *A_const* (2-dimensional); a) isopycnally varying and b) equally labelled initial tracer condition (diffusion acts on tracer, temperature and salinity, isopycnals are non-horizontal).

As expected, the results of the weighted diffusivity $\kappa_{w,\sigma}$ and the diagnosed diffusivity $\kappa_{var,\sigma}$ in experiment *A_const* (Figure 8.24) closely reproduce the results of the analogous experiment where diffusion acts on the tracer only and are independent of the initial tracer condition used. The values of $\kappa_{w,\sigma}$ are consistent with the constant value of $4\,cm^2/s$ of the explicit diffusivity.

Using the isopycnally varying initial tracer condition (Figure 8.24 a), the results of the diagnosed diffusivity $\kappa_{var\_int,\sigma}$ are smaller than the results of $\kappa_{var,\sigma}$, 10% at the beginning and 5% after the second month converging to a difference of $\sim 2\%$ at the end of the experiment. Using the equally labelled initial tracer condition (Figure 8.24 b), the diagnosed diffusivity $\kappa_{var\_int,\sigma}$ is systematically smaller than $\kappa_{var,\sigma}$ ($\sim 1\%$) during the first four months and shows a small increase during the last two months of the experiment. This is also similar to the results of the analogous experiment with stationary isopycnals.

Increasing the number of layers of the transformation axis by a factor of 2 (Figure 8.25) does not lead to changes in the results of $\kappa_{w,\sigma}$ and $\kappa_{var,\sigma}$. Using the isopycnally varying initial tracer condition (Figure 8.25 a), the diagnosed diffusivity $\kappa_{var\_int,\sigma}$ (red) shows non-periodic fluctuations with a maximal amplitude of $\pm 1.5\,cm^2/s$. A further increase in the number of layers used for the mapping leads to an increase in amplitude and frequency

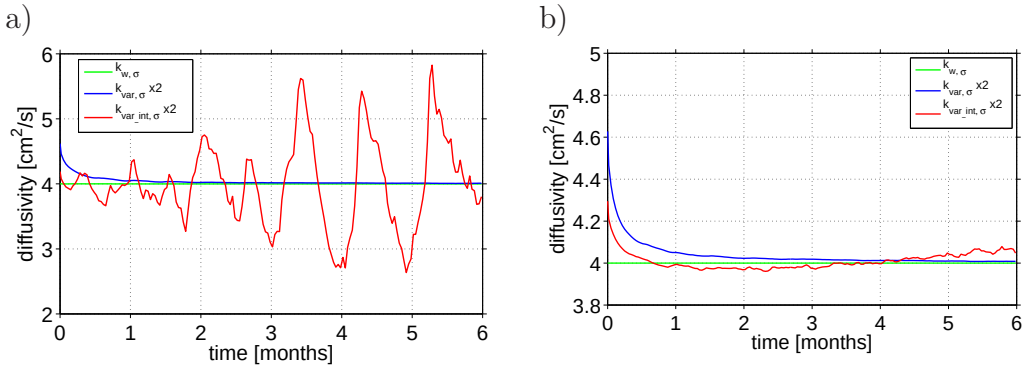

Figure 8.25: Weighted diffusivity $\kappa_{w,\sigma}$ (green) and diagnosed diffusivities $\kappa_{var,\sigma}$ and $\kappa_{var\_int,\sigma}$ using twice as may layers than levels for the mapping, for *A_const* (2-dimensional); a) isopycnally varying and b) equally labelled initial tracer condition (diffusion acts on tracer, temperature and salinity, isopycnals are non-horizontal).

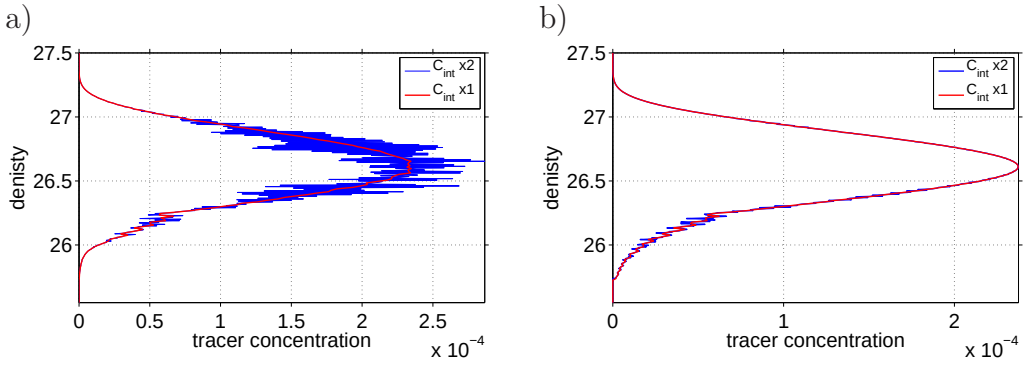

Figure 8.26: Profile of the along isopycnal integrated tracer at the end of experiment *A_const*, a) isopycnally varying initial tracer condition and b) equally labelled along one isopycnal.

of these fluctuations. When on the other hand the equally labelled initial tracer condition is used (Figure 8.25 b), the results for the diagnosed diffusivity $\kappa_{var\_int,\sigma}$ are consistent with the ones shown in Figure 8.24 b), except for the small fluctuations.

The reason of this large increase in the fluctuations of the diagnosed diffusivity $\kappa_{var\_int,\sigma}$ using the higher resolved transformation can be ascribed to the mapping-integration error, which is large in experiments where the isopycnally varying initial tracer condition is used. Figure 8.26 shows the vertical profiles of the isopycnally integrated tracer concentration at the end of experiment *A_const* using the same amount of layers as levels

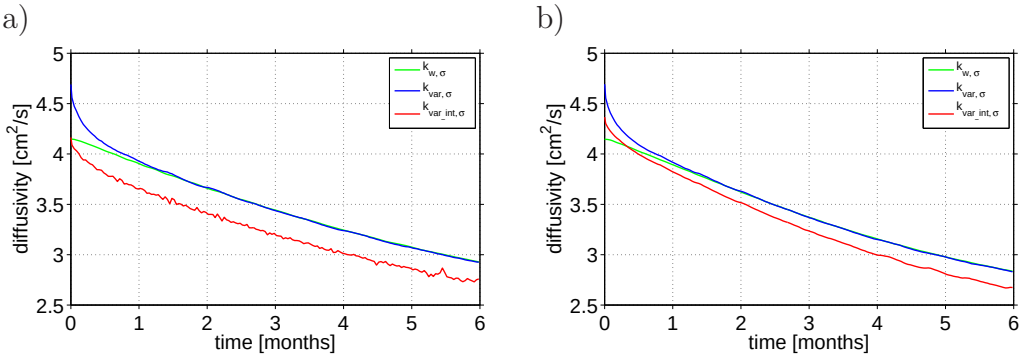

Figure 8.27: Weighted diffusivity $\kappa_{w,\sigma}$ (green) and diagnosed diffusivities $\kappa_{var,\sigma}$ and $\kappa_{var\_int,\sigma}$ using the same number of layers as levels for the mapping, for A_incr (2-dimensional); a) isopycnally varying and b) equally labelled initial tracer condition (diffusion acts on tracer, temperature and salinity, isopycnals are non-horizontal).

for the transformation (red) and twice as many than levels (blue). In contrast to Figure 8.17 higher transformations are not considered here.

Only the experiment using the isopycnally varying initial tracer condition shows a high vertical variation in the profile of the integrated tracer concentration for the case, where twice as many layers than levels have been used for the mapping. As this effect leads to a large mapping-integration error in the results or $\kappa_{var\_int,\sigma}$, only the results using the same amount of layers as levels will be shown for the following experiments.

As expected, also for experiment A_incr (Figure 8.27), the results for $\kappa_{w,\sigma}$ and $\kappa_{var,\sigma}$ closely reproduce the ones of the analogous experiment in which the diffusion acts on the tracer only. For both initial tracer conditions, the results for the diagnosed diffusivity $\kappa_{var\_int,\sigma}$ are systematically smaller than the values of $\kappa_{var,\sigma}$. Using the isopycnally varying initial tracer condition (Figure 8.27 a), $\kappa_{var\_int,\sigma}$ shows high frequency fluctuations with a very small amplitude and the difference to $\kappa_{var,\sigma}$ is $\sim 7\%$. When on the other hand the equally labelled initial tracer condition is used (Figure 8.27 b) the diagnosed diffusivity $\kappa_{var\_int,\sigma}$ is $\sim 2\%$ smaller than $\kappa_{var,\sigma}$ at the beginning of the experiment and $\sim 5\%$ smaller towards the end of the experiment. For both initial tracer conditions the mapping-integration error leads to a spurious diffusivity in $\kappa_{var\_int,\sigma}$ which is larger than the

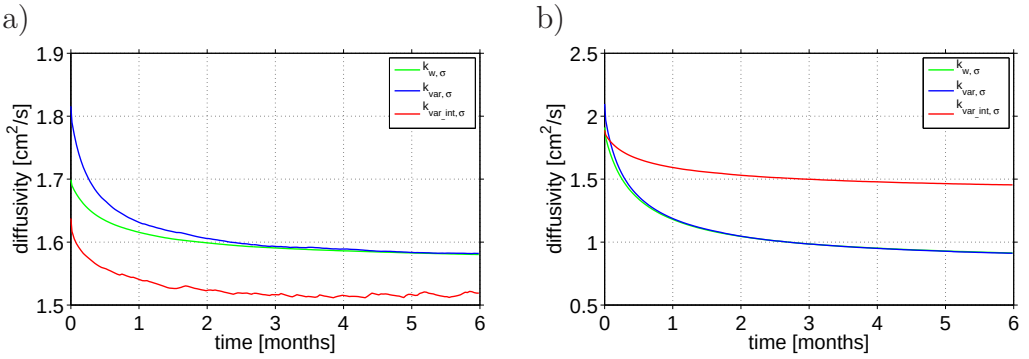

Figure 8.28: Weighted diffusivity $\kappa_{w,\sigma}$ (green) and diagnosed diffusivities $\kappa_{var,\sigma}$ and $\kappa_{var\_int,\sigma}$ using the same number of layers as levels for the mapping, for *A_horiz* (2-dimensional); a) isopycnally varying and b) equally labelled initial tracer condition (diffusion acts on tracer, temperature and salinity, isopycnals are non-horizontal).

numerically induced diffusivity.

In experiment *A_horiz* (Figure 8.28), the results for $\kappa_{w,\sigma}$ and $\kappa_{var,\sigma}$ are also independent on the interfacial movement of the isopycnal layers and closely reproduce the results of the analogous experiment with stationary isopycnals. Using the isopycnally varying initial tracer condition (Figure 8.28 a), the diagnosed diffusivity $\kappa_{var\_int,\sigma}$ underestimates the values of $\kappa_{var,\sigma}$ constantly by $\sim 6\%$. When the equally labelled initial tracer condition is used (Figure 8.28 b), the results for the diagnosed diffusivity $\kappa_{var\_int,\sigma}$ are almost identical with the one of the analogous experiment, with stationary isopycnals.

Also in the last experiment, *A_oc* (Figure 8.29), the results of $\kappa_{w,\sigma}$ and $\kappa_{var,\sigma}$ are almost identical with the ones shown in Section 8.3.2. Using the isopycnally varying initial tracer condition (Figure 8.29 a), the diagnosed diffusivity $\kappa_{var\_int,\sigma}$ is $\sim 10\%$ smaller than the values of $\kappa_{var,\sigma}$, whereas using the equally labelled initial tracer condition the difference is only $\sim 3\%$ (Figure 8.29 b).

In summary it can be said, that the interfacial movement of the isopycnals itself does not cause any spurious mixing in the model itself, as the results of the diagnosed diffusivity $\kappa_{var,\sigma}$ are almost identical with the ones of the analogous experiment with stationary isopycnals.

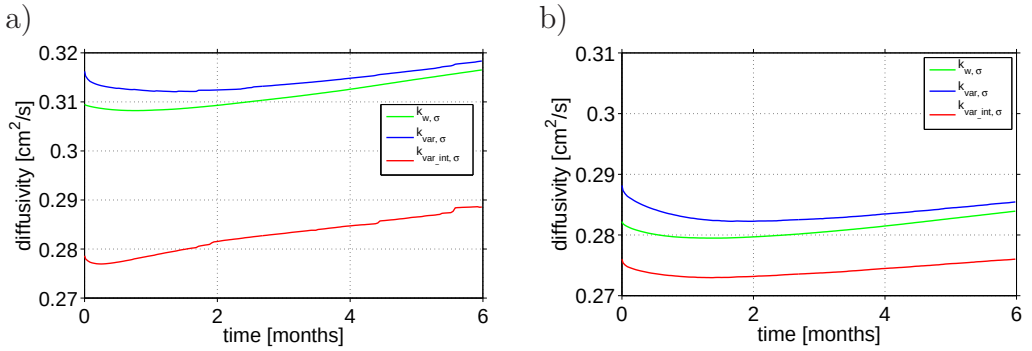

Figure 8.29: Weighted diffusivity $\kappa_{w,\sigma}$ (green) and diagnosed diffusivities $\kappa_{var,\sigma}$ and $\kappa_{var\_int,\sigma}$ using the same number of layers as levels for the mapping, for A_oc (2-dimensional; a) isopycnally varying and b) equally labelled initial tracer condition (diffusion acts on tracer, temperature and salinity, isopycnals are non-horizontal).

Using the equally labelled initial tracer condition, the integration of the tracer leads to an additional spurious diffusivity in $\kappa_{var\_int,\sigma}$ only in experiment A_horiz, similar to the results shown in Section 8.3.2. In the other experiments, $\kappa_{var\_int,\sigma}$ underestimates the values of $\kappa_{var,\sigma}$ by at most $\sim 10\%$.

Using the isopycnally varying initial tracer condition, the combination of a high resolution in the transformation axis used and the along isopycnal integration of the tracer leads to a spurious diffusivity, the mapping-integration error, in the results. Therefore, a relatively low resolution for the transformation axis was used. The resulting values of $\kappa_{var\_int,\sigma}$ are generally $10 - 20\%$ too small compared to the reference values of $\kappa_{var,\sigma}$.

In all experiments, the spurious diffusivity which is a result of the mapping-integration error is larger than the numerically induced diffusivity, which is given by the difference between $\kappa_{var,\sigma}$ and $\kappa_{w,\sigma}$.

For the analysis of tracer fields in OGCMs this implies that the spurious diffusivity as a result of the mapping-integration error, which is generated by the analysis of $\kappa_{var\_int,\sigma}$ is mostly larger than the numerically induced diffusivity. Therefore it does not seem to be useful to analyse the numerically induced diffusivity in complex models by the variance method.

As the results of the diagnosed diffusivity $\kappa_{var,\sigma}$ are robust, it is still possible to analyse the diffusivity, which is caused only by the parameterisation of the (vertical) explicit diffusion scheme in the model. This analysis can be done, as diffusion and advection are usually treated separately in different model steps.

8.4 Summary

In this chapter the robustness of the variance method in 2-dimensional experiments was tested. To this extent, experiments used an initial density field with horizontal isopycnals and non-horizontal isopycnals, as one would expect in the oceans interior. In order to obtain more general information about the sensitivity of the method all experiments are performed for two different initial tracer conditions: first, with the initial tracer concentration varying along the isopycnal layer and second, with the tracer concentration initialised equally along the isopycnal surface.

Horizontal isopycnals The results of the basic experiments in which the isopycnals are horizontal showed that as long as the mixing, either due to vertical diffusion or vertical advection, is constant along the isopycnal layers, it is possible to analyse the diapycnal diffusivity separately by integrating the tracer isopycnally before estimating its variance decay. Only in these cases, there is no spurious diffusivity in the results of $\kappa_{var\_int,\sigma}$ caused by the along isopycnal integration of the tracer.

For experiments which include vertical advection, the transformation of the tracer onto isopycnals leads to spurious diffusivities in the results for $\kappa_{var\_int,\sigma}$ and $\kappa_{var,\sigma}$, so the diapycnal diffusivity cannot be estimated for each time-step. Nevertheless, mean values taken over at least one wavelength give close results to the diagnosed diffusivity $\kappa_{var,z}$ estimated in z-levels.

Non-horizontal isopycnal The results of the experiments with non-horizontal isopycnals showed that, using the isopycnally varying initial tracer condition, the integration of the tracer along the isopycnals leads to large instabilities in the results of $\kappa_{var\_int,\sigma}$. The results for $\kappa_{var\_int,\sigma}$ are highly sensitive to an increase in the resolution used for the mapping, which results in a large amount of spurious diffusivity as a result of the mapping-integration error.

The spurious diffusivity as a result of the mapping-integration error arise from the combined effect of the transformation and the along isopycnal integration of the tracer. Contrary, the numerically induced diffusion in the current idealised case studies arises from discretisation errors of the vertical diffusion and the vertical advection as a result of insufficient vertical and horizontal resolution. The spurious diffusivity of the mapping-integration error is always larger than the numerically induced diffusivity and therefore masks its signal.

As long as the diffusion acts on the tracer only, there is no mapping-integration error in the experiments when the equally labelled initial tracer condition is used. In experiments in which the diffusion acts on tracer, temperature and salinity, the spurious diffusivity, which is caused by the mapping-integration error is larger than the signal of the numerically induced diffusivity.

In experiments with implemented vertical advection, the spurious diffusivity resulting from the mapping-integration error leads to an increase in the amplitude of the high frequency fluctuations of the diagnosed diffusivity. The tracer mapping on its own also results in artificial fluctuations in the results of $\kappa_{var,\sigma}$, as shown in Chapter 5 in detail. Using the equally labelled initial tracer condition, it is still possible to estimate mean values of the diagnosed diffusivity $\kappa_{var\_int,\sigma}$ which give close results to the expected value. Whereas using the isopycnally varying initial tracer condition, also the mean values are affected by the spurious mixing of the mapping-integration error.

In general, it seems not useful to analyse the diapycnal diffusivity in

complex OGCMs by the variance method. As long as it is not necessary to separate between the isopycnal and the diapycnal diffusivity, it is always possible to use the variance method in order to analyse the numerically induced diffusivity in more dimensional models.

The results of the 1-dimensional experiments already showed, that depending on the grid used (examples are shown for uniform and non-uniform grids), there is induced diffusion, as a result of the discretisation of the explicit diffusion and which does not necessarily decrease with a reduction of the time-step. The vertical diffusion in OGCMs is generally computed in a separate step as well as the vertical advection. By implementing the analysis presented here into the model itself, it should be possible to analyse the numerically induced diffusivities due to discretisation errors of the explicit vertical diffusion and compare it with the weighted one and also the numerically induced diffusion as a result of the vertical advection. This can be also done for the analysis of tracers in e.g. biogeochemical models, where it should be possible to generate a horizontal map of the diagnosed diffusivities, determined only by the explicit vertical diffusion. It can be expected, that the difference between the weighted and the diagnosed diffusivity is only significant in regions, where the difference between the analytical distribution and the discretisation onto the model grid is large, as it was shown in the 1-dimensional experiments. This is usually the case when the tracer gradient is strong or the model grid is coarse.

Chapter 9

2-dimensional case study: Diagnostics using the tracer flux method

The studies of the 1-dimensional experiments showed that the results analysed by the tracer flux method are more robust in experiments with a high vertical resolution in the model set-up. In this chapter, the results of the tracer flux method for 2-dimensional experiments will be shown using a fine resolved vertical model grid with an equidistant level thickness of $5\,m$.

First, the changes in the tracer flux method for the analysis of 2-dimensional experiments will be shown. Second, the set of experiments will be analysed, (i) including vertical diffusion only in the tracer field, (ii) including vertical advection and (iii) including vertical diffusion of tracer, temperature and salinity, using horizontal isopycnals and third using non-horizontal isopycnals.

9.1 Changes in the method

For the analysis of 2-dimensional experiments using the tracer flux method (Section 2.2) it is generally necessary to use the cumulative integral of the transformed advection-diffusion equation in order to analyse the diapycnal

diffusivity. Only in the idealised case, where the isopycnals are horizontal this is not necessary. In the following the analysis will be only done in σ-coordinates.

In general it can be said, that the cumulative sum of the advection-diffusion equation is valid in each column of the model, as

$$\sum_{s_1=1}^{s} \left(\frac{\Delta \left(C_t(i,s_1) \cdot \Delta z_t(i,s_1) \right)}{\Delta t} \right) \Big|_i = \kappa \frac{\Delta C_t(i,s)}{\Delta z_t(i,s)} \Big|_{i,s+1} - w_I C_t(i,s) \Big|_{i,s+1}, \quad (9.1)$$

where C_t denotes the transformed tracer concentration, Δz_t the transformed layer thickness, s the density layer this equation is given for and i the index of the horizontal unit. The transformed tracer concentration C_t and the layer thickness Δz_t both depend on the horizontal and the vertical grid, in the following the notation will be reduced to $C_t(i,s) = C_t$ and $\Delta z_t(i,s) = \Delta z_t$. The diagnosed diffusivity κ_{diag_G} and the interfacial velocity w_I are both vertical mean values, but depend on the horizontal distance.

Diagnosed diffusivity In order to analyse vertical and horizontal mean values of the diagnosed diffusivity and the interfacial velocity, it is necessary to integrate Equation 9.1 along the isopycnals. In the following the mean diagnosed diffusivity is denoted as $\kappa_{G\_int,\sigma}$ and the interfacial velocity as $\overline{w_I}$. Note, $\kappa_{G\_int,\sigma}$ and $\overline{w_I}$ are taken are taken as vertically and horizontally independent, but time dependent. The horizontal sum of Equation 9.1 is then given by

$$\begin{aligned} \sum_{i=1}^{m} \left(\sum_{s_1=1}^{s} \left(\frac{\Delta \left(C_t \cdot z_t \right)}{\Delta t} \right) \cdot \Delta x \right) = -\kappa_{G\_int,\sigma} \cdot \sum_{i=1}^{m} \left(\frac{\Delta C_t}{\Delta z_t} \Big|_{i,s+1} \cdot \Delta x \right) \\ + \overline{w_I} \sum_{i=1}^{m} \left(C_t \Big|_{i,s+1} \cdot \Delta x \right). \end{aligned} \quad (9.2)$$

Solving Equation 9.2 with the method of the least squares fit, mean values

for the diagnosed diffusivity $\kappa_{G\_int,\sigma}$ and the interfacial velocity $\overline{w_I}$ can be found.

In the idealised experiments, in which either the vertical diffusion acts on the tracer only or there is only vertical advection implemented in the model set-up, the interfacial velocity is zero. Additionally, the results of the 1-dimensional experiments showed, that the diagnostics of the interfacial velocity only has a minor effect on the results of the diagnosed diffusivity. The transformation of the tracer onto isopycnals by using a high resolution in the transformation leads to large errors in the results of the diagnosed interfacial velocity. Therefore, it is useful to neglect the analysis of the mean interfacial velocity, assuming $\overline{w_I} = 0$ in the following.

In this case, the change of the total amount of tracer mass above an isopycnal layer will be compared with the sum of the diapycnal fluxes through the isopycnal. The method of the least squares fit requires

$$\sum_{s=1}^{l} \left(\left[\sum_{i=1}^{m} \left(\sum_{s_1=1}^{s} \left(\frac{\Delta \left(C_t \cdot \Delta z_t \right)}{\Delta t} \right) \cdot \Delta x \right) + \kappa_{G\_int,\sigma} \cdot \sum_{i=1}^{m} \frac{\Delta C_t}{\Delta z_t}\Big|_{i,s+1} \cdot \Delta x \right]^2 \cdot \Delta\sigma \right) \doteq min, \tag{9.3}$$

where $\Delta\sigma$ is the difference of the density classes used for the transformation. As the sum over $\Delta\sigma$ is required to be a minimum, the derivative $\partial / \partial \kappa_{G\_int,\sigma}$ has to be equal to zero leading to

$$\sum_{s=1}^{l} \left[\left(\sum_{i=1}^{m} \left(\sum_{s_1=1}^{s} \left(\frac{\Delta \left(C_t \cdot \Delta z_t \right)}{\Delta t} \right) \cdot \Delta x \right) + \kappa_{G\_int,\sigma} \sum_{i=1}^{m} \left(\frac{\Delta C_t}{\Delta z_t}\Big|_{i,s+1} \cdot \Delta x \right) \right) \cdot \left(\sum_{i=1}^{m} \frac{\Delta C_t}{\Delta z_t}\Big|_{i,s+1} \cdot \Delta x \right) \cdot \Delta\sigma \right] = 0. \tag{9.4}$$

Solving Equation 9.4 for the term of the diagnosed diffusivity $\kappa_{G\_int,\sigma}$ gives

$$\kappa_{G\_int,\sigma} = \frac{-\sum_{s=1}^{l}\left[\sum_{i=1}^{m}\left(\sum_{s_1=1}^{s}\left(\frac{\Delta(C_t\cdot\Delta z_t)}{\Delta t}\right)\cdot\Delta x\right)\cdot\sum_{i=1}^{m}\left(\frac{\Delta C_t}{\Delta z_t}\Big|_{i,s+1}\cdot\Delta x\right)\cdot\Delta\sigma\right]}{\sum_{s=1}^{l}\left[\left\{\sum_{i=1}^{m}\left(\frac{\Delta C_t}{\Delta z_t}\Big|_{i,s+1}\cdot\Delta x\right)\right\}^2\cdot\Delta\sigma\right]}. \tag{9.5}$$

For the analysis of the diagnosed diffusivity $\kappa_{G\_int,\sigma}$, Equation 9.5 needs to be discretised on the model grid in exactly the same way as done in the discretisation of the model set-up (see also Section 2.2 for more detail). In order to analyse the numerically induced diffusivity, it is necessary to weight the explicit diffusion coefficient in a comparable way as it is done for the diagnosed diffusivity.

Weighted diffusivity The weighted explicit diffusion coefficient will be denoted as $\kappa_{w\_G,\sigma}$ in the following and is vertically and horizontally independent, but time dependent. The analysis has to be done on the transformed σ-grid, similar as used for the analysis of the diagnosed diffusivity. Therefore, the explicit diffusion coefficient needs to be interpolated onto isopycnals. The linearly interpolated explicit diffusivity will be denoted as $\kappa_{expl,\sigma}$ in the following. Note, $\kappa_{expl,\sigma}$ is a function of density and depth, whereas the weighted diffusivity $\kappa_{w\_G,\sigma}$ is a vertical and horizontal mean value.

The change of the total amount of tracer mass above the isopycnal σ which is only caused by the flux of the explicit diffusion is given by

$$\sum_{i=1}^{m}\left(\sum_{s_1=1}^{s}\left(\frac{\Delta\left(C_t\cdot\Delta z_t\right)}{\Delta t}\right)\cdot\Delta x\right) = -\sum_{i=1}^{m}\left(\kappa_{expl,\sigma}\cdot\frac{\Delta C_t}{\Delta z_t}\Big|_{i,s+1}\cdot\Delta x\right) \tag{9.6}$$

Substituting Equation 9.6 into Equation 9.2 yields for the weighted diffusivity $\kappa_{w,\sigma}$

$$-\sum_{i=1}^{m}\left(\kappa_{expl,\sigma}\cdot\frac{\Delta C_t}{\Delta z_t}\Big|_{i,s+1}\cdot\Delta x\right)=-\kappa_{w,\sigma}\cdot\sum_{i=1}^{m}\left(\frac{\Delta C_t}{\Delta z_t}\Big|_{i,s+1}\cdot\Delta x\right). \quad (9.7)$$

Similar to the method for the 1-dimensional models, Equation 9.7 can be solved using the method of the least squares fit, leading to

$$\kappa_{w\_G,\sigma}=\frac{\sum_{s=1}^{l}\left[\sum_{i=1}^{m}\left(\kappa_{expl,\sigma}\cdot\frac{\Delta C_t}{\Delta z_t}\Big|_{i,s+1}\cdot\Delta x\right)\cdot\sum_{i=1}^{m}\left(\frac{\Delta C_t}{\Delta z_t}\Big|_{i,s+1}\cdot\Delta x\right)\cdot\Delta\sigma\right]}{\sum_{s=1}^{l}\left[\left\{\sum_{i=1}^{m}\left(\frac{\Delta C_t}{\Delta z_t}\Big|_{i,s+1}\cdot\Delta x\right)\right\}^2\cdot\Delta\sigma\right]}. \quad (9.8)$$

In order to analyse the weighted diffusivity $\kappa_{w,\sigma}$ in numerical models, Equation 9.8 needs to be discretised on the model grid.

In the present analysis, the diagnostics of $\kappa_{w\_G,\sigma}$ and $\kappa_{G\_int,\sigma}$ are based on the least squares fit taken in σ-coordinates. This can be interpreted as a weighting of the results by the spacing of the isopycnal grid. In contrast, the results of the 1-dimensional experiments (Chapter 3) were weighted by the level thickness. This means, that the results for the diagnosed and the weighed diffusivities shown in this chapter will not necessarily be identical to the ones shown in the 1-dimensional experiments.

In the following, first the results of experiments using horizontal isopycnals will be shown and second, the same experiments will be repeated using non-horizontal isopycnals. As long as only the tracer is diffusive, $\kappa_{G\_int,\sigma}$ and $\kappa_{w\_G,\sigma}$ should give identical results.

9.2 Results: horizontal isopycnals

In order to test the robustness of the tracer flux method in 2-dimensional models, idealised experiments with horizontal isopycnals are analysed first. The initial tracer conditions and the experimental set-up are identical to

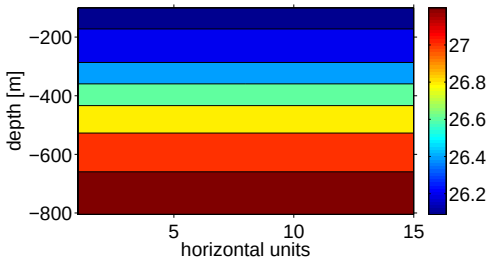

Figure 9.1: Initial density field for the 2-dimensional case studies with horizontal isopycnals.

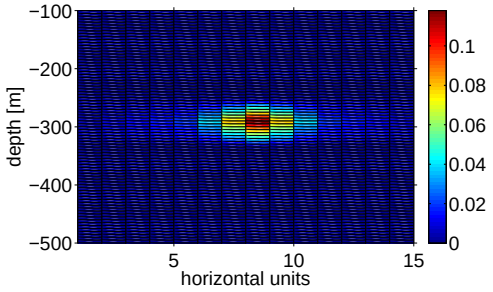

Figure 9.2: Initial tracer field, with a tracer maximum in the middle and fading concentration towards the outer sides (horizontal isopycnals).

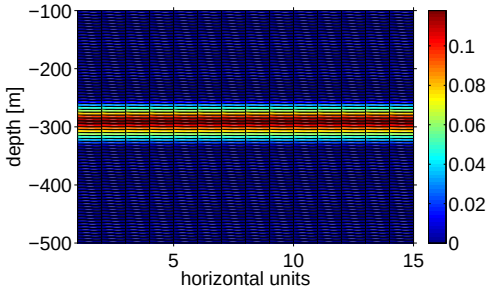

Figure 9.3: Initial tracer field, where the tracer is equally labelled along one isopycnal layer (horizontal isopycnals).

the ones used in Chapter 8 and will be repeated first. Second, the results of experiments, in which only the tracer is diffusive, are shown. Third, experiments including vertical advection are analysed and in the last subsection, experiments including vertical diffusion of tracer, temperature and salinity will be shown.

9.2.1 Initial conditions

The experimental set-up of the experiments shown in this section is the same as already described in Section 8.2.1. To get a quick overview, Figure 9.1 (identical with Figure 8.1) shows the initial density condition, with horizontal isopycnals. Note, that density is not linearly increasing with depth.

In Figure 9.2 (the same as Figure 8.2) shows the initial tracer condition, where the tracer maximum is located in the middle of the horizontal field

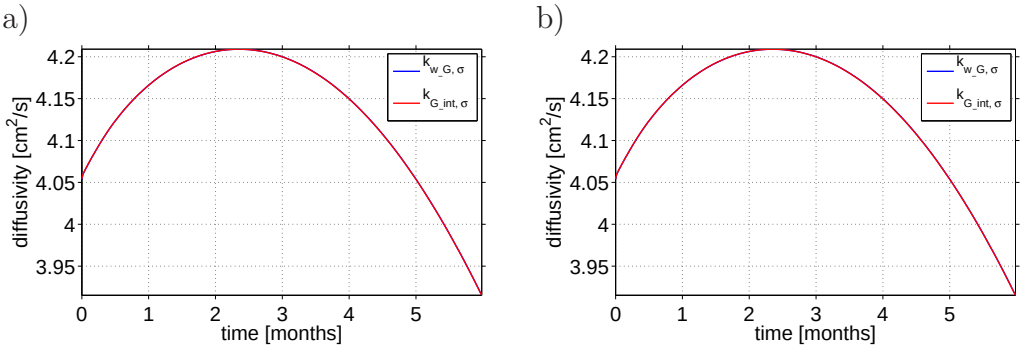

Figure 9.4: Weighted diffusivity $\kappa_{w\_G,\sigma}$ equal to diagnosed diffusivity $\kappa_{G\_int,\sigma}$ for *A_incr* (2-dimensional, diffusion acts on tracer, horizontal isopycnals): a) horizontally varying and b) equally labelled initial tracer condition.

with a fading concentration towards the outer sides, denoted as horizontally varying initial tracer condition. Figure 9.3 (Figure 8.3) shows the equally labelled initial tracer condition, where the tracer mass is equally spread along the isopycnal layer.

9.2.2 Diffusion acts on the tracer only

The sensitivity studies in the 1-dimensional experiments (see also Section 4.3) showed, that it is necessary to use more layers than levels in order to get robust results for the diagnosed diffusivity. Indeed the results for the diagnosed diffusivity $\kappa_{G\_int,\sigma}$ are independent on the used number of layers for the mapping as long as the resolution of the transformation is not getting coarser than the density profiles in the model. In the following there are twice as many layers than levels used for the tracer mapping onto isopycnals. Note, the tracer gradient is also transformed linearly onto isopycnals as introduced in Section 4.3.

The easiest experiment is *A_const*, where the explicit diffusion coefficient is constant with depth and also along the horizontal direction. Irrespective which initial tracer condition is used, the results for the weighted diffusivity $\kappa_{w\_G,\sigma}$ and also for the diagnosed diffusivity $\kappa_{G\_int,\sigma}$ are identical with the value of $4\,cm^2/s$ of the constant explicit diffusion coefficient.

The results for experiment *A_incr* (Figure 9.4) are also independent of the

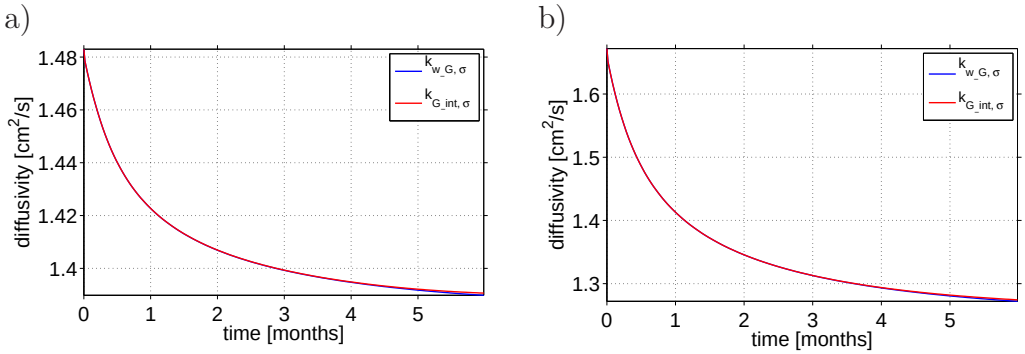

Figure 9.5: Weighted diffusivity $\kappa_{w\_G,\sigma}$ equal to diagnosed diffusivity $\kappa_{G\_int,\sigma}$ for *A_horiz* (2-dimensional, diffusion acts on tracer, horizontal isopycnals): a) horizontally varying and b) equally labelled initial tracer condition.

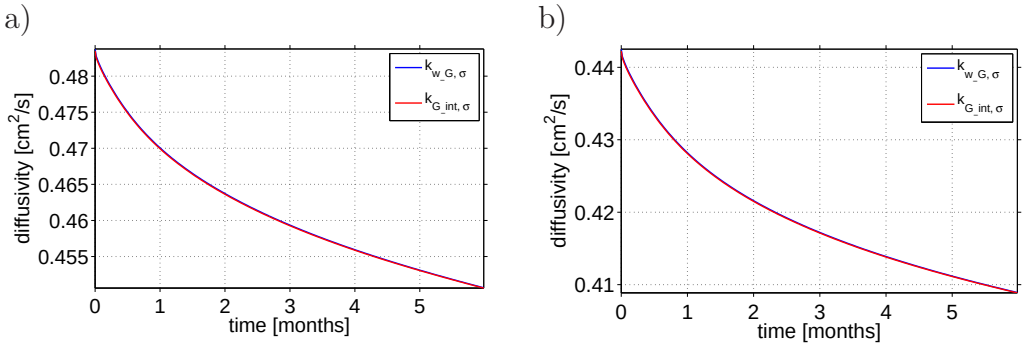

Figure 9.6: Weighted diffusivity $\kappa_{w\_G,\sigma}$ equal to diagnosed diffusivity $\kappa_{G\_int,\sigma}$ for *A_oc* (2-dimensional, diffusion acts on tracer, horizontal isopycnals): a) horizontally varying and b) equally labelled initial tracer condition.

used initial tracer condition, which can be ascribed to the constancy of the explicit diffusion coefficient along the isopycnal layers. The values of the diagnosed diffusivity $\kappa_{G\_int,\sigma}$ are almost identical to the ones of the weighted diffusivity $\kappa_{w\_G,\sigma}$.

Independent of the used initial tracer condition, the values for $\kappa_{G\_int,\sigma}$ and $\kappa_{w\_G,\sigma}$ of experiment *A_horiz* (Figure 9.5) are also almost identical. Using the horizontally varying initial tracer condition (Figure 9.5 a), the values for $\kappa_{G\_int,\sigma}$ and $\kappa_{w\_G,\sigma}$ are slightly lower ($1.48\,cm^2/s$ decreasing to $\sim 1.39\,cm^2/s$) compared to the ones for the equally labelled initial tracer condition ($\sim 1.65\,cm^2/s$ decreasing to $1.29\,cm^2/s$, Figure 9.5 b).

Also in the results for experiment *A_oc*, the values for $\kappa_{G\_int,\sigma}$ are consistent with the ones of $\kappa_{w\_G,\sigma}$ (Figure 9.6). Using the horizontally

varying initial tracer condition, the values decrease from $\sim 0.485\,cm^2/s$ to $\sim 0.45\,cm^2/s$. For the equally labelled initial tracer condition, the values for the weighted and the diagnosed diffusivity vary between $\sim 0.44\,cm^2/s$ and $\sim 0.41\,cm^2/s$.

As expected, the results for the diagnosed diffusivity $\kappa_{G\_int,\sigma}$ and the weighted diffusivity $\kappa_{w\_G,\sigma}$ are almost identical independent on the vertical or horizontal structure of the explicit diffusivity used. Here, it should be added, that in analogous experiments using models with a coarser vertical resolution, the results of the diagnosed and the weighted diffusivity are also almost identical, although the values might vary compared the ones shown.

The reason can be found in the origin of the tracer flux method. The change in the total amount of tracer mass above an isopycnal is compared with the tracer flux through the isopycnal. As the different terms are discretised in exactly the same way as it is done in the model set-up, the values for $\kappa_{G\_int,\sigma}$ and $\kappa_{w\_G,\sigma}$ should be consistent, independent of the resolution of the model grid.

9.2.3 The effect of vertical advection

In this section, the experiment with an implemented constant vertical advection in the tracer, the temperature and the salinity fields are shown. The explicit vertical velocity is constant and has a value of $4 \times 10^{-6}\,m/s \approx 0.35\,m/day$.

The results of the 1-dimensional experiments with implemented vertical advection showed that the combination of the transformation of the tracer and the vertical movement of the isopycnals cause high frequency fluctuations in the values of the diagnosed diffusivity. The implemented vertical advection was restricted to a parallel movement of the isopycnals by defining the density equation to be linear. Defining the density to be linear in the experiments with horizontal isopycnals, the results for the diagnosed diffusivity are, as expected, exactly the same as the ones previously shown for the 1-dimensional experiments.

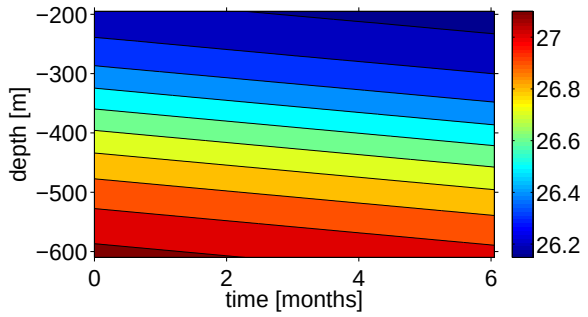

Figure 9.7: Density profile with time for experiment with implemented vertical advection: isopycnals are parallel, although temperature and salinity are non-linear and the density equation is non-linear.

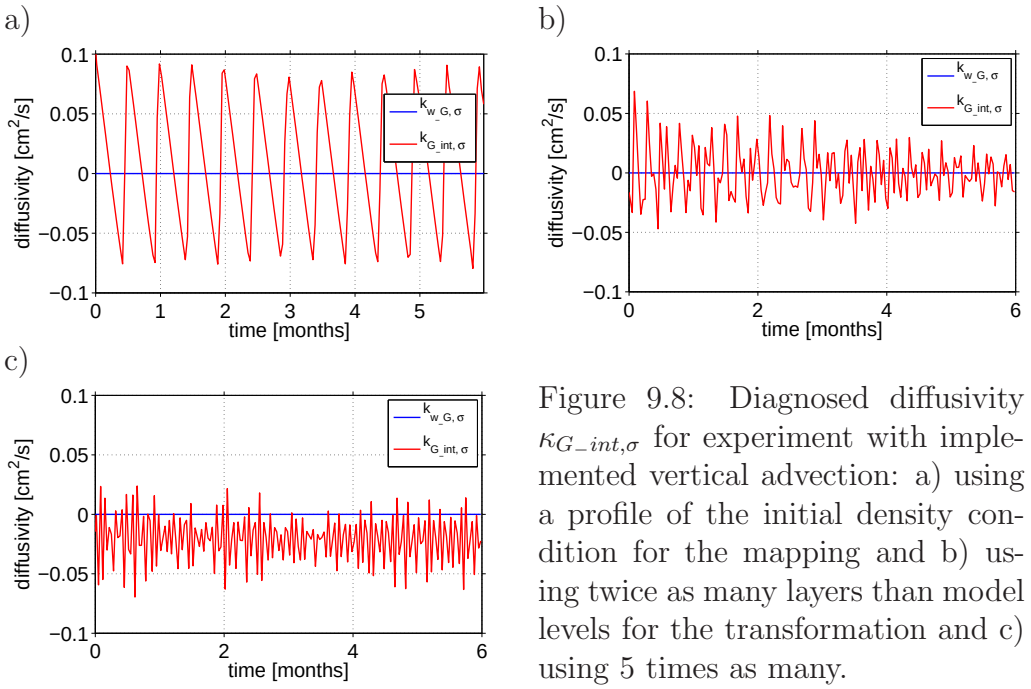

Figure 9.8: Diagnosed diffusivity $\kappa_{G\_int,\sigma}$ for experiment with implemented vertical advection: a) using a profile of the initial density condition for the mapping and b) using twice as many layers than model levels for the transformation and c) using 5 times as many.

Using the non-linear density equation in combination with non-linear initial temperature and salinity fields, the advection does not only lead to an exact parallel downward movement of the isopycnals, but might also result in a small amount of divergence or convergence of density classes. As the initial temperature and salinity fields in this experiment are horizontally uniform, the density fields stay horizontal throughout the whole experiment.

Figure 9.7 shows the temporal development of the isopycnals with time. Although temperature and salinity vary non-linearly with depth and the used density equation is non-linear as well, the downward movement of the isopycnals with time is almost parallel. The divergence and convergence in the Figure is so small, that it cannot be seen.

Figure 9.8 a) shows the results for the diagnosed diffusivity $\kappa_{G\_int,\sigma}$, where a profile of the initial density is used as the transformation axis of the mapping. The values and the frequency are still similar compared to the results of the 1-dimensional case studies and also the mean value of $\kappa_{G\_int,\sigma}$ is consistent with a value of $7.7 \times 10^{-3}\, cm^2/s$. The numerically induced diffusivity analysed by the variance method has a value of $\sim 6.7 \times 10^{-3}\, cm^2/s$ (see Section 8.2.3). The results are independent of the initial tracer condition used, therefore only one Figure is shown.

Increasing the resolution of the transformation by using twice as many layers than levels, the amplitude of the fluctuations in $\kappa_{G\_int,\sigma}$ is reduced by $\sim 50\%$ and the mean value is $-0.14 \times 10^{-3}\, cm^2/s$ (Figure 9.8 b). A further increase in the number of layers used for the mapping (5× more layers) leads to a further reduction in the amplitude of the fluctuations and also to a further decrease of the mean value to $-0.02\, cm^2/s$ (Figure 9.8 c). The spurious effect of the increase in the number of layers used for the tracer mapping leads to negative mean values of $\kappa_{G\_int,\sigma}$, similar as found in the 1-dimensional case studies. The negative mean values are an artificial effect of the tracer mapping.

In summary, the amplitude of the fluctuations in the diagnosed diffusivity is of the same order as the explicit diffusivity expected in the ocean interior of OGCMs. The time averaged values of $\kappa_{G\_int,\sigma}$ are of the order of $o(10^{-3}\, cm^2/s)$. An increase in the resolution used for the mapping results in a decrease of the averaged $\kappa_{G\_int,\sigma}$ to negative values of the order of $o(10^{-2}\, cm^2/s)$. Depending on the periodic structure of the fluctuations of $\kappa_{G\_int,\sigma}$, the mean should be taken over at least one wavelength. The spurious effect of the mapping is too large for a robust analysis at each time-step and also leads to large errors on the mean values of $\kappa_{G\_int,\sigma}$, which mask the signal of the numerically induced diffusivity.

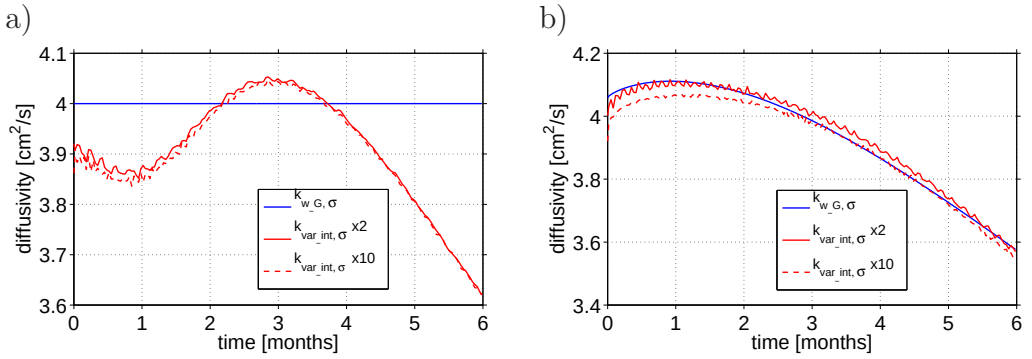

Figure 9.9: Diagnosed diffusivity $\kappa_{G\_int,\sigma}$ (red, solid line) using twice as many layers than levels for the mapping and 10× more layers than levels (red, dashed line) and weighted explicit diffusivity coefficient $\kappa_{w\_G,\sigma}$ (blue) for a) experiment *A_const* and b) experiment *A_incr* (diffusion acts on tracer, temperature and salinity; horizontal isopycnals).

9.2.4 Diffusion acts on tracer, temperature and salinity

In this section, experiments are analysed, in which the vertical diffusion acts not only on the tracer, but also on temperature and salinity. The corresponding effect in the density can be interpreted as an additional small scale movement of the isopycnal interfaces. Because the experiments are reduced to the cases with horizontal isopycnals, only the results for experiment *A_const* and *A_incr* will be shown.

The results for the diagnosed diffusivity $\kappa_{G\_int,\sigma}$ and the weighted diffusivity $\kappa_{w\_G,\sigma}$ for both experiments are consistent to ones in the analogous 1-dimensional experiments. Additionally, $\kappa_{G\_int,\sigma}$ and $\kappa_{w\_G,\sigma}$ are independent of the initial tracer condition used, therefore only one figure will be shown for each experiment. The mean interfacial velocity $\overline{w_I}$, has only a minor ($<< 0.1\%$) effect on the result of $\kappa_{G\_int,\sigma}$. Therefore, $\overline{w_I} = 0$ can be assumed in the following analysis.

Figure 9.9 a) shows the results of experiment *A_const* for the diagnosed diffusivity $\kappa_{G\_int,\sigma}$ using twice as many layers than levels (red, solid) and 10 times more layers than levels (red, dashed) and the weighted diffusivity $\kappa_{w\_G,\sigma}$ (blue). The results for $\kappa_{w\_G,\sigma}$ are identical to the value of the

explicit diffusion coefficient. An increase in the resolution of the transformation leads to a decrease in the values of $\kappa_{G\_int,\sigma}$. The maximum difference of $\sim 1\%$ is very small and decreases with time.

The results for the diagnosed diffusivity in experiment *A_incr* (Figure 9.9 b) are also robust with respect to changes in the transformation axis used as the maximal difference in the values of $\kappa_{G\_int,\sigma}$ is smaller than 1%.

As long as the isopycnals are horizontal the results of the 2-dimensional experiment are consistent to the results of the analogous 1-dimensional experiments. Additionally, the results are robust according to the transformation onto isopycnal layers, which can be ascribed by the high vertical resolution in the model itself.

9.3 Results: isopycnals as in the ocean interior

In this section the effect of the non-horizontal density field on the diagnostics of the tracer flux method will be analysed. One effect of the different initial density field is that the values of the diagnosed and the weighted diffusivity are not necessarily identical with the results shown in the previous section.

In the following, first the initial conditions of the experimental set-up will be repeated (same conditions as shown in Section 8.3.1). Second, experiments where vertical diffusion acts on the tracer only will be shown, third, the effect of implemented vertical advection is analysed and last the effect of diffusion in tracer, temperature and salinity.

9.3.1 Initial conditions

Figure 9.10 (identical with Figure 8.12) shows the initial density field, were the isopycnal layers are sloping and diverge along the horizontal direction. In Figure 9.11 (the same as Figure 8.13) the isopycnally varying initial

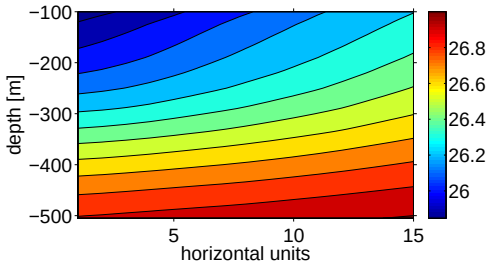

Figure 9.10: Initial density field with non-horizontal isoycnals for the 2-dimensional case studies.

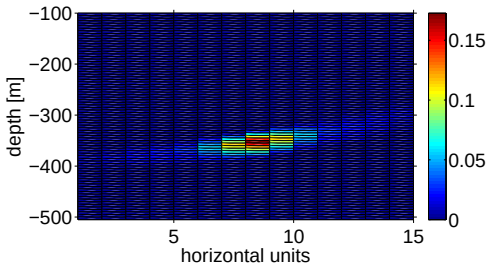

Figure 9.11: Isopycnally varying initial tracer condition for non-horizontal isopycnals: initial tracer field, with a tracer maximum in the middle and fading concentration towards the outer sides.

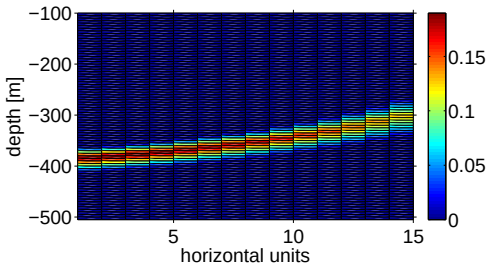

Figure 9.12: Equally labelled initial tracer condition for non-horizontal isopycnals: tracer is equally labelled along one isopycnal layer.

tracer condition is shown, the tracer maximum is located in the middle of the horizontal field with a fading concentration towards the outer sides. Figure 9.12 (Figure 8.14) shows the equally labelled initial tracer condition, where one isopycnal layer is labelled with the equal tracer mass.

The vertical model grid is chosen to be equidistant with a level thickness of $5\,m$. The horizontal grid is also chosen to be equidistant with a box width equal to 1. The model set-up is the same as the one introduced in Section 8.2.1.

9.3.2 Diffusion acts on the tracer only

In the experiments shown in this section the vertical diffusion acts on the tracer only, temperature and salinity are both stationary. The results for the diagnosed and the weighted diffusivity base on the integrated

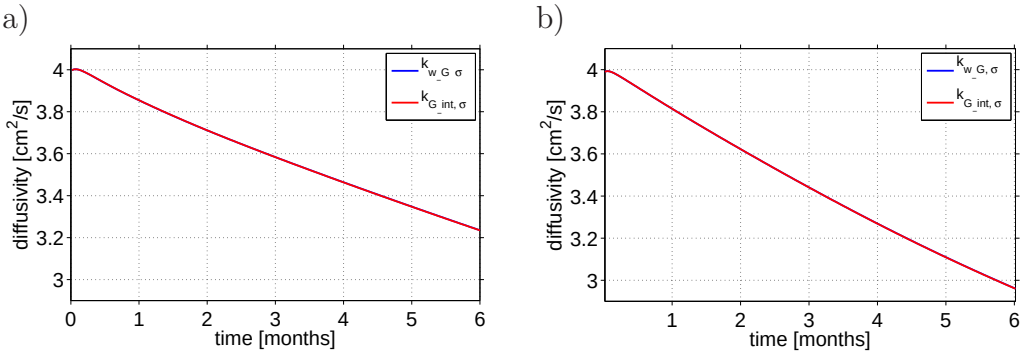

Figure 9.13: Weighted diffusivity $\kappa_{w\_G,\sigma}$ equal to diagnosed diffusivity $\kappa_{G\_int,\sigma}$ for *A_incr* (2-dimensional, diffusion acts on tracer, non-horizontal isopycnals): a) isopycnally varying and b) equally labelled initial tracer condition.

advection-diffusion equation. Similar as in the analogous experiments with horizontal isopycnals, the tracer flux through the isopycnal layer and the change of the total amount of tracer mass above the isopycnal is discretised in the analysis in exactly the same way as it is done in the model discretisation. Therefore, it can be expected that the results for $\kappa_{G\_int,\sigma}$ and $\kappa_{w\_G,\sigma}$ are very similar in this section.

In the following the results for the diagnosed diffusivity are independent of the number of layers used for the transformation of the tracer into σ-coordinates, as long as the transformation is not getting coarser than the density profiles in the model. For the results shown, twice as many layers than levels are chosen for the tracer mapping.

In the results of experiment *A_const*, the diagnosed diffusivity $\kappa_{G\_int,\sigma}$ and the weighted diffusivity $\kappa_{w\_G,\sigma}$ are identical to the constant value of $4\,cm^2/s$ of the explicit diffusion coefficient. The results are independent of the initial tracer condition used.

Irrespective which initial tracer condition is used, the results for the diagnosed diffusivity $\kappa_{G\_int,\sigma}$ and the weighted diffusivity $\kappa_{w\_G,\sigma}$ in experiment *A_incr* are almost identical (Figure 9.13). Because the explicit diffusion coefficient in this experiments is defined to be constant along the isopycnal layers, the results for the two initial tracer conditions differ only slightly towards the end of the experiment. This effect is caused by the

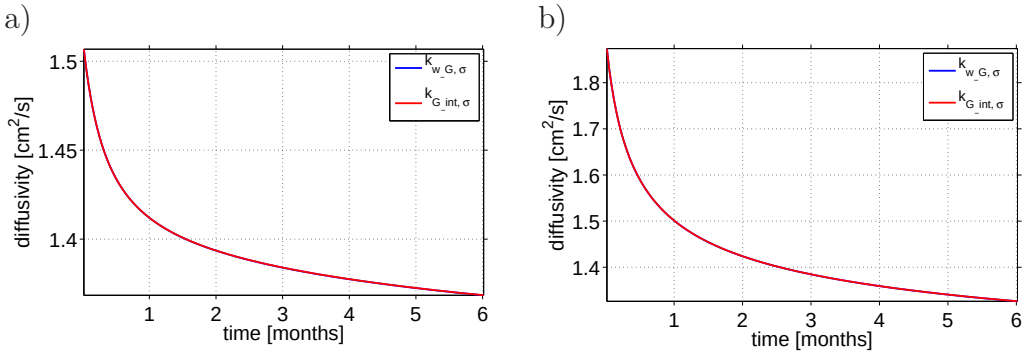

Figure 9.14: Weighted diffusivity $\kappa_{w\_G,\sigma}$ equal to diagnosed diffusivity $\kappa_{G\_int,\sigma}$ for A_horiz (2-dimensional, diffusion acts on tracer, non-horizontal isopycnals): a) isopycnally varying and b) equally labelled initial tracer condition.

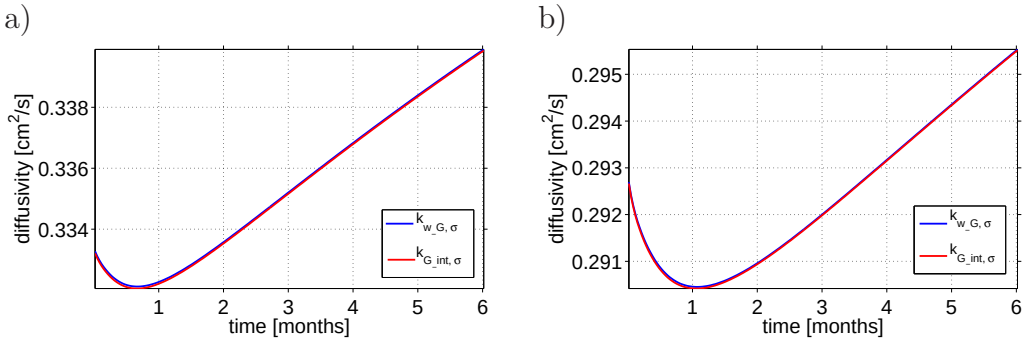

Figure 9.15: Weighted diffusivity $\kappa_{w\_G,\sigma}$ equal to diagnosed diffusivity $\kappa_{G\_int,\sigma}$ for A_oc (2-dimensional, diffusion acts on tracer, non-horizontal isopycnals): a) isopycnally varying and b) equally labelled initial tracer condition.

slightly diverging isopycnals along the horizontal direction.

Also in experiment A_horiz, $\kappa_{G\_int,\sigma}$ and $\kappa_{w,\sigma}$ show almost identical results (Figure 9.14) for both initial tracer conditions. The similar effect can be found in experiment A_oc. The values of $\kappa_{G\_int,\sigma}$ and $\kappa_{w,\sigma}$ are consistent for both initial tracer conditions, although the explicit diffusivity is non-linear with depth and non-linear along the isopycnal layers.

In summary it can be said, that as long as the isopycnals layers are stationary and the diffusion acts on the tracer only, the results for the diagnosed diffusivity $\kappa_{G\_int,\sigma}$ and the weighted diffusivity $\kappa_{w\_G,\sigma}$ are almost identical and robust with respect to the mapping of the tracer onto isopycnals.

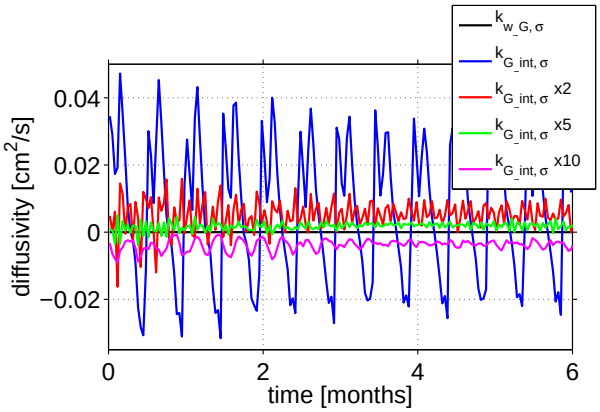

Figure 9.16: Diagnosed diffusivity $\kappa_{G\_int,\sigma}$ for experiment including advection (non-horizontal isopycnals) using the isopycnally varying initial tracer condition, using the same amount of layers as levels (blue), twice as many (red), 5 times more (green) and 10 times more layer than levels (magenta).

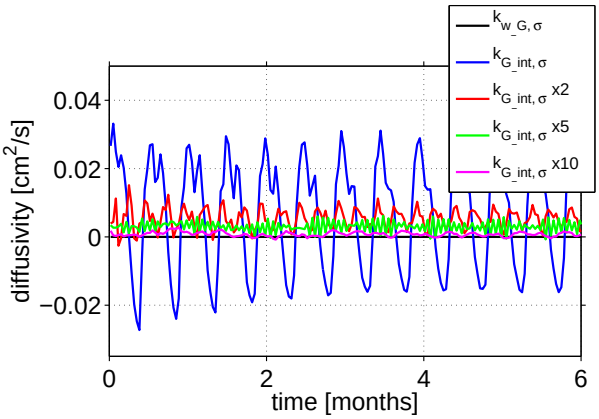

Figure 9.17: Diagnosed diffusivity $\kappa_{G\_int,\sigma}$ (red) for experiment including advection (non-horizontal isopycnals) using the equally labelled initial tracer condition, using the same amount of layers as levels (blue), twice as many (red), 5 times more (green) and 10 times more layer than levels (magenta).

9.3.3 The effect of vertical advection

In this section, the experiment with an implemented constant vertical advection in tracer, temperature and salinity are shown. The explicit vertical velocity is $4 \times 10^{-6}\, m/s$ which is equal to $0.35\, m/day$. For these experiments, the used density equation is non-linear in order to be more realistic. The change in the density field is already shown in Figure 8.21 in Section 8.3.3 and will therefore not be repeated.

Figure 9.16 shows the results for the diagnosed diffusivity $\kappa_{G\_int,\sigma}$ where the isopycnally varying initial tracer condition is used. For the mapping of the tracer onto isopycnals, results are shown using the same amount of layers as levels (blue), twice as many (red), 5 times more (green) and 10 times (magenta) more layers than levels for the mapping of the tracer onto isopycnals. As a reference the weighted diffusivity (black) which is equal to

zero is shown as well.

Already an increase of the number of layers used for the mapping from the same amount as levels to twice as many leads to a reduction in the amplitude of the high frequency fluctuations of 75%. A further increase in the number of layers leads to a further reduction in the amplitude. The time averaged values of $\kappa_{G\_int,\sigma}$ vary between values of $6.7 \times 10^{-3}\, cm^2/s$ ($\kappa_{G\_int,\sigma}$) and $1.7 \times 10^{-3}\, cm^2/s$ ($\kappa_{G\_int,\sigma}, 5\times$), except using 10 times more layers than levels, the mean value gets negative ($-3.8 \times 10^{-3}\, cm^2/s$). The analysis of the variance method (Section 8.3.3) showed that the numerically induced diffusivity in this experiment is $6.7^{-3}\, cm^2/s$. The time averaged diagnosed diffusivity, when the same amount of layers as levels is used for the transformation, is consistent with the numerically induced diffusivity.

In Figure 9.17 the results for the diagnosed diffusivity are shown where the equally labelled initial tracer condition is used. The amplitudes for all shown realisations of the used number of layers for the tracer transformation are smaller compared to the results of the experiments with the isopycnally varying initial tracer condition. Additionally, the results using 10 times more layers than levels are staying almost always positive.

The time averaged diagnosed diffusivity, when the same number of layers as levels is used for the transformation, has a value of $6.9 \times 10^{-3}\, cm^2/s$ and overestimates the numerically induced diffusivity by $\sim 3\%$. An increase in the resolution of the transformation leads to a decrease of the time averaged values of $\kappa_{G\_int,\sigma}$ ($5.3 \times 10^{-3} - 0.78 \times 10^{-3}\, cm^2/s$).

The results of these experiments show, that the analysis of a tracer field, which is uniformly distributed along the isopycnals, leads to a smaller amplitude in the fluctuations of the diagnosed diffusivity, which are caused by the tracer mapping. By analysing time averaged values for the diagnosed diffusivities, close results to the numerically induced diffusivity can be found for the cases where the same number of layers as levels is used for the transformation of the tracer. These close results might be a result of averaging effects by the horizontal integration of the tracer mass and the tracer gradient. Similar to the results of the experiments with horizontal

isopycnals, the time-scale of the mean values depends on the periodic structure of the fluctuations and should last at least over one wavelength. An increase in the resolution of the tracer transformation leads to a decrease of the time averaged diapycnal diffusivities.

9.3.4 Diffusion acts on tracer, temperature and salinity

In the experiments shown in this section tracer, temperature and salinity are diffusive. The corresponding effect of the diffusion acting on temperature and salinity can be interpreted as an interfacial movement of the isopycnals. The effect of the interfacial velocity is of minor importance for the analysis of the diagnosed diffusivity in experiments with a high vertical resolution ($< 1\%$), therefore $w_I = 0$ is assumed in the following.

The results for the weighted diffusivity $\kappa_{w\_G,\sigma}$ in the experiments shown in the following are, as expected, identical to the ones of Section 9.3.2. The results of the diagnosed diffusivity $\kappa_{G\_int,\sigma}$ are robust with respect to changes in the resolution of the transformation axis used ($< 0.1\%$), as long as the resolution is not getting coarser than the density profiles in the model.

In experiment *A_const* (Figure 9.18), the results for the diagnosed diffusivity $\kappa_{G\_int,\sigma}$ are smaller compared to the weighted one for both initial tracer conditions. The interfacial movement of the isopycnal layers with time is so small, that a direct comparison between the isopycnal fields does not show a diverging or converging behaviour. Therefore, Figure 9.19 shows the difference of the initial density field and the density field at the end of the experiment, to get an idea about the temporal change of the isopycnal field. The difference of the interfacial velocities can be interpreted as a divergence or convergence of the isopycnal layers.

Negative values in the difference of the densities can be interpreted as an upward movement of the isopycnals. The tracer in these experiments is released at a depth between $300\,m$ (eastern side) and $400\,m$ (western side).

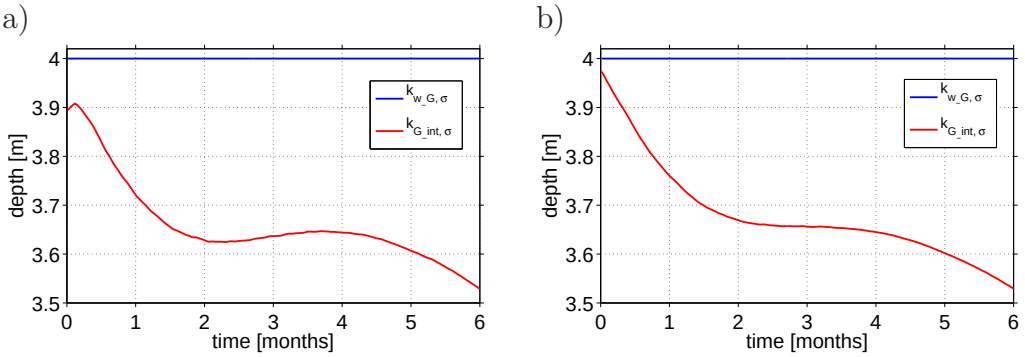

Figure 9.18: Weighted diffusivity $\kappa_{w\_G,\sigma}$ and diagnosed diffusivity $\kappa_{G\_int,\sigma}$ for A_const (2-dimensional): a) isopycnally varying and b) equally labelled initial tracer condition (diffusion acts on tracer, temperature and salinity, non-horizontal isopycnals).

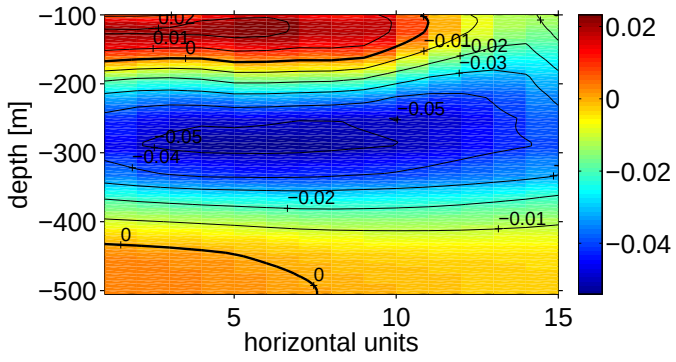

Figure 9.19: Difference of the density field at the beginning and at the end of experiment A_const.

The upward movement of the isopycnals at 300 m depth is large compared to the one at 400 m depth, which means that the isopycnals are diverging. The smaller values in the diagnosed diffusivity $\kappa_{G\_int,\sigma}$ can be ascribed to the divergence of the isopycnals.

Also in experiment A_incr, the diagnosed diffusivity $\kappa_{G\_int,\sigma}$ (red) is constantly smaller $(1 - 20\%)$ than the weighted diffusivity $\kappa_{w\_G,\sigma}$ (blue), independent of the initial tracer condition used (Figure 9.21). The difference of the initial density field with the one at the end of the experiment is shown in Figure 9.21. Similar to the difference shown for experiment A_const, the values of the difference in the depth region between 300 and 400 m are negative and increase with depth, which can also be interpreted as a divergence of the isopycnals. This means, that the

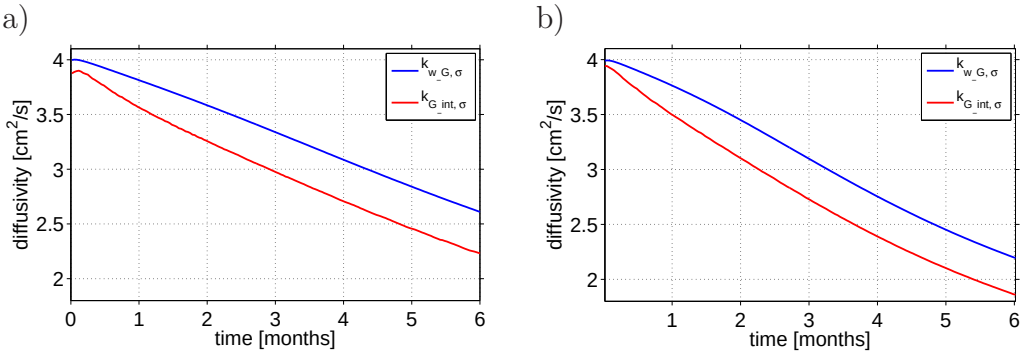

Figure 9.20: Weighted diffusivity $\kappa_{w\_G,\sigma}$ and diagnosed diffusivity $\kappa_{G\_int,\sigma}$ for *A_incr* (2-dimensional): a) isopycnally varying and b) equally labelled initial tracer condition (diffusion acts on tracer, temperature and salinity, non-horizontal isopycnals).

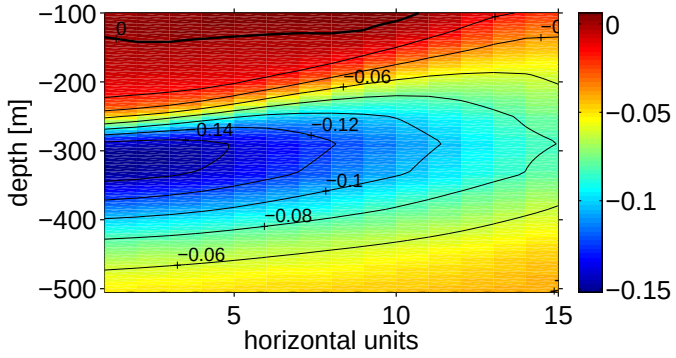

Figure 9.21: Difference of the density field at the beginning and at the end of experiment *A_incr*.

divergence of the isopycnals leads to a negative induced diffusivity in the results for the diagnosed diffusivity $\kappa_{G\_int,\sigma}$ of experiment *A_incr*.

A similar effect can be seen in the results of experiment *A_horiz* (Figure 9.23), where $\kappa_{G\_int,\sigma}$ is smaller than $\kappa_{w\_G,\sigma}$ for both initial tracer conditions. The difference in the density fields (Figure 9.23) gives the impression that the slightly diverging isopycnals in the depth between 300 and 400 m lead to a negative induced diffusivity.

Contrary, in the results for the last experiment, *A_oc* (Figure 9.24), the diagnosed diffusivity is not constantly smaller than the weighted diffusivity. Using the isopycnally varying initial tracer condition (see Figure 9.24 a.), $\kappa_{G\_int,\sigma}$ starts at a lower value than $\kappa_{w\_G,\sigma}$, but increases constantly and from the second month onwards, $\kappa_{G\_int,\sigma}$ is larger than $\kappa_{w\_G,\sigma}$. In Figure

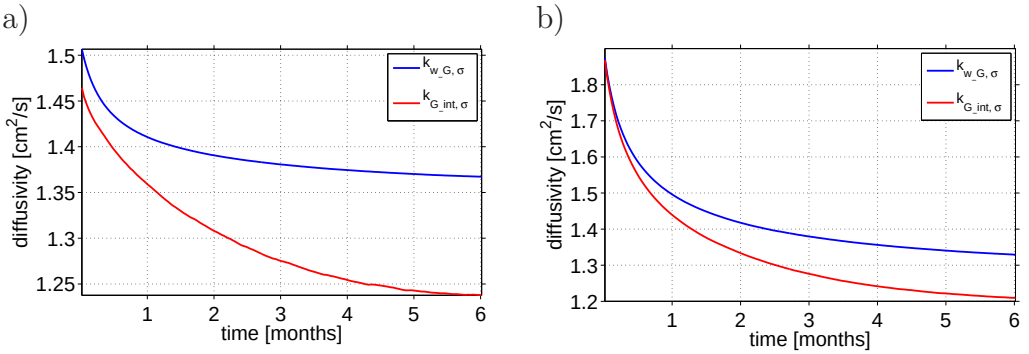

Figure 9.22: Weighted diffusivity $\kappa_{w\_G,\sigma}$ and diagnosed diffusivity $\kappa_{G\_int,\sigma}$ for *A_horiz* (2-dimensional): a) isopycnally varying and b) equally labelled initial tracer condition (diffusion acts on tracer, temperature and salinity, non-horizontal isopycnals).

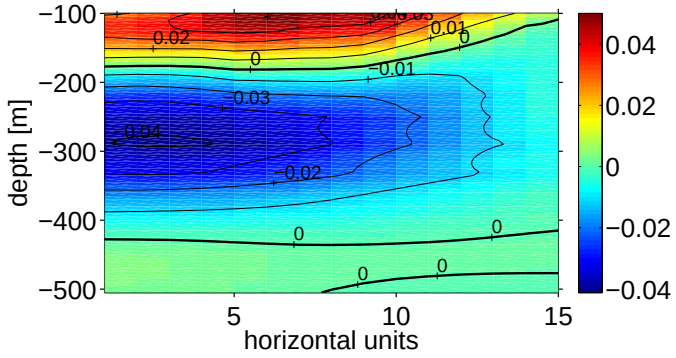

Figure 9.23: Difference of the density field at the beginning and at the end of experiment *A_horiz*.

9.24 b), where the results of the equally labelled initial tracer condition are shown, the values for $\kappa_{G\_int,\sigma}$ are nearly constantly higher ($\sim 1\%$).

The positive values in the difference of the density field in the depth between 300 and 400 m, as shown in Figure 9.25, represent a downward movement of the isopycnals. The values close to the depth of 300 m are larger than the ones in 400 m depths, which can be interpreted as a convergence of the isopycnals. This means that the positive induced diffusivity can be ascribed to a convergence of the isopycnal layers.

In summary it can be said that the results presented in this section are robust with respect to changes in the resolution of the tracer transformation, as long as the used transformation is not getting coarser

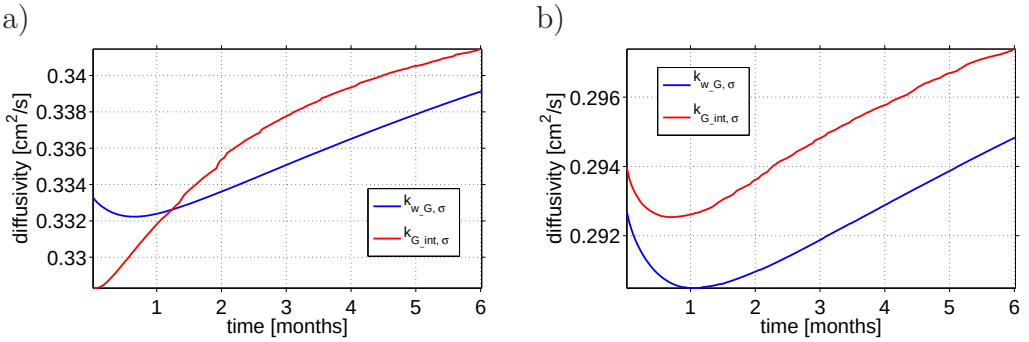

Figure 9.24: Weighted diffusivity $\kappa_{w\_G,\sigma}$ and diagnosed diffusivity $\kappa_{G\_int,\sigma}$ for A_oc (2-dimensional): a) isopycnally varying and b) equally labelled initial tracer condition (diffusion acts on tracer, temperature and salinity, non-horizontal isopycnals).

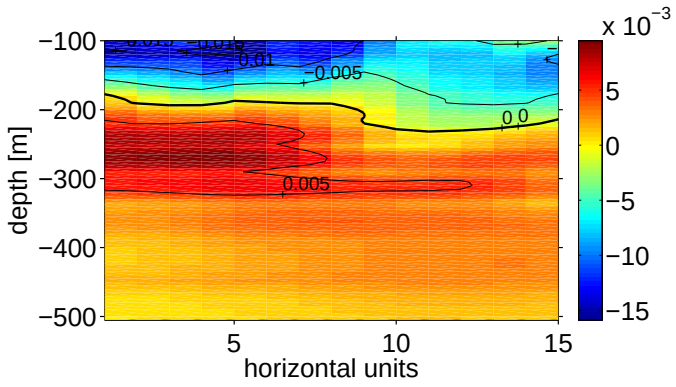

Figure 9.25: Difference of the density field at the beginning and at the end of experiment A_oc.

than the density profiles which can be found in the model. The rate of change in the density fields, which is realised here by taking the difference of the density at the beginning and the end of the experiment, gives an idea about the diverging and converging behaviour of the isopycnals with time. The results suggest, that diverging isopycnals lead to negative values, and converging isopycnals to positive values of the numerically induced diffusivity.

9.4 Summary

The experiments in which the vertical diffusion acts on the tracer only show almost identical results for the diagnosed and the weighted diffusivity

independent of the used initial tracer condition and the slope of the isopycnals. Additionally, these results showed that this method is robust according to the transformation of the tracer onto isopycnals, as long as the resolution does not get coarser than the density profiles of the model.

Also the analysis of experiments in which the vertical diffusion acts on tracer, temperature and salinity showed that the results for the diagnosed and the weighted diffusivity are robust with respect to changes in the resolution of the transformation used. The criterion, that the resolution of the transformation used should not be coarser than the density profiles in the model, is identical to the one mentioned above. The comparison between the values of the diagnosed and the weighted diffusivity in relation to the temporal change in the isopycnal layers showed that a divergence of the isopycnals leads to negative values and a convergence to positive values of the numerically induced diffusivity.

Already the results of the 1-dimensional experiments showed that experiments which include a constant vertical advection lead to spurious fluctuations in the values of the diagnosed diffusivity. Also the spurious effect on the time averaged values of the diagnosed diffusivity was at least one order of magnitude larger than the numerically induced diffusivity. These spurious fluctuations can also be found in the results of the 2-dimensional experiments. Using a higher resolution of the transformation than the resolution of the z-level model grid, the amplitude of these high frequency fluctuations is reduced by more than 50%.

The time average values of the diagnosed diffusivity give close results to the numerically induced diffusivity, but only when the transformation of the tracer is kept close to the resolution of the density profiles in the model. An increase of the resolution of the transformation leads to a decrease of the mean diagnosed diffusivities, which masks the numerically induced diffusivity. Depending on the periodic structure of the high frequency fluctuations, the mean values should be estimated at least over one wavelength.

Chapter 10

Summary: Part II

In the following, the applicability of the variance and the tracer flux method to infer diapycnal diffusivities in a set of idealised 2-dimensional case studies is summarised.

Variance method

For the analysis of the diagnosed diffusivity using OGCMs it is necessary to separate the variance decay of the total tracer volume between diffusivities caused by diapycnal mixing from those caused by isopycnal mixing. The separation of these two processes is carried out in the present study by interpolating the tracer along isopycnal layers before estimating its variance decay. Additionally, the uncertainty resulting from the transformation of the tracer concentration onto isopycnal layers is separated from the mapping-integration error (combined uncertainty due to transformation of the tracer onto isopycnals and along isopycnal integration). The results show that:

(i) analysing the diagnosed diffusivity without separating the diapycnal from the isopycnal diffusion, the mapping of the tracer onto isopycnals leads to minor uncertainties in the diagnosed diffusivities.

(ii) for horizontal isopycnals and constant along-isopycnal explicit diffusion coefficients, the diagnosed diffusivities are independent of the horizontal

distribution of the tracer concentration and insensitive to the vertical resolution of the transformation.

(iii) in more general experiments, where the isopycnals are non-horizontal or the explicit diffusion coefficient changes along the isopycnal layers, the along-isopycnal integration of the tracer concentration results in a spurious mixing of the tracer (mapping-integration error). This leads to spurious changes in the variance decay of the integrated tracer concentration in all experiments. This spurious diffusivity is larger than the numerically induced diffusivity. The latter arises from discretisation errors of the vertical advection and diffusion as a result of the Eulerian backwards time-stepping scheme.

Conclusions The variance method cannot be used reliably for the analysis of mean diapycnal diffusivities of passive tracers in models with an isopycnal component in the tracer flow, which is always the case in OGCMs.

In general, diffusion and advection in OGCMs are computed as separate steps. Therefore, it is possible to analyse vertically averaged fields of diagnosed diffusivities, which can be inferred from the spatial discretisation of the explicit diffusion only. This limited analysis is not restricted to z-level models, but can also be used in σ-layer models.

In σ-layer models, numerically induced diffusion is generated by the diapycnal (vertical) advection. In general, diapycnal and isopycnal advection are computed in separate steps. In these models it is possible to analyse the numerically induced diffusion by the variance method. The diagnosed diffusivity analysed by the variance decay of the total tracer gives the value for the numerically induced diffusivity.

Tracer flux method

The modification of the tracer flux method to analyse 2-dimensional experiments leads to robust estimates of diagnosed diffusivities in experiments where vertical diffusion acts on the tracer only, independent of the horizontal distribution of the tracer and of the density distribution.

Diagnosed diffusivities from the experiments in which vertical diffusion acts on tracer, temperature and salinity are insensitive to changes of the spatial resolution of the transformation. The corresponding effect of diffusion in temperature and salinity can be interpreted as a divergence or convergence of the isopycnal layers. In the diagnosed diffusivities converging isopycnals lead to positive induced diffusivities and diverging isopycnals to negative induced diffusivities. The resolution of the transformation should not be coarser than the resolution of the density profiles in the model. The diagnosed diffusivities are even more robust compared to those from analogous experiments in the 1-dimensional case studies.

Diagnosed diffusivities from experiments including vertical advection show spurious fluctuations. These result from the transformation of the tracer concentration onto isopycnals and from the vertical movement of the isopycnal layers. The amplitude in these fluctuations is smaller than that of the analogous experiment of the 1-dimensional case studies. This might be a result of averaging effects. Considering the time mean values over one or more wavelengths of the fluctuations in the diagnosed diffusivity, the values of the diagnosed diffusivity are of $o(10^{-3}\, cm^2/s)$, which is the same order of magnitude as the numerically induced diffusivity. In fact, if the transformation of the tracer is chosen to be similar to the density profiles in the model, the mean diagnosed diffusivity differs from the numerically induced diffusivity only by about 3%. An increase of the resolution of the transformation leads to a spurious decrease of the mean diagnosed diffusivities which masks numerically induced diffusivity.

Conclusions Using the tracer flux method it is not possible to directly analyse the diagnosed diffusivity at each time step, but it should be possible to analyse time mean values over longer periods. The minimum suitable averaging integral depends on the periodic structure of the spurious fluctuations and should at least include one wavelength.

It is necessary to repeat the set of experiments in 3-dimensional case studies. There, one may assume, that again only results for experiments including vertical advection are sensitive to the transformation of the tracer

onto isopycnals. In the 2-dimensional case studies the spurious effects in the time averaged values of the diagnosed diffusivity is less than in 1-dimensional cases due to averaging effects. One can speculate that 3-dimensional case studies may possibly show a further reduction of these spurious effects caused by the tracer mapping.

A fine resolved vertical grid is important for the analysis of diagnosing diffusion. Increasing the vertical resolution can be done in OGCMs at relatively low computational costs in comparison to an increase in horizontal resolution. Direct comparison of weighted and diagnosed diffusivities provides a measure of the numerically induced diffusivity. This might shed light on the mechanisms driving the meridional overturning circulation in models. Additionally the tracer flux method can be used for the analysis of any passive tracer in any model.

Chapter 11

Summmary and Outlook

Summary Three different diagnostics have been introduced to analyse the mean diapycnal diffusivity of a passive tracer. The methods were tested in a set of 1-and 2-dimensional case studies. The effect of a parallel vertical movement and of converging and diverging isopycnal layers is shown separately.

The first method is the divergence method, which infers the mean diapycnal diffusion from the advection-diffusion equation. It turns out that the results are very sensitive to the resolution of the density grid that is used. The errors are small, only if the thickness of the isopycnal layers onto which the tracer is reassigned is close to the thickness of the original model levels.

In the method of choice, the tracer flux method, the temporal change of the total amount of tracer above an isopycnal equals the diapycnal flux through the isopycnal. This method works reasonably well: In order to keep errors as small as possible longer time mean values should be analysed, as the combination of the advection and the transformation of the tracer onto isopycnals induce oscillations. As long as the vertical velocity is constant, the frequency of the oscillations are proportional to relation of the vertical velocity to the layer thickness of the transformed grid ($\frac{w}{\Delta z_t}$). The amplitude is proportional to the vertical change in the tracer concentration (ΔC). This means that either increasing the resolution of the vertical model grid or changing the initial tracer condition by decreasing ΔC lead to a decrease

of the spurious oscillations.

The third method is the variance method, that links the tracer variance decay to a mean diffusivity. In 2- and 3-dimensional experiments it is not possible to separate the diapycnal from the isopycnal diffusion.

Discussion and Outlook The results of the tracer flux method indicate that it should, in principle, be possible to analyse diapycnal diffusivities in OGCMs. However further analysis is still required to determine better the conditions required for the methods to work well. The comparison between the 1- and 2-dimensional experiments indicates that the biasing effect resulting from the tracer mapping and the relative movement of the isopycnals can be reduced by analysing a wider area with weak tracer gradients.

The 1- and 2-dimensional case studies also indicate that for diagnosing diffusivities a finely resolved vertical model grid is necessary. Increasing the vertical resolution can be done in OGCMs at relatively low computational costs in comparison to an increase in horizontal resolution. To what extent an increase in the vertical resolution or an initial tracer field with relatively weak gradients is important for a robust analysis of the diagnosed diffusivity in OGCMs needs to be verified in the future work.

The aim of this thesis was to analyse mean values of the diapycnal diffusivity for tracer fields in order to find a tool to analyse values which can be directly compared to the observational studies. This also helps to understand how far the results of the observational studies depend on the method used. How well can vertical profiles of the diagnosed diffusivity be analysed in z-level models? In principle, it should be possible, analogously to the studies of Griffies et al. (2000), to analyse the vertical behaviour of the diapycnal diffusivity by the tracer flux method.

As a further outlook, the analysis of diapycnal mixing in biogeochemical coupled models is also an important tool in order to analyse basic processes in these models, as these processes are currently poorly understood. The tracer flux method, as introduced in this thesis, analyses the mean

diapycnal diffusivity of the whole tracer volume. In order to analyse tracers which are not restricted to a local tracer patch, it is necessary to modify the tracer flux method for the analysis of a fixed region. Therefore it is necessary to consider the lateral tracer fluxes leaving the region of interest. Additionally, sinks and sources of tracers such as e.g. nutrients needs to be included in the diagnostic method as well.

Knowing the amount of numerical mixing in a z-level models, will, for example, allow a quantitative study of the interaction between diapycnal mixing and the absorption of carbon dioxide (CO_2) in the ocean in connection with climate change on glacial and interglacial time-scales.

Bibliography

Bryan, K., 1987: Potential vorticity in models of the ocean circulation. *Quart. J. Roy. Meteor. Soc.*, **113**, p 713 – 734.

Burchard, H. and H. Rennau, 2007: Comparative quantification of physically and numerically induced mixing in ocean models. *Ocean Modelling*.

Fick, A., 1855: On liquid diffusion, Philos. Mag. *J.Sci.*, **10**, p 31 – 39.

Garabato, A. C. N., K. I. Polzin, B. A. King, K. J. Heywood and M. Visbeck, 2004: Widespread intense turbulent mixing in the Southern Ocean. *Science*, **303**, p 210 – 213.

Gregg, M. C., T. B. Sanfort and D. P. Winkel, 2003: Reducing mixing from the breaking of internal waves in equatorial waters. *Nature*, **422**, p 513 – 515.

Griffies, S. M., R. C. Pacanowski and R. W. Halberg, 2000: Spurious diapycnal mixing associated with advection in a z-coordinate ocean model. *Mon. Wea. Rev.*, **128**, p 538 – 564.

Jeffreys, H., 1925: On fluid motions produced by differences of temperature and humidity. *Q.J.R. Meteorol. Soc.*, **51**, p 347 – 356.

Jenkins, W. J. and S. C. Doney, 2003: The subtropical nutrient spiral. *Global Biogeochem. Cycles*, **17 (4)**, 1110, doi: 10.1029/2003GB002085.

Kuhlbrodt, T., A. Griesel, M. Montoya, A. Levermann, M. Hofmann and S. Rahmstorf, 2007: On the driving processes of

the Atlantic Meridional Overturning Circulation. *Rev. Geophys.*, (RG2001, doi:10.1029/2004RG000166).

Ledwell, J., A. Watson and C. Law, 1993: Evidence for slow mixing across the pycnocline from an open-ocean tracer-release experiment. *Nature*, **364** (6439), p 701 – 703.

Ledwell, J. R. and B. M. Hickey, 1995: Evidence for enhanced boundary mixing in the Santa-Monica Basin. *J. Geophys. Res.*

Ledwell, J. R., E. Montgomery, K. Polzin, L. St. Laurent, R. Schmitt and J. Toole, 2000: Evidence for enhanced mixing over rough topography in the abyssal ocean. *Nature*, p 179 – 182.

Ledwell, J. R., A. J. Watson and C. Law, 1998: Mixing of tracer in the pycnocline. *J. Geophys. Res.*, **103** (C10), p 21499 – 21529.

Lee, M.-M., C. C. Andrew and A. J. G. Nurser, 2002: Spurious diapycnal mixing of the deep water in an eddy-permitting global ocean model. *J. Phys. Oceanogr.*, **32**, p 1522 – 1535.

Marotzke, J., 1997: Boundary mixing and the dynamics in the three-dimensional thermohaline circulation. *J. Phys. Oceanogr.*, **27**, p 1713 – 1728.

Marshall, J. and F. Schott, 1999: Open ocean deep convection: observations, models and theory. *Rev. Geophys.*, **37**, p 1 – 64.

Mignot, J., A. Levermann and A. Griesel, 2006: A decomposition of the Atlantic meridional overturning circulation into physical components using its sensitivity to vertical mixing. *J. Phys. Oceanogr.*, **36**, p 636 – 650.

Morales Maqueda, M. and G. Holloway, 2006: Second-order moment advection scheme applied to Arctic Ocean simulation. *Ocean Modelling*, **14**, p 197 221.

Moum, J., D. Caldwell, J. Nash and G. Gunderson, 2002: Observations of boundary mixing over the continental slope. *J. Phys. Oceanogr.*, **32**, p 2113 – 2130.

Moum, J. and T. Osborn, 1986: Mixing in the main thermocline. *J. Phys. Oceanogr.*, **16**, p 1250 – 1259.

Munk, W., 1966: Abyssal recipes. *Deep-Sea Res.*, **13**, p 707 – 730.

Munk, W. and C. Wunsch, 1998: Abyssal recipes II: energetics of tidal and wind mixing. *Deep-Sea Res.*, **45**, p 1976 – 2009.

Oakey, N., B. Ruddick, D. Walsh and J. Burke, 1994: Turbulence and microstructure measurements during North Atlantic Tracer Release Programm. *Eos Trans. AGU*, **75 (3)**, p 130, Ocean Sci. Meet. Suppl.

Osborn, T. R., 1980: Estimates of the local rate of vertical diffusion from dissipation measurements. *J. Phys. Oceanogr.*, **10**, p 83 – 89.

Osborn, T. R. and C. S. Cox, 1972: Oceanic fine structure. *Geophys. Fluid Dyn.*, **3**, p 321 – 345.

Oschlies, A. and V. Garcon, 1999: An eddy-permitting coupled physical-biological model of the North Atlantic 1. Sensitivity to advection numerics and mixed layer physics. *Global Biogeochem. Cycles*, **13**, p 135 – 160.

Pacanowski, R. C., 1995: MOM 2 Documentation, User's Guide and Reference Manual. technical report 3, GFDL Ocean Group.

Paparella, F. and W. R. Young, 2002: Horizontal convection is non-turbulent. *J. Fluid Mech.*, **466**, p 205 – 214.

Pelegri, J. L. and G. T. Csanady, 1991: Nutrient transport and mixing in the gulf stream. *J. Geophys. Res.*, **96** (C2), p 2577–2583.

Pelegri, J. L., G. T. Csanady and A. Martins, 1996: The North Atlantic nutrient stream. *Journal of Oceanography*, **52** (3), p 275 – 299.

Polzin, K. L., J. M. Toole, J. R. Ledwell and R. W. Schmitt, 1997: Spatial variability of turbulent mixing in the abyssal ocean. *Science*, **276**, p 93 – 96.

Sandström, J., 1908: Dynamische Versuche mit Meerwasser. *Ann. Hydrogr. Mar. Meteorol.*, **36**, p 6 – 23.

Sandström, J., 1916: Meteorologische Studien im Schwedischen Hochgebirge. *Göteborgs K. Vetensk. Vitterhetssamhällets Handkl.*, **27**, p 48.

Scott, J. R. and J. Marotzke, 2002: The location of diapycnal mixing and the meridional overturning circulation. *J. Phys. Oceanogr.*, **32**, p 3578 – 3595.

Stommel, H. and A. B. Arons, 1960: On the abyssal circulation of the world ocean - I. Stationary planetary flow patterns on a sphere. *Deep–Sea Res.*, **6**, p 140 – 154.

Winters, K. B. and E. A. D'Asaro, 1996: Diascalar flux and the rate of fluid mixing. *J. Fluid Mech.*, **317**, p 179 – 193.

Winters, K. B., P. N. Lombard, J. J. Riley and E. A. D'Asaro, 1995: Available potential energy and mixing in density-stratified fluids. *J. Fluid Mech.*, **289**, p 115 – 128.

Wuest, A. and A. Lorke, 2003: Small-scale hydrodynamics in lakes. *Ann. Rev.Fluid Mech.*, **35**, p 373 – 412.

Wunsch, C. and R. Ferrari, 2004: Vertical Mixing, Energy, and the General Circulation of the Oceans. *Ann. Rev. Fluid Mech.*, **36**, p 281 – 314.

Zhang, J., R. Schmitt and R. Huang, 1999: The relative influence of diapycnal mixing and hydrologic forcing on the stability of the thermohaline circulation. *J. Phys. Oceanogr.*, **29**, p 1096 – 1108.